NASA CONTRACTOR REPORT

NASA CR-2659

NASA CR-2659

DESIGN OF A 4½ STAGE TURBINE WITH A STAGE LOADING FACTOR OF 4.66 AND HIGH SPECIFIC WORK OUTPUT

P. F. Webster

Prepared by
PRATT & WHITNEY AIRCRAFT
East Hartford, Conn. 06108
for Lewis Research Center

NATIONAL AERONAUTICS AND SPACE ADMINISTRATION • WASHINGTON, D. C. • MARCH 1976

1. Report No.	2. Government Accession No.	3. Recipient's Catalog No.
CR-2659		

4. Title and Subtitle	5. Report Date
DESIGN OF A 4½ STAGE TURBINE WITH A STAGE LOADING FACTOR OF 4.66 AND HIGH SPECIFIC WORK OUTPUT	March 1976
	6. Performing Organization Code
7. Author(s)	8. Performing Organization Report No.
P. F. Webster	PWA-5101
	10. Work Unit No.
9. Performing Organization Name and Address	11. Contract or Grant No.
Pratt & Whitney Aircraft 400 Main Street East Hartford, Connecticut 06108	NAS3-18033
12. Sponsoring Agency Name and Address	13. Type of Report and Period Covered
National Aeronautics and Space Administration Washington, D.C. 20546	Contractor Report
	14. Sponsoring Agency Code

15. Supplementary Notes

Final Report. Project Manager, Warren J. Whitney, Fluid System Components Division, NASA Lewis Research Center, Cleveland, Ohio

16. Abstract

The aerodynamic design of a highly loaded multistage fan drive turbine is discussed. Turbine flowpath and airfoil sections are presented along with respective pressure and velocity distributions. Vibrational modes are identified in the expected turbine operating range.

17. Key Words (Suggested by Author(s))	18. Distribution Statement
Aerodynamic design High airfoil loading High specific work	Unclassified - unlimited STAR category 07 (rev.)

19. Security Classif. (of this report)	20. Security Classif. (of this page)	21. No. of Pages	22. Price*
Unclassified	Unclassified	137	$5.75

* For sale by the National Technical Information Service, Springfield, Virginia 22161

TABLE OF CONTENTS

LIST OF ILLUSTRATIONS

LIST OF ILLUSTRATIONS (Cont'd)

LIST OF ILLUSTRATIONS (Cont'd)

LIST OF ILLUSTRATIONS (Cont'd)

Figure

LIST OF ILLUSTRATIONS (Cont'd)

Figure

LIST OF TABLES

SUMMARY

A highly loaded, high work four-stage turbine has been aerodynamically designed with an axial inlet and with exit guide vanes to eliminate exit swirl with minimal loss. This design features controlled vortex flow, terraced inner flowpath, transitional boundary layer flow on each airfoil row, localized airfoil recambering, and zero seal leakage flow. The result is a turbine with high levels of gas turning and Mach numbers relative to a conventional design.

The predicted efficiency for this turbine is 89.3% without the exit guide vane.

INTRODUCTION

The application of highly loaded, high work fan-drive turbines is found in advanced subsonic cruise and lift fan engines. These engines must be lightweight, have high overall performance, and meet low noise requirements. In these types of engines high by-pass ratios are used to improve cycle performance, which results in large fan diameters and increased work requirements for the low pressure turbine. The combination of low rotative speeds and increased work output in the low pressure turbine necessitates the use of high stage loading and high specific work technology to keep engine weight, size and complexity at a minimum. A study conducted at Pratt & Whitney Aircraft of the engine for an advanced transport airplane indicated that a 4½ stage turbine (4 stages plus exit guide vanes) with a stage loading factor of 4.66 and high specific work output would be required to drive the fan. If conventional stage loading factors (2.0 or lower) were used, this turbine would consist of 8 or more stages.

The objective of this program is to design and fabricate the 4½ stage turbine and to determine its performance in a cold air investigation. This report describes the initial phase of the program, the turbine aerodynamic design.

TURBINE AERODYNAMIC DESIGN

The turbine aerodynamic design encompasses the discussion of the turbine requirements, the design philosophy and the turbine flowpath, velocity diagrams, and airfoil definitions.

DESIGN REQUIREMENTS

The aerodynamic design parameters required for this turbine design approximate those resulting from a Pratt & Whitney Aircraft engine study for an advanced transport airplane application. These requirements are summarized as follows:

Number of Stages	n	4 Plus Exit Guide Vanes
Average Stage Load Factor	$\dfrac{g J \Delta h}{n U_m^2}$	4.66 Based on Root Mean Square Pitch Diameter

Equivalent Specific Work	$\frac{\Delta h}{\theta}$	104,430 Joules/kg (44.9 BTU/lb)
Equivalent Rotative Speed	$\frac{N}{\sqrt{\theta}}$	2980 RPM
Equivalent Mass Flow	$\frac{W\sqrt{\theta}}{\delta}$	6.078 kg/sec (13.4 lb/sec)
Equivalent Mean Diameter	D_m	48.006 cm (18.90 in.)

The last three of the requirements result from applying a 0.5 linear scale factor to the study engine turbine to make the cold air turbine compatible with existing NASA Lewis test facilities. The turbine was designed to be investigated with inlet total state conditions of 422°K (300°F) and 1.565 atmospheres. These test conditions duplicate the study engine turbine Reynolds number at cruise flight conditions. The turbine was also specified to have an axial inlet flow so that the test results could be compared to those obtained from previous tests of turbines designed with high stage loading factors. No requirements were made on the turbine exit guide vanes (denoted EGV hereafter) other than the elimination of exit swirl.

DESIGN PHILOSOPHY

The turbine design personnel at Pratt & Whitney Aircraft believe that the achievement of an efficient turbine design for this application requires the incorporation of certain aerodynamic concepts into the turbine design. These concepts are discussed in the following paragraphs.

Controlled Vortex Flow

The design of a highly loaded, high specific work low pressure turbine presents the problem of obtaining adequate levels of root reaction especially when a free vortex flow design philosophy is used. Reaction is defined as the ratio of the static pressure change across the moving blade row to the static pressure change across the turbine stage. It has been found that low stage reactions lead to extreme pressure gradients on the suction surface of the airfoil which increases the danger of boundary layer separation. For this turbine, a controlled vortex flow principle was used which enhances the design by altering the spanwise work distribution to increase the root reaction and decrease the tip reaction. The reduction in tip reaction also is beneficial since this reduces the potential for blade tip leakage. The use of controlled vortex flow as a design tool is discussed in Reference 1, and has been incorporated into the turbine design procedure used at Pratt & Whitney Aircraft.

Terraced Inner Diameter Flowpath

In a typical controlled vortex design, the vane exit angle is redistributed, relative to free vortex flow by increasing the vane root angle and decreasing the vane tip angle. This results in a reduction in the vane exit static pressure gradient. Investigation into the effects of flowpath inner wall geometry on streamline curvature has shown that the combination of a conical vane endwall followed by a cylindrical blade endwall (referred to herein as "terraced") forces the local streamline curvatures in a way which also decrease the vane exit radial static pressure gradient. However, with a terraced flowpath, the reduced radial pressure gradient is accompanied by a reduction in streamline diffusion through the following blade row which does not occur with the vane angle redistribution. It is believed that the reduction in diffusion may result in reduced secondary flow losses. Therefore, this turbine design incorporates a combination of the vane exit redistribution and a terraced inner flowpath.

Transitional Boundary Layer

Experimental cascade research conducted by H. Schlichting and A. Das (2), H. Hebble (3) and K. Gersten (4) have clearly established that the profile performance of cascades in the Reynolds number range from 1.5×10^5 to 13.0×10^5 is strongly influenced by the nature of the transition from a laminar to a turbulent boundary layer on the airfoil suction side. As the Reynolds number decreases from a level where the suction side boundary layer is primarily turbulent, the laminar boundary layer transition moves further downstream towards the minimum pressure point. Upon reaching a Reynolds number where transition does not occur naturally before the minimum pressure, it appears that the boundary layer undergoes transition in a laminar separation bubble and reattaches to the profile surface as a turbulent boundary layer. At still lower Reynolds numbers, reattachment fails to occur, and the profile is separated in the classic sense.

A new calculation procedure has recently been developed by Pratt & Whitney Aircraft which accounts for the transitional nature of the airfoil boundary layer, the end product being a predicted airfoil profile loss. The results of this calculation are shown in Figure 1 for a typical airfoil design. A predicted turbulent boundary layer solution is also shown which has been used as a base for design performance estimation. As can be seen, the change in the boundary layer characteristics are reflected in the airfoil profile loss, i.e., the loss decreases as the transition point moves toward the minimum pressure point. The loss then increases gradually until boundary layer reattachment fails to occur. Therefore a minimum loss exists for each airfoil which is dependent on the transitional nature of the boundary layer, and which has been verified by cascade performance testing. The present four stage turbine design aims to capitalize on this loss characteristic by designing to an airfoil Reynolds number in the minimum loss region of each row through the variation of the airfoil chord.

Turbine Endwall Loss

The presence of divergent endwalls, high airfoil turning and high Mach numbers in a turbine design may result in large endwall losses. One of the mechanisms believed to cause end loss is the build up of the boundary layer as the fluid flows through the airfoil channel. Because of the pressure gradient across the channel, the lower momentum fluid is drawn to the interface of the suction surface and the inner wall where it forms a strong vortex, resulting in high losses. An investigation was made into the effects of airfoil recambering in the root endwall to reduce the cross channel pressure gradient. The results of this study are discussed in Reference 5, but the main conclusion was that a local recambering of the turbine airfoil by reducing the airfoil inlet and exit metal angle can lead to loss reductions in the root endwall regions. This approach has now been used in the 4½ stage turbine design between the root and quarter root sections.

Inner and Outer Seal Leakage

Gas path leakage past the rotating blade tip seals and the inner diameter spacer seals is known to have a large impact on turbine efficiency. One method for minimizing these leakage flows has been the use of abradable seal land materials that make very small running clearances possible. Since abradable seals are now being used in many turbine applications, the assumption of near zero leakage for the inner and outer seal configurations has been made.

DESIGN PROCEDURE

Meanline Analysis

The turbine flowpath and stage work distribution were set as a result of a parametric study using a Mean Line Design analysis approach. The Mean Line Design analysis offers a relatively fast meanline calculation by which a variety of turbine configurations can be compared and the optimum configuration selected. For this design, the inlet annulus was sized to give an inlet Mach number of 0.3 without inlet swirl. The fourth stage exit annulus was initially set to give 30° of swirl and a 0.46 exit Mach number. A parametric study was then carried out which varied the exit annulus area and stage work split while maintaining the average turbine mean diameter at 48.006 cm (18.9 inches). Varying the annulus area results in a trade-off between airfoil turning and turbine Mach number. The meanline results giving the effect of annulus area variation on efficiency are shown in Figure 2 for a stage work split of 27%, 27%, 27%, 19% in stages 1 through 4 respectively. The efficiency levels in this figure do not represent the final turbine design. This curve indicates that little improvement in efficiency is obtained by increasing the annulus area more than 15% above the base.

The variation of the fourth stage work determines the optimum overall turbine efficiency including the exit guide vane turning loss. The remainder of the turbine work was split equally in the first three stages. The exit guide vane loss was calculated using diffusion factors of 0.4 and 0.6, and the loss correlation from Reference 6. The meanline analysis results for this study are also shown in Figure 2 for the 15% increased exit annulus turbine. These curves indicate that the optimum turbine efficiency including the EGV loss would be obtained by designing the turbine with a near equal work split (25.5%, 25.9%, 24.5%, 24.1%) and a diffusion factor of 0.6. This means that the exit guide vane will be a highly loaded cascade with average inlet swirl of 45°. A reduction in the diffusion factor would result in the necessity to shift work out of the fourth stage, producing low fourth stage root reactions and high losses.

Streamline Analysis

Having determined the basic turbine flowpath, stage work split and the average (meanline) velocity triangles, the radial distribution of aerodynamic properties was determined using the Streamline Design Analysis. The basis of this analysis is a streamline design computer program which accounts for the radial component of gas velocity by using a streamline curvature solution to the equation of motion for an axisymmetric, inviscid, compressible flow. The most important aspect of the streamline procedure is the ability to use controlled vortex principles to maximize the turbine efficiency.

The results of the Meanline Design Study provide predicted airfoil profile and endwall loss levels which are distributed across the span by using Pratt & Whitney Aircraft's design experience. The airfoil chords were set to obtain airfoil Reynolds numbers between 3.0 and 4.0×10^5. This Reynolds number range was found to give a minimum profile loss in the cascade test mentioned earlier. The root and tip reaction levels were adjusted by the use of controlled vortex flow through a redistribution of vane exit angles and the "terracing" of the inner flowpath. A 30% to 40% root reaction level in all airfoil rows was the goal. Once a satisfactory solution was obtained, the turning in the airfoil roots was reduced to relieve the endloss as previously discussed.

The results of the streamline analysis are shown in the flowpath of Figure 3 and the velocity triangles at five radial locations in Figures 4 and 5. The flowpath is convergent through the exit guide vane to reduce the local diffusion factor. The number of turbine airfoils shown in Figure 3 was based on the application of the compressible form of the Zweifel lift coefficient in the range of 0.9 and 1.1 which is within Pratt & Whitney's experience for good profile efficiency. A tabulation of aerodynamic properties from the streamline analysis is given in Table I for the root, mean and tip sections, with typical airfoil nomenclature shown in Figure 6.

Airfoil Design

The airfoil contours were designed through an analysis of the airfoil surface pressure distribution, channel convergence, and surface boundary layer behavior. An airfoil design computer program generates suction and pressure surfaces based on input geometric parameters such as inlet and exit gas angles, solidity, throat dimensions and leading and trailing edge thickness. Inlet metal angles were determined by applying 3° to 6° of negative airfoil incidence, which is based on Pratt & Whitney Aircraft's experience on high performance turbine airfoils. Exit metal angles were determined by applying a gas angle deviation criterion derived from design experience, and influenced by the airfoil exit Mach number and gaging angle. Trailing edge diameter was to be 0.0253 cm (0.010 in.) to maintain the 0.5 scale factor between the cold air turbine and engine turbine. However, this diameter was increased to 0.038 cm (0.015 in.) to reduce fabrication costs.

Once the airfoil contours are defined, a surface pressure distribution is calculated by means of either a computer program which calculates the two-dimensional, irrotational flow of a perfect, compressible, inviscid gas through an entirely subsonic airfoil channel, or a program which applies a transient technique of the conservation laws to small control volumes in the flow field for a transonic airfoil channel.

The transient technique permits a mixed flow solution without advance knowledge of the interface regions of subsonic and supersonic flows. The resulting pressure distributions are then appraised on the basis of accelerating suction surface velocity while the suction surface diffusion is minimized in the uncovered regions where the airfoil is susceptible to boundary layer separation. The channel geometry is also reviewed to ensure that a minimum amount of channel diffusion exists near the airfoil leading edge. This is to prevent the occurrence of a pressure side separation and reattachment with a subsequent increase in profile loss.

Surface boundary layer behavior of each airfoil defining section is also examined for possible separation through a program which uses a finite difference procedure to compute the laminar, transitional, and turbulent development of the airfoil surface boundary layer. This problem also calculates momentum and displacement thicknesses for the suction and pressure sides at the trailing edge which are used in a control volume wake mixing computation for determining the profile loss.

The results of the airfoil design procedure, i.e., the airfoil contours, pressure and velocity distributions and channel area ratios are presented in Figures 7 through 86. A summary of the defining section airfoil geometry is given in Table II, and the associated airfoil nondimensional coordinates in Table III. The results of the total pressure loss calculations for the mean sections over a range in Reynolds numbers are shown in Figure 87. This figure indicates that the selection of airfoil chord to give Reynolds numbers between 3 and 4.0 x 10^5 does result in minimum losses in most airfoil rows.

EXIT GUIDE VANE DESIGN

The establishment of an equal work distribution in the turbine stages results in the need for a highly loaded, high turning exit guide vane design. The exit guide vane was therefore designed using fan exit guide vane technology based on stator data from the NASA high tip speed, low tip speed and 1800 fps tip speed fan programs discussed in References 7, 8 and 9 respectively.

The requirements for the exit guide vanes, as determined from the streamline analysis, are shown in Figure 88 which give the inlet angle and inlet Mach number distributions. The EGV airfoil sections were chosen to be 65 series thickness distributions in circular arc meanlines (656A) and were designed on conical surfaces approximating a stream surface of revolution. These sections were chosen to best accommodate the anticipated range of Mach numbers and Reynolds numbers. The resulting EGV design has 28 vanes an an 8.636 cm (3.4 in.) true chord which is constant spanwise. The aspect ratio is 1.6 based on average blade length and an axially projected chord at the hub. Maximum thickness to chord ratio varies linearly with radius from 0.06 at the hub to 0.10 at the tip. The convergence of the flowpath is the result of iterations aimed at controlling root loadings and wall diffusion rates while maintaining levels of solidity, Mach number and aspect ratio within P&WA experience. The incidence angles were set to correspond with past experience and to provide some additional choke margin for off-design requirements while the EGV deviation angles were determined by applying Carters Rule plus an adjustment based on P&WA experience. The EGV incidence and diffusion factors are shown in Figure 89 as a function of span and the resulting airfoil contours are shown in Figure 90 for 5 radial locations. Non-dimensional coordinates for the EGV are given in Table IV. EGV surface pressure distributions were also computed by means of a compressible potential flow solution program per T. Katsanis (Reference 10).

These results are shown in Figures 91 through 95, and indicate satisfactory flow at all sections.

The EGV losses were calculated by using a correlation of loss parameter versus diffusion factor and percent span. The correlation as reported in Reference 11 was modified slightly to represent more closely the stator data from other NASA fan programs. Because the Reynolds number at the design conditions is lower than those normally encountered in compressor designs, the loss calculation was adjusted assuming loss proportional to $Re^{-.2}$ and using $Re = 10^6$ for the parameter data. The resultant loss is shown in the spanwise curve of Figure 89, the average loss being 2.1% $\Delta P_T/P_T$.

EFFICIENCY ESTIMATION

The result of the Meanline Design and Streamline Studies was the establishment of the turbine flowpath, work distribution and velocity diagrams. The estimated efficiency for this turbine based on those diagrams is 88.1% for airfoils with 0.010" trailing edge thickness, exclusive of the EGV loss. Increasing the airfoil trailing edge diameter to 0.015" reduces this efficiency to 87.9%. Application of the minimum profile loss assumed for the transitional boundary layer design procedure will result in an improvement of 1.4% to 89.3%. The exit guide vane loss of 2.1% would then give an overall turbine efficiency with EGV of 88.6%.

Airfoil Vibration Analysis

The airfoils defined in this report have been analyzed for vibratory resonance and airfoil flutter. The vibratory analysis idealizes one blade as vibrating in a complete rotor stage. The turbine disk is modeled via thin disk and ring equations. The shroud is modeled with equations as a continuous ring. The root and disk dead rim flexibilities are entered as connector springs between disk and blade. The disk and shroud are then assumed to undergo a sinusoidal vibratory mode with an integral number of waves around the rim and the system natural frequency is then found.

The results of this analysis are shown in the resonance diagrams of Figures 96 through 99 for each rotor. The first stage blade is shown to be free of all critical resonances within the anticipated steady-state operating range of the turbine. (±25% of design speed). Rotors 2 through 4 do have nozzle passing frequency resonances within the operating range. These resonances are first and second bending, and first torsional modes of vibration. The magnitude of the vibratory stress levels are not known due to the lack of engine experience with airfoils of such high thickness to chord ratios, and high camber which make for a stiff airfoil. However, engine experience on conventional LPT airfoil designs has resulted in vane passing vibratory stress levels of 7720 kg/m^2 (11.0 ksi) which is half of the vibratory stress capability as shown on the Goodman Diagram of Figure 100. Mechanical damping and the low pressure levels of a cold flow rig versus an engine will also minimize the excitation energy. Therefore no vibratory resonance problems are anticipated for these airfoils.

REFERENCES

Dorman, T. E, Welna, H., and Lindlauf, R. W, "The Application of Controlled Vortex Aerodynamics to Advanced Axial Flow Turbines," Trans. ASME, Journal Engineering for Power, July 1968, pp 245.

Schlichting, H. and Das, A. "Recent Research on Cascade-Flow Problems," Journal of Basic Engineering, Trans. ASME, Series D, pp 221-228, 1966.

Hebbel, H., "The Influence of the Mach Number and Reynolds Number on the Aerodynamic Coefficients of Turbine Cascades at Various Turbulence Intensities of the Flow (Uber den Einfluss der Machzahl und der Reynoldszal auf die Aerodynamischen Deiwerte von Turbineneschaufelgittern bie verschiedener Turbulenz der Stromung)," Forschung im Ingenieurwesen, vol. 30, Nr. 3 pp 65-77, 1964.

Gersten, K., "The Influence of the Reynolds Number on Flow Losses in Two-Dimensional Cascades (Der Einfluss derReynoldszahl auf die Stromung in ebenen Schaufelgittern)," Abhandungen der Braunschweigischen Wissenschaftlichen Gesellschaft, vol. 11, pp 5-19, 1959.

Welna, H. Dahlberg, D., Heiser, W. H., "Investigation of a Highly Loaded Two-Stage Fan Drive Turbine," AFAPL-TR-69-92, vol. VI, Final Report.

Aerodynamic Design of Axial Flow Compressor, NASA SP-36, 1965.

Sulam, D. H., Keenan, M. J., and Flynn J. T., Single-Stage Evaluation of Highly-Loaded High-Mach Number Compressor Stages, II - Data and Performance Multiple-Circular-Arc Rotor, NASA CR-72694, PWA-3772, 1970.

Harley, K. G., Odegard, P. A., and Burdsall, E. A., High-Loading Low-Speed Fan Study, IV - Data and Performance with Redesign Stator and Including a Rotor Tip Casing Treatment, NASA CR-120866, PWA 4326, 1972.

Morris, A. L., and Sulam, D. H., High-Loading, 1800 ft/sec Tip Speed Transonic Compressor Fan Stage, II - Final Report, NASA CR-120991, PWA-4463, 1972.

Katsanis, T., Fortran Program for Calculating Transonic Velocities on a Blade-to-Blade Stream Surface of a Turbomachine, NASA TN D-5427, 1969.

Monsarrat, N. T., Keenan, M. J., and Tramn, P. C., Design Report, Single Stage Evaluation of Highly-Loaded, High-Mach-Number Compressor Stages, NASA CR-72562, PWA 3546, 1969.

SYMBOLS AND DEFINITIONS

A	area (cm^2, $in.^2$)
B	axial chord (cm, in.)
C_L	compressible lift coefficient
C_x	axial velocity (m/sec, ft/sec)
D	diameter (cm, in.)
D_f	diffusion factor for incompressible 2 dimensional cascade
ΔH	turbine total work (joules, BTU)
Δh	turbine specific work (joules/kg, BTU/lbm)
L	blade or vane height at airfoil throat (cm, in.)
LED	leading edge diameter (cm, in.)
M	Mach number
n	number of stages
N	turbine rotor speed (rev/min)
P	static pressure (newtons/cm^2, psia)
P_T	total pressure (newtons/cm^2, psia)
R_N	Reynolds number
S	suction surface length (cm, in.)
TED	trailing edge diameter (cm, in.)
TER	trailing edge radius (cm, in.)
T_T	total temperature (°K, °R)
U	wheel speed (m/sec, ft/sec)
V	air velocity (m/sec, ft/sec)
W	turbine airflow (kg/sec, lbm/sec)

τ	airfoil pitch (cm, in.)
λ	airfoil throat (cm, in.)
ρ	density (kg/m^3, lbm/ft^3)
σ	airfoil solidity, ratio of chord to spacing
α	absolute air angle, degrees
β	relative air angle, degrees
θ_r	ratio of air temperature to standard sea level temperature
θ	turning through an airfoil
ϕ^2	ratio of the square of the airfoil absolute exit velocity to the ideal exit velocity
μ	viscosity (kg/sec-m, lbm/sec ft)

Subscripts

m	mean
o	vane inlet
1	vane exit
1.5	blade inlet
2	blade exit
V	vane
B	blade
A	absolute reference
R	relative reference

Superscripts

*	metal angles

SYMBOLS AND DEFINITIONS (Cont'd)

Definitions

α gaging	$= \arcsin \lambda/\tau$
D_f	$= \dfrac{1 - \cos\beta_1}{\cos\beta_2} + \dfrac{\cos\beta_1 \; (\tan\beta_1 + \tan\beta_2)}{2\sigma}$
R_N	$= \dfrac{\rho V S}{\mu}$
Reaction	$= (P_1 - P_2)/(P_o - P_2)$
Uncovered Turning	= turning angle depicted by Γ in Figure 6

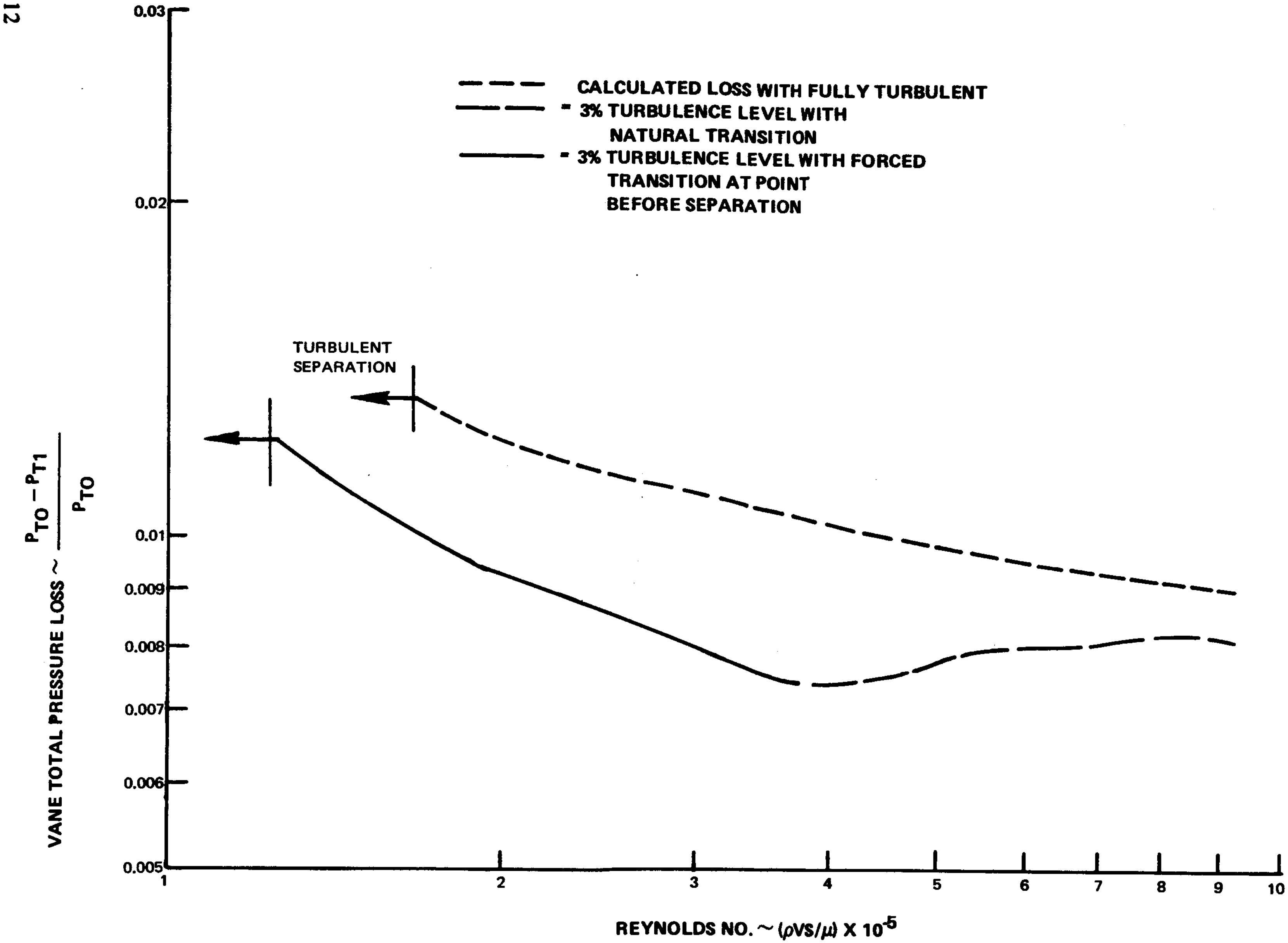

FIGURE 1 CASCADE PROFILE LOSS VS REYNOLDS NUMBER

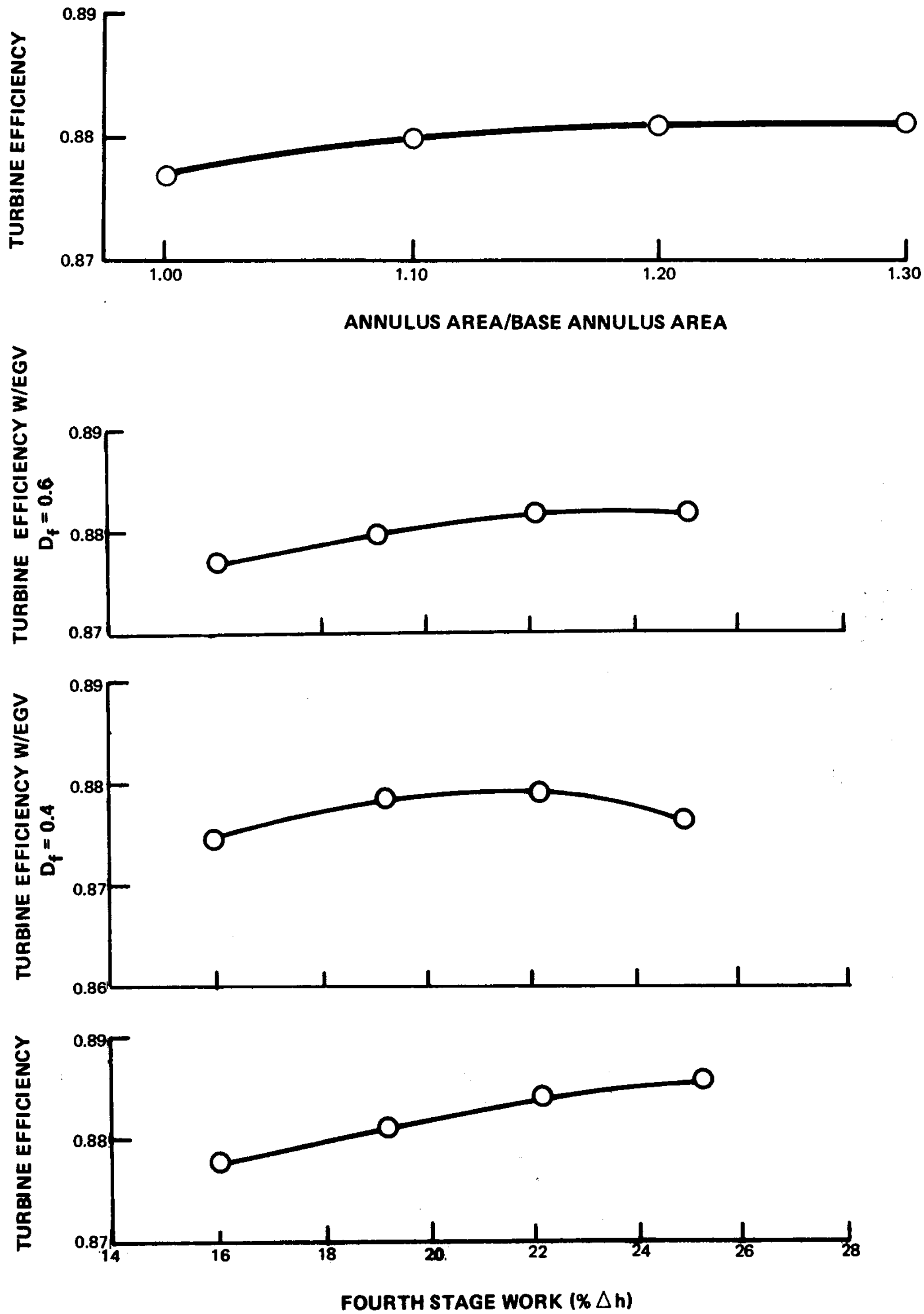

FIGURE 2 TURBINE EFFICIENCY VS. FOURTH STAGE WORK AND EXIT ANNULUS AREA

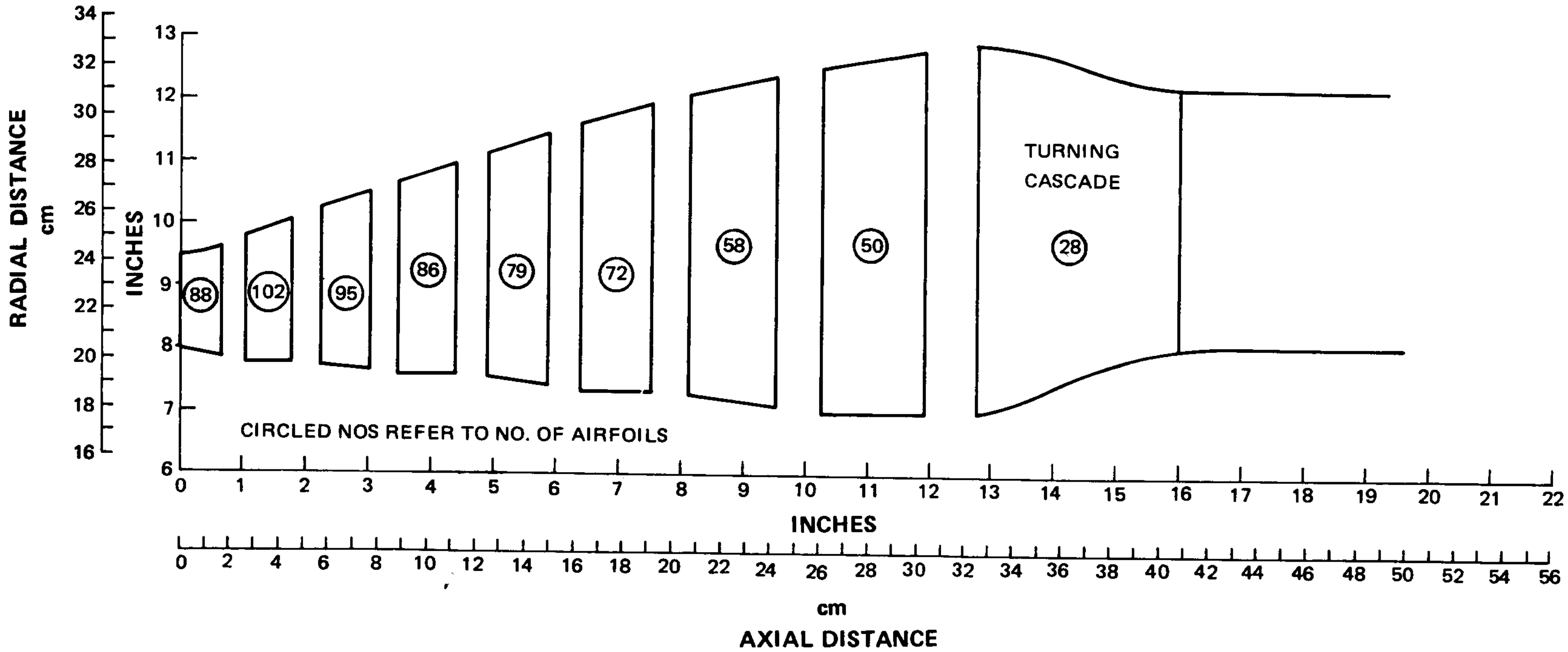

FIGURE 3 TURBINE FLOWPATH

25% SPAN

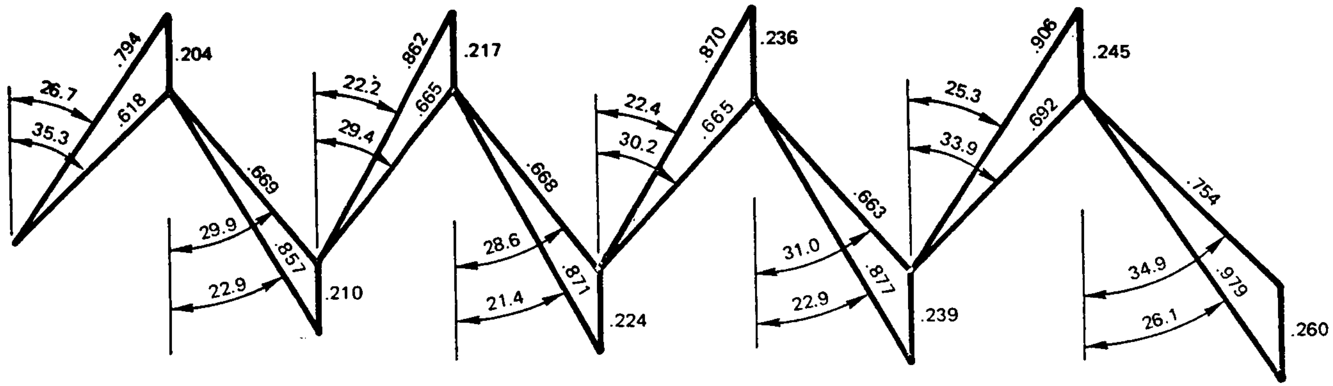

NUMBERS SHOWN ARE ANGLES IN DEGREES AND MACH NUMBERS AT THE AIRFOIL EXIT

ROOT

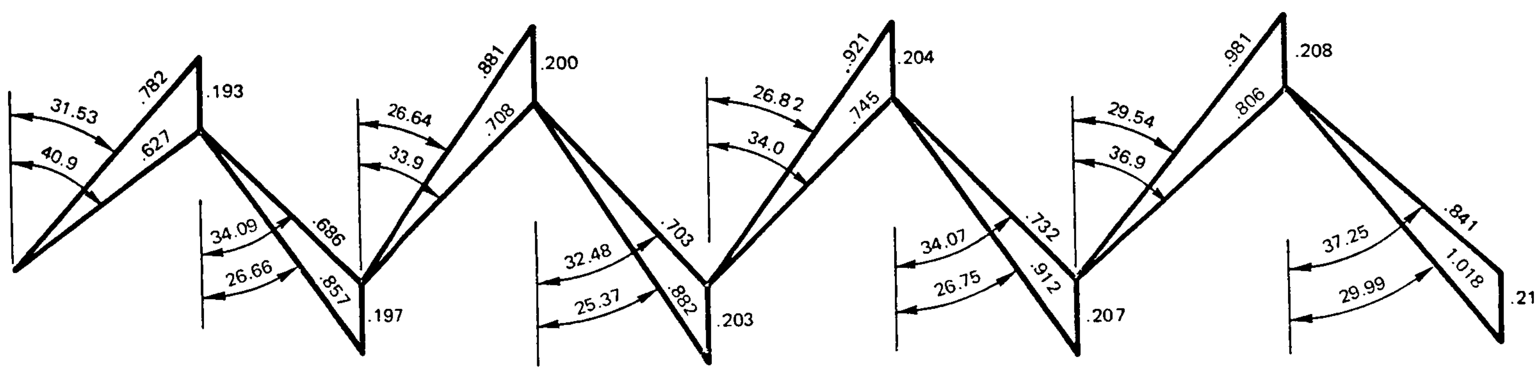

FIGURE 4 VELOCITY DIAGRAMS

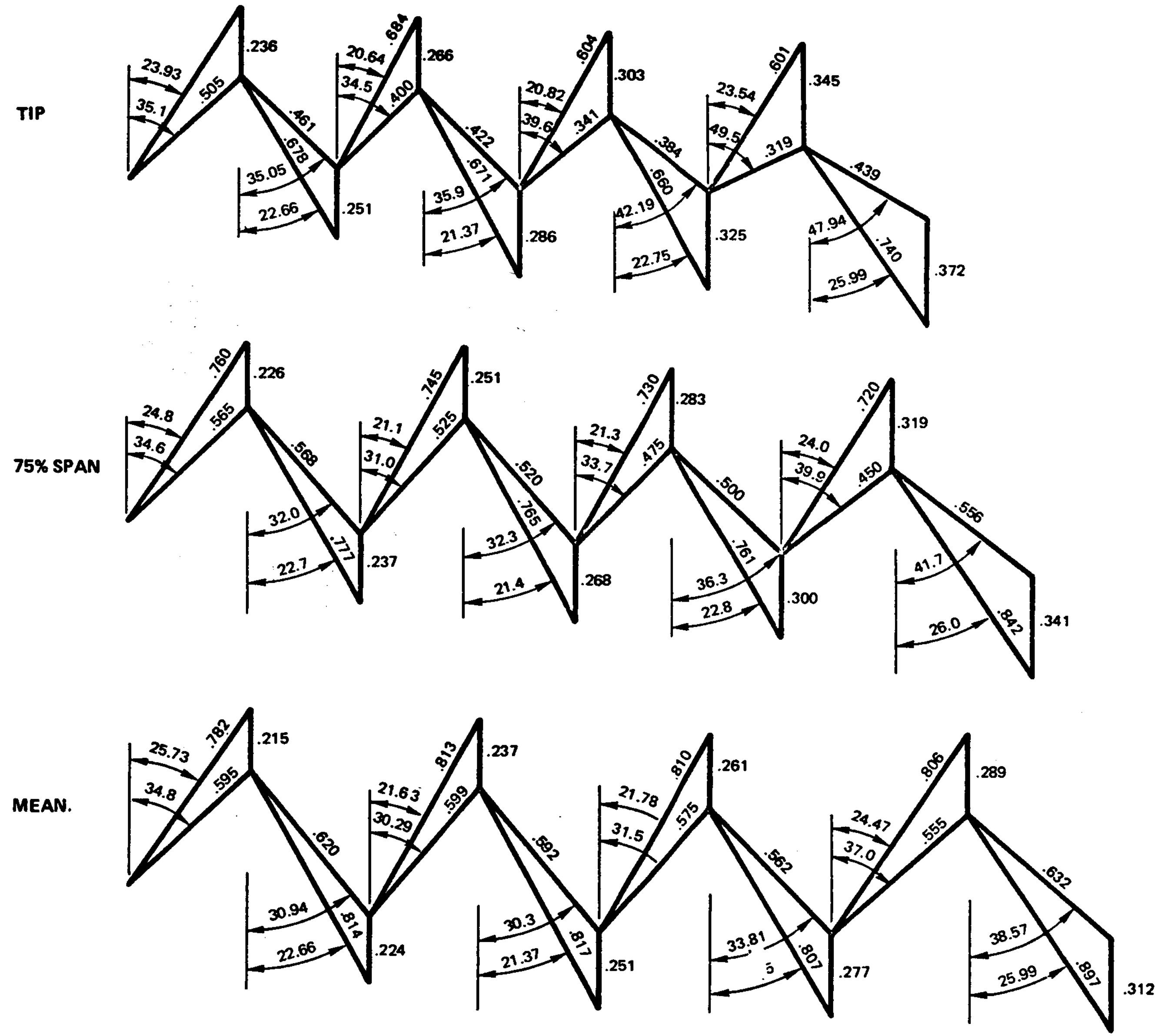

NUMBERS SHOWN ARE ANGLES IN DEGREES AND MACH NUMBERS AT THE AIRFOIL EXIT

FIGURE 5 VELOCITY DIAGRAMS

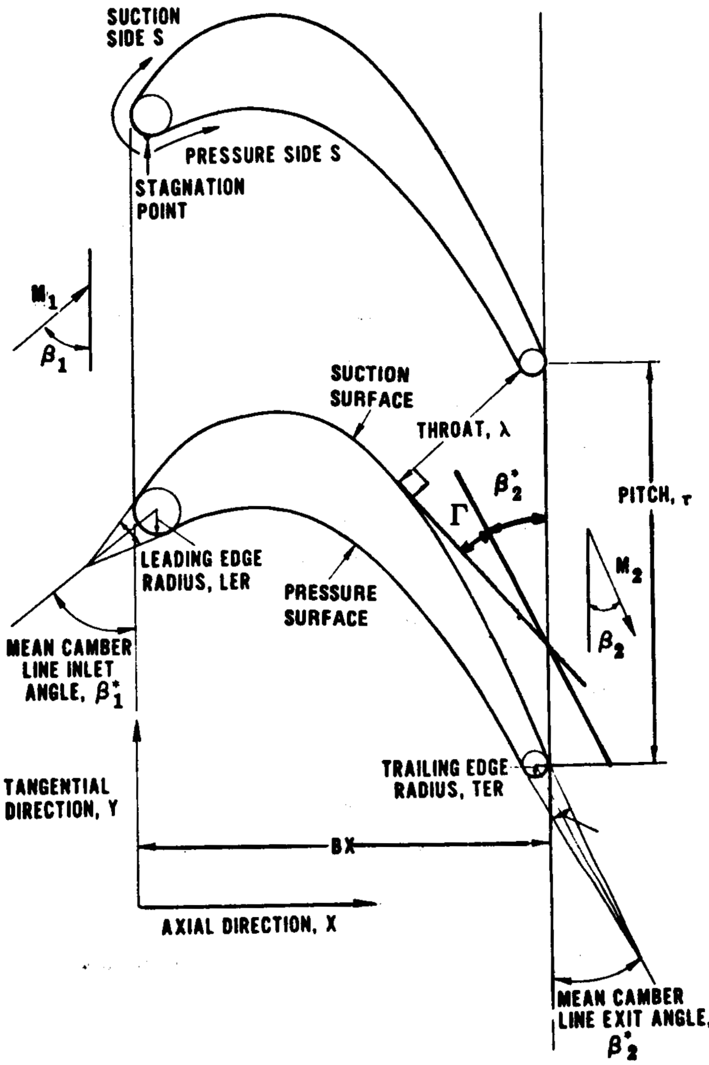

NOMENCLATURE IN FIGURE IS FOR A BLADE. FOR A VANE REPLACE "β" to "α"

FIGURE 6 AIRFOIL NOMENCLATURE

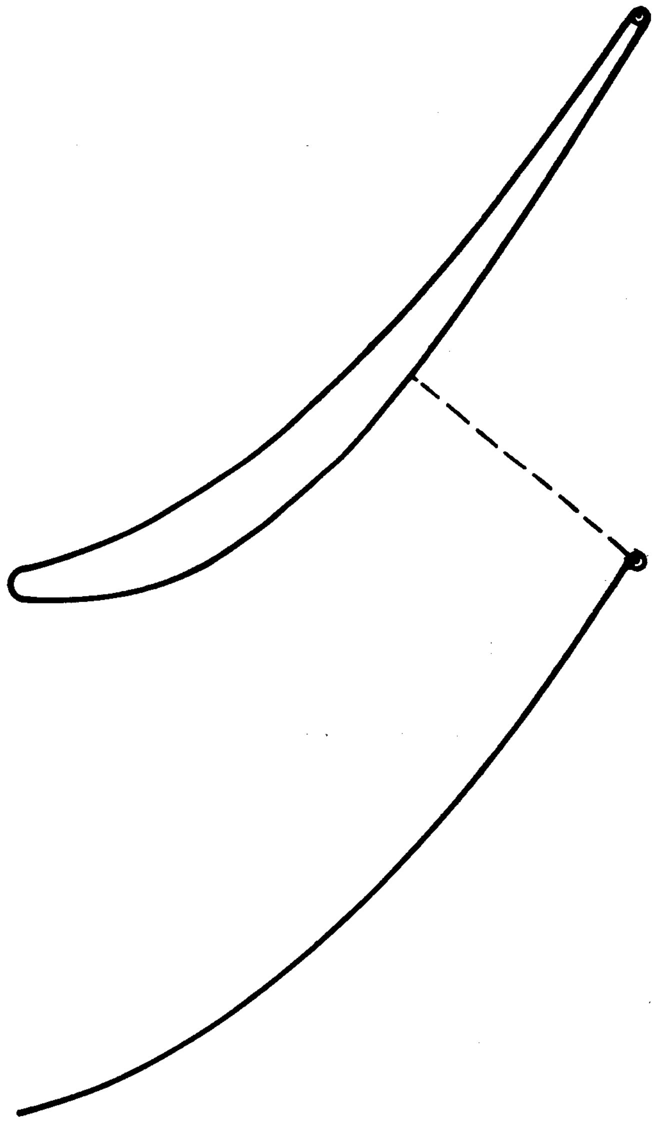

FIG. 7 FIRST STAGE VANE ROOT 5.0 SCALE

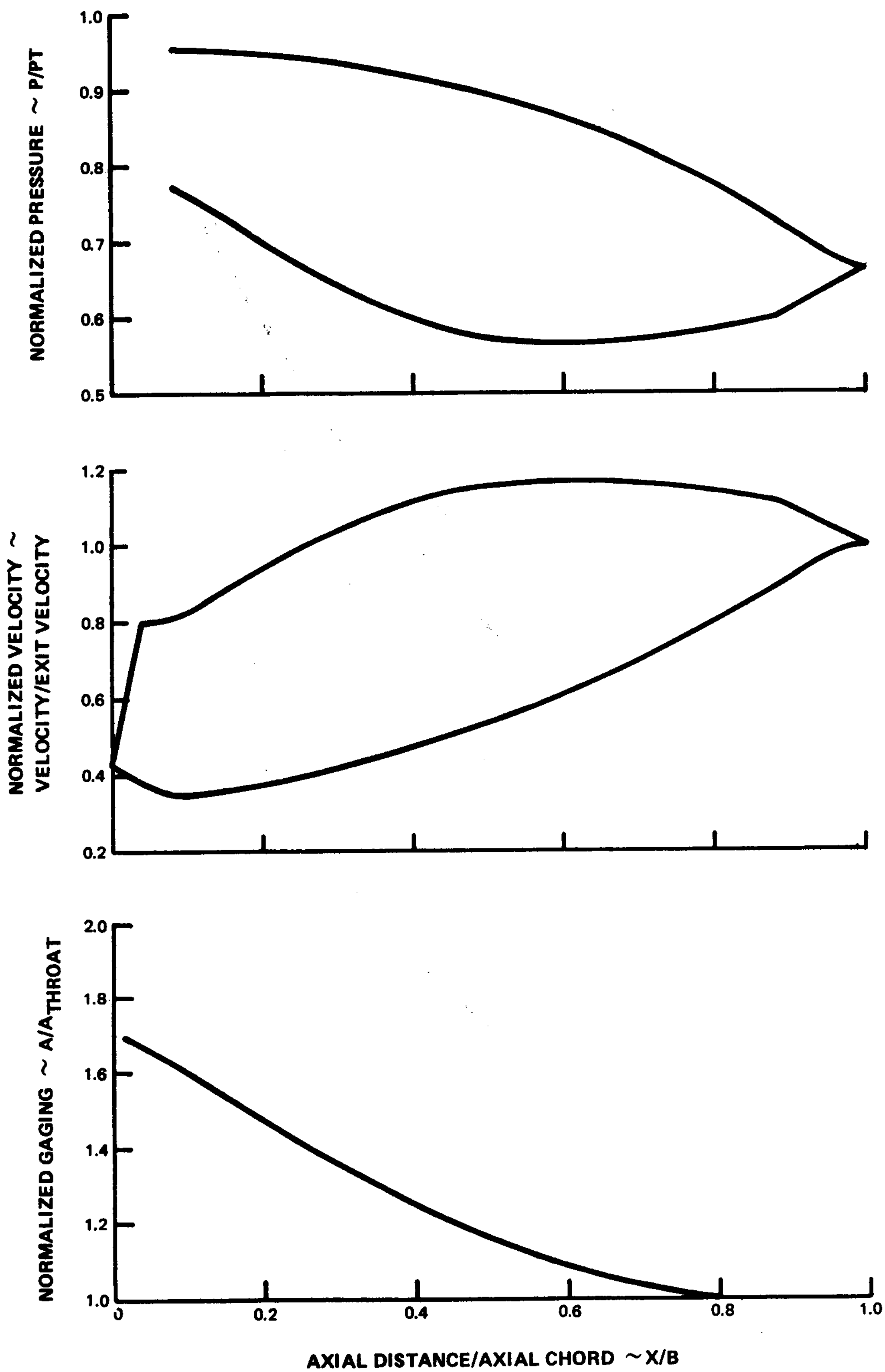

FIG. 8 FIRST STAGE VANE ROOT NORMALIZED PRESSURE VELOCITY AND GAGING DIAGRAMS

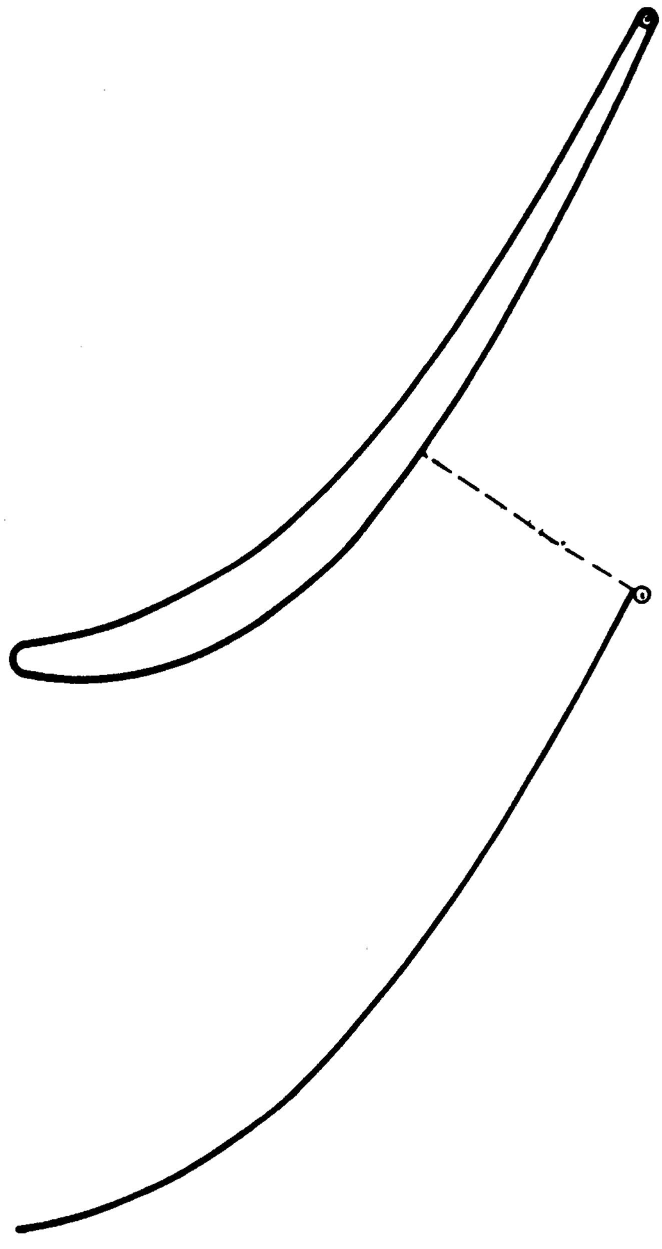

FIG. 9 FIRST STAGE VANE QUARTER ROOT 5.0 SCALE

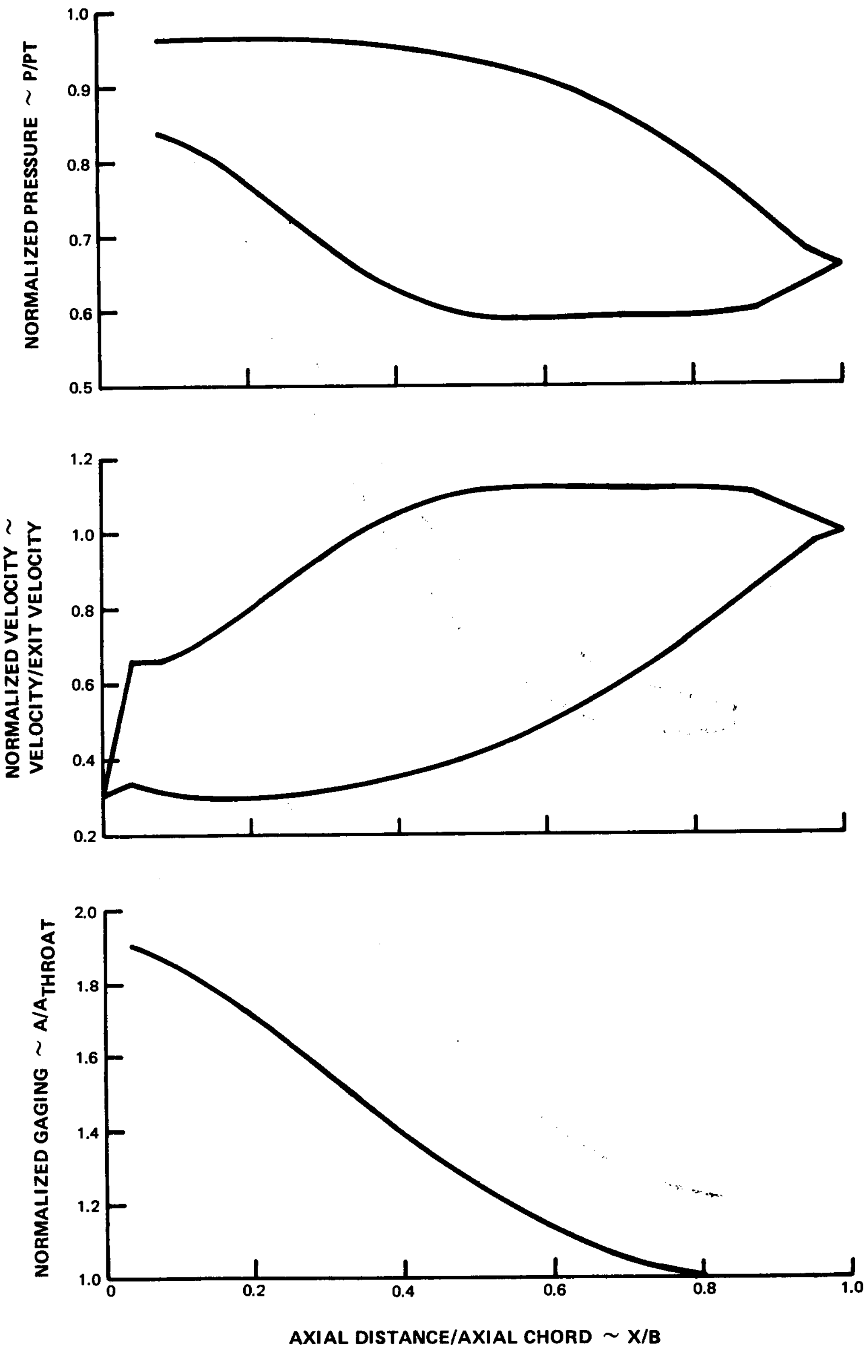

FIG. 10 FIRST STAGE VANE QUARTER ROOT NORMALIZED PRESSURE VELOCITY AND GAGING DIAGRAMS

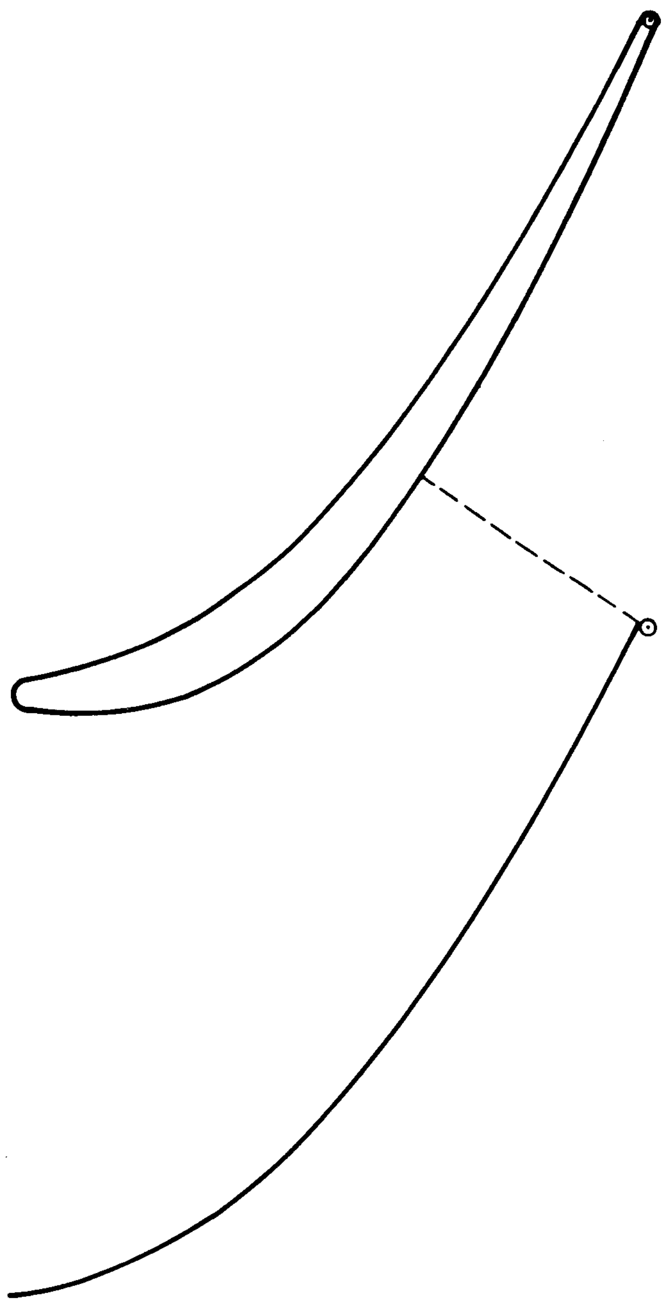

FIG. 11 FIRST STAGE VANE MEAN 5.0 SCALE

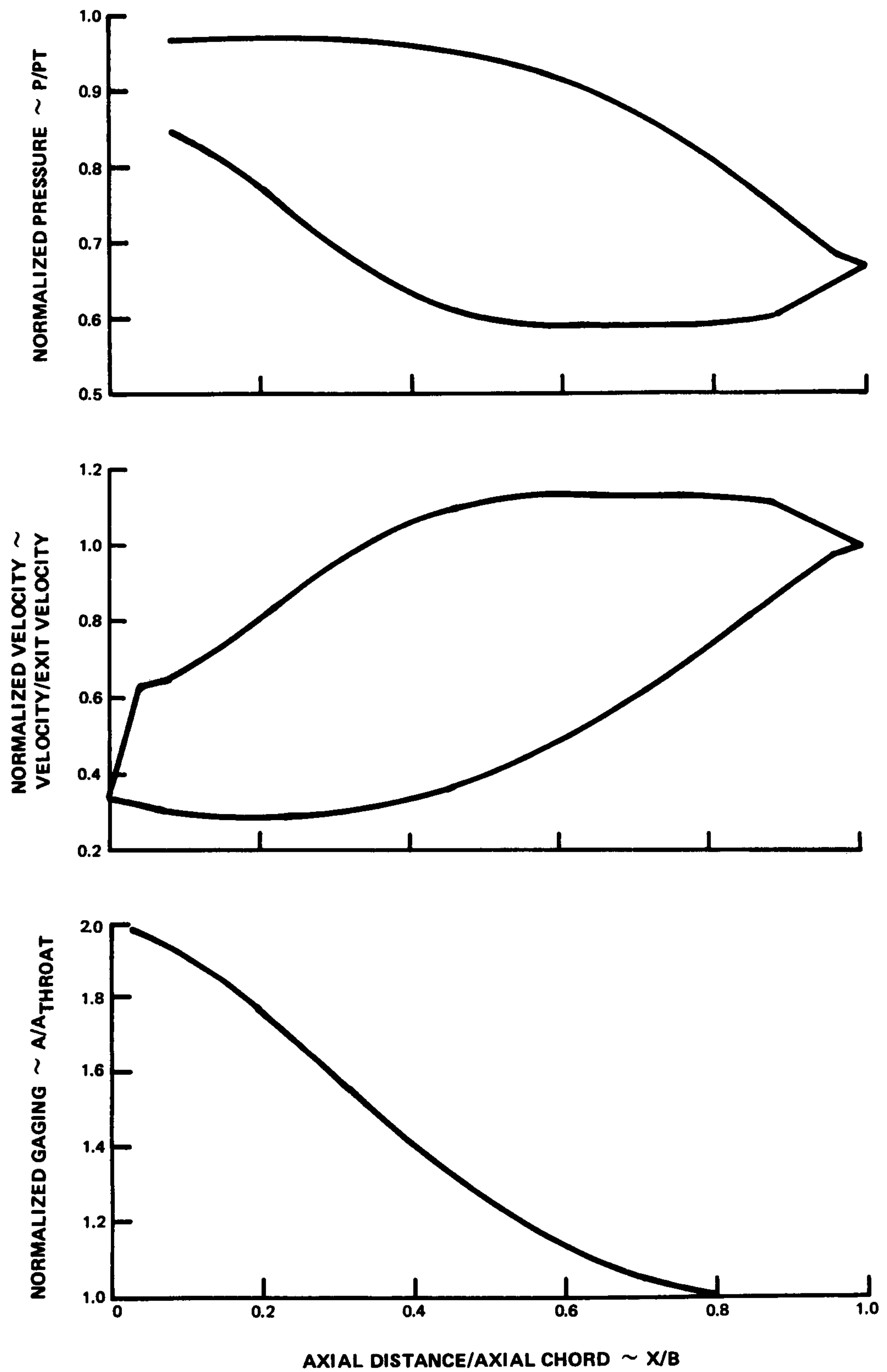

FIG. 12 FIRST STAGE VANE MEAN NORMALIZED PRESSURE VELOCITY AND GAGING DIAGRAMS

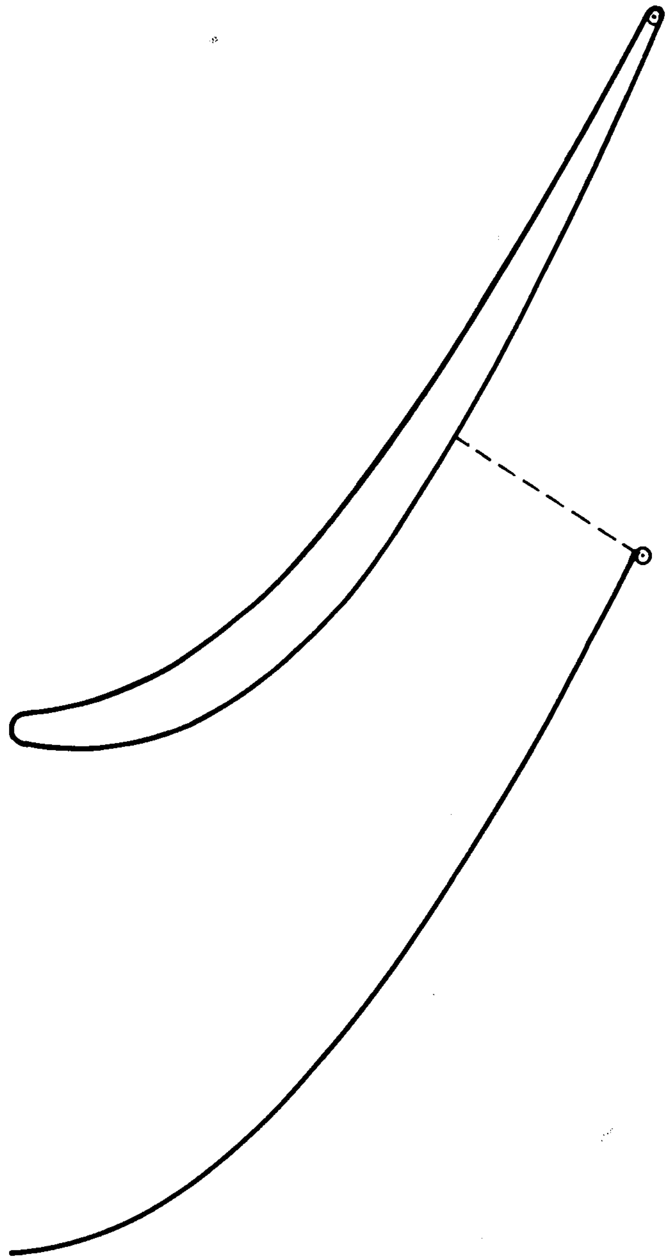

FIG. 13 FIRST STAGE VANE QUARTER TIP 5.0 SCALE

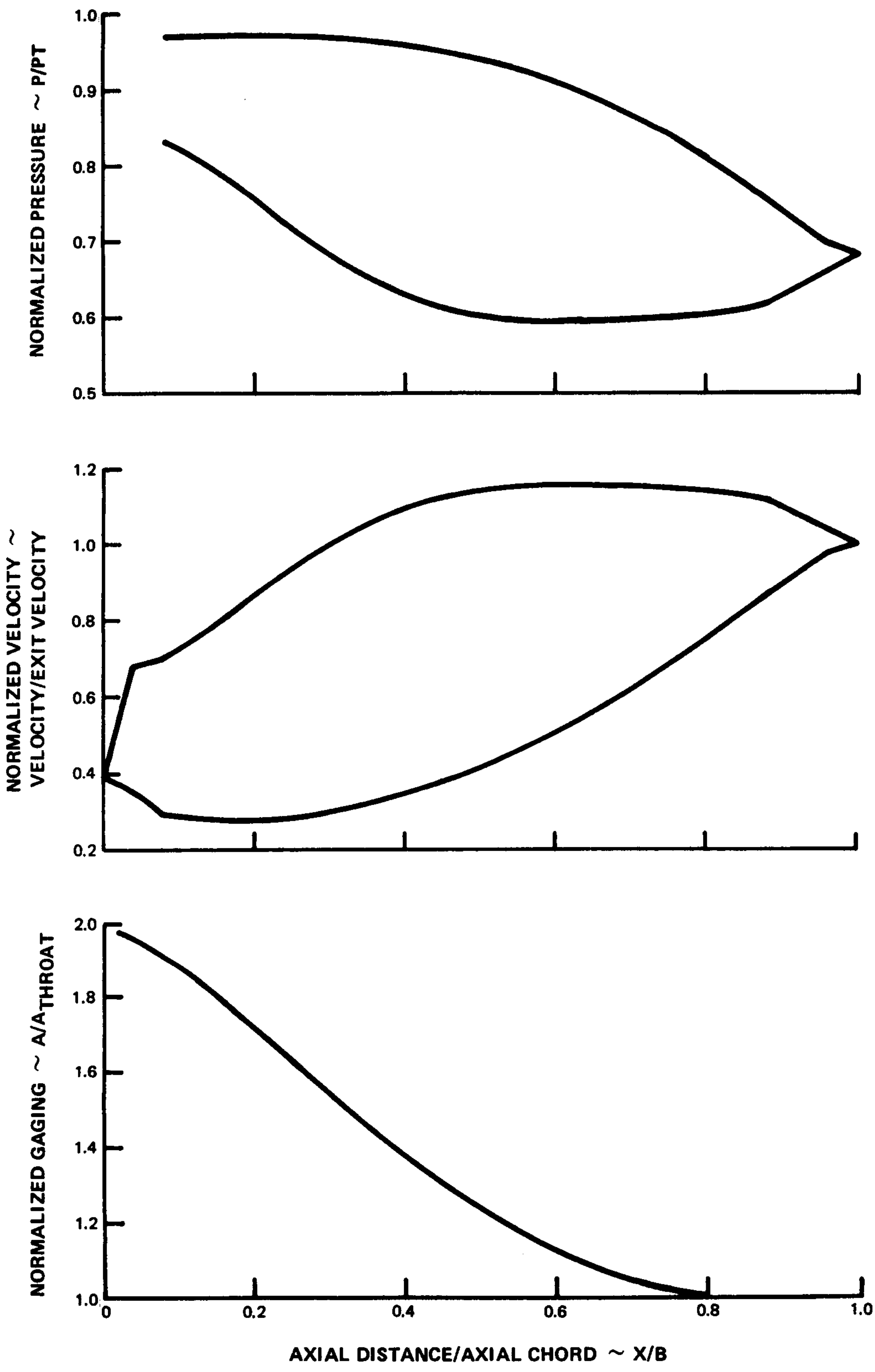

FIG. 14 FIRST STAGE VANE QUARTER TIP NORMALIZED PRESSURE VELOCITY AND GAGING DIAGRAMS

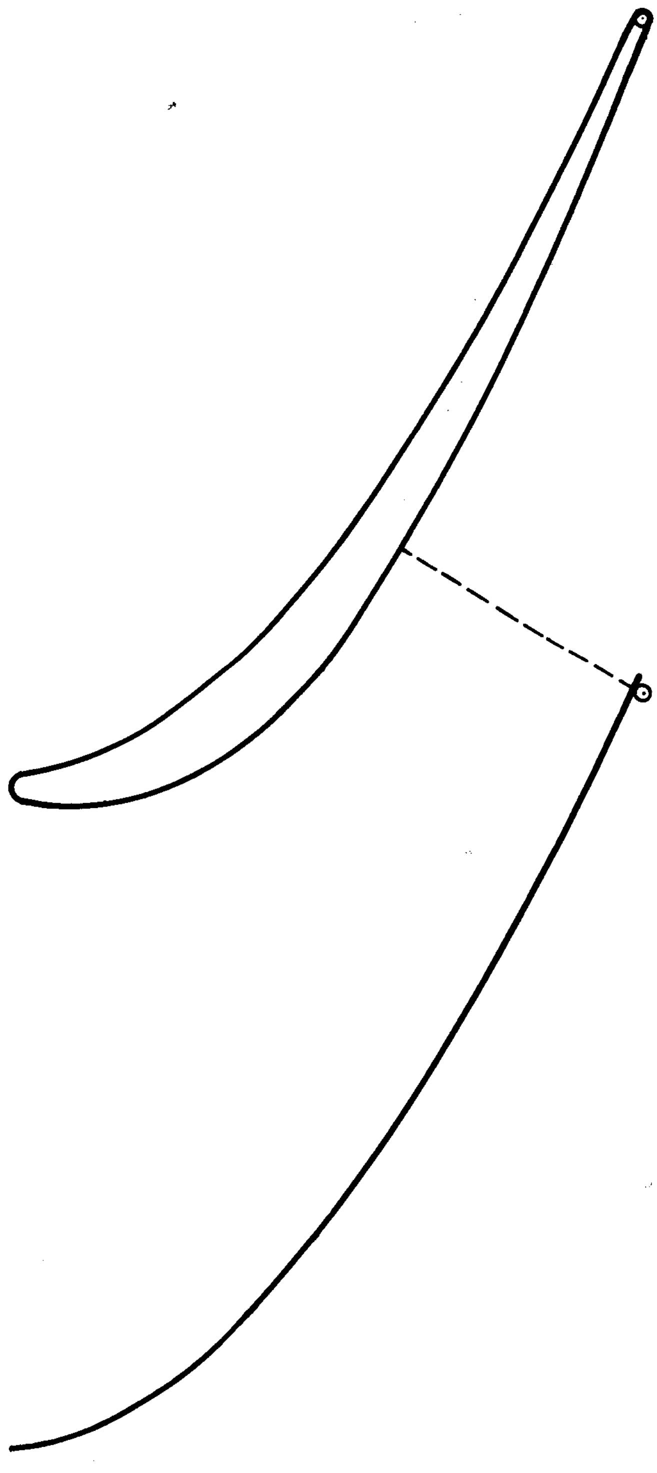

FIG. 15 FIRST STAGE VANE TIP 5.0 SCALE

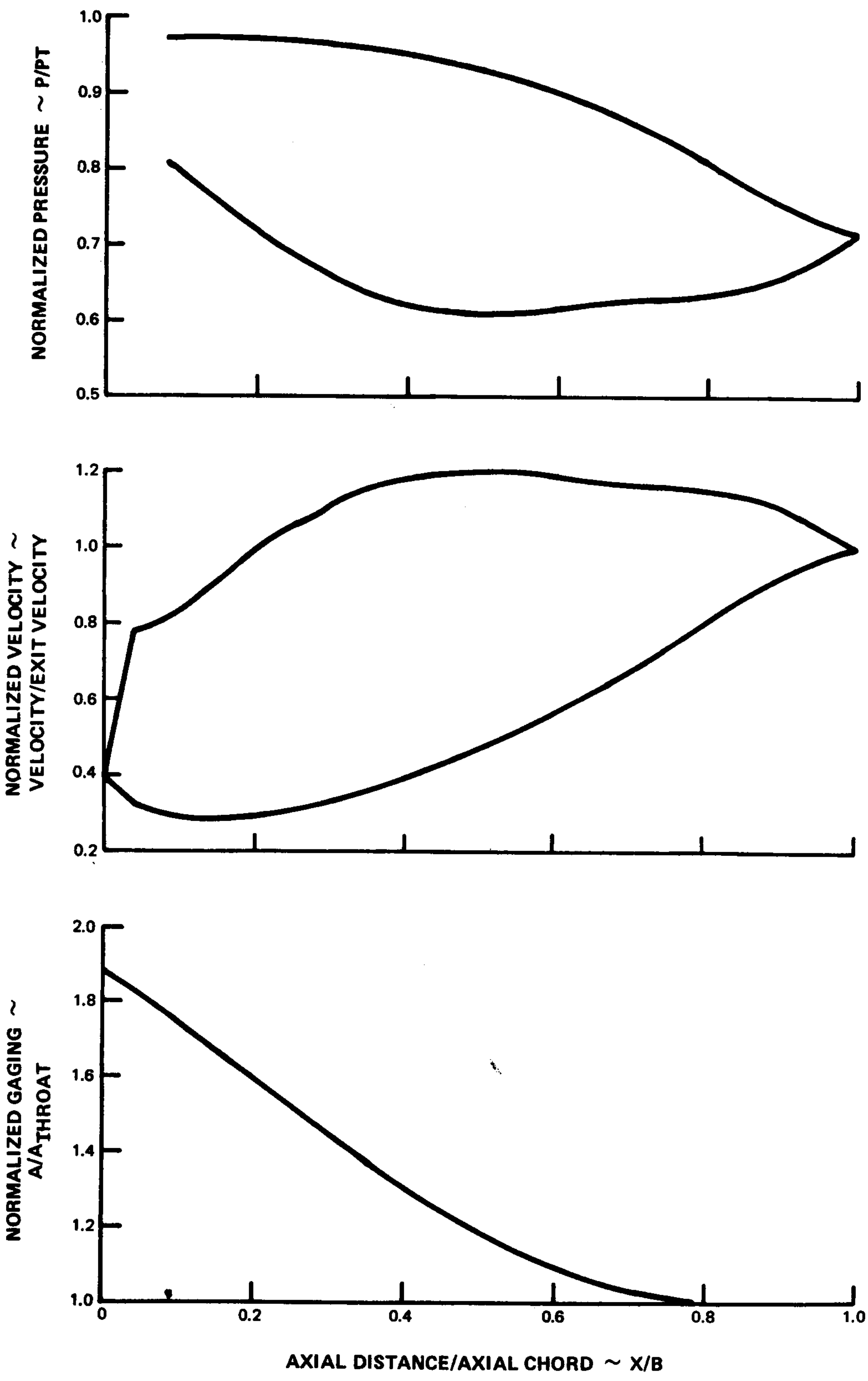

FIG. 16 FIRST STAGE VANE TIP NORMALIZED PRESSURE VELOCITY AND GAGING DIAGRAMS

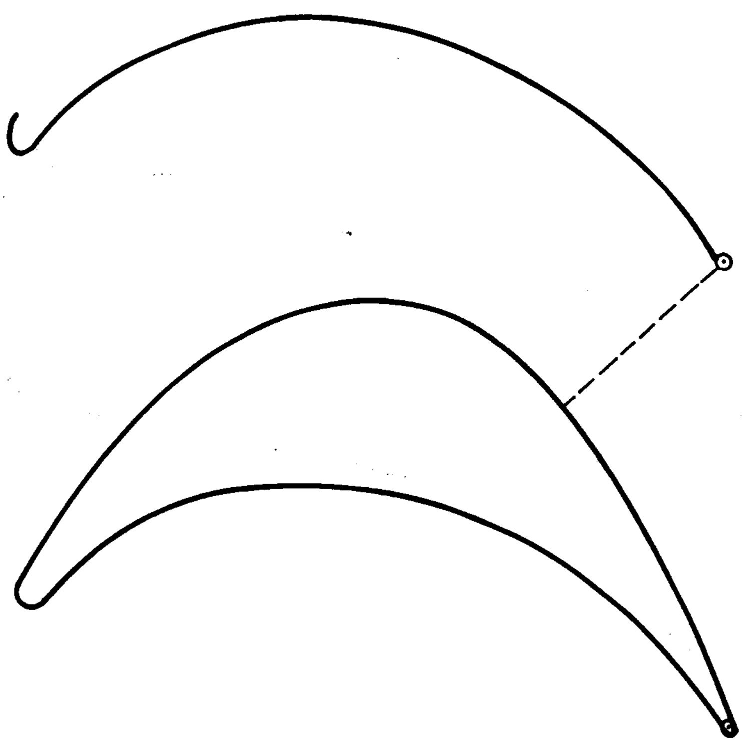

FIG. 17 FIRST STAGE BLADE ROOT 5.0 SCALE

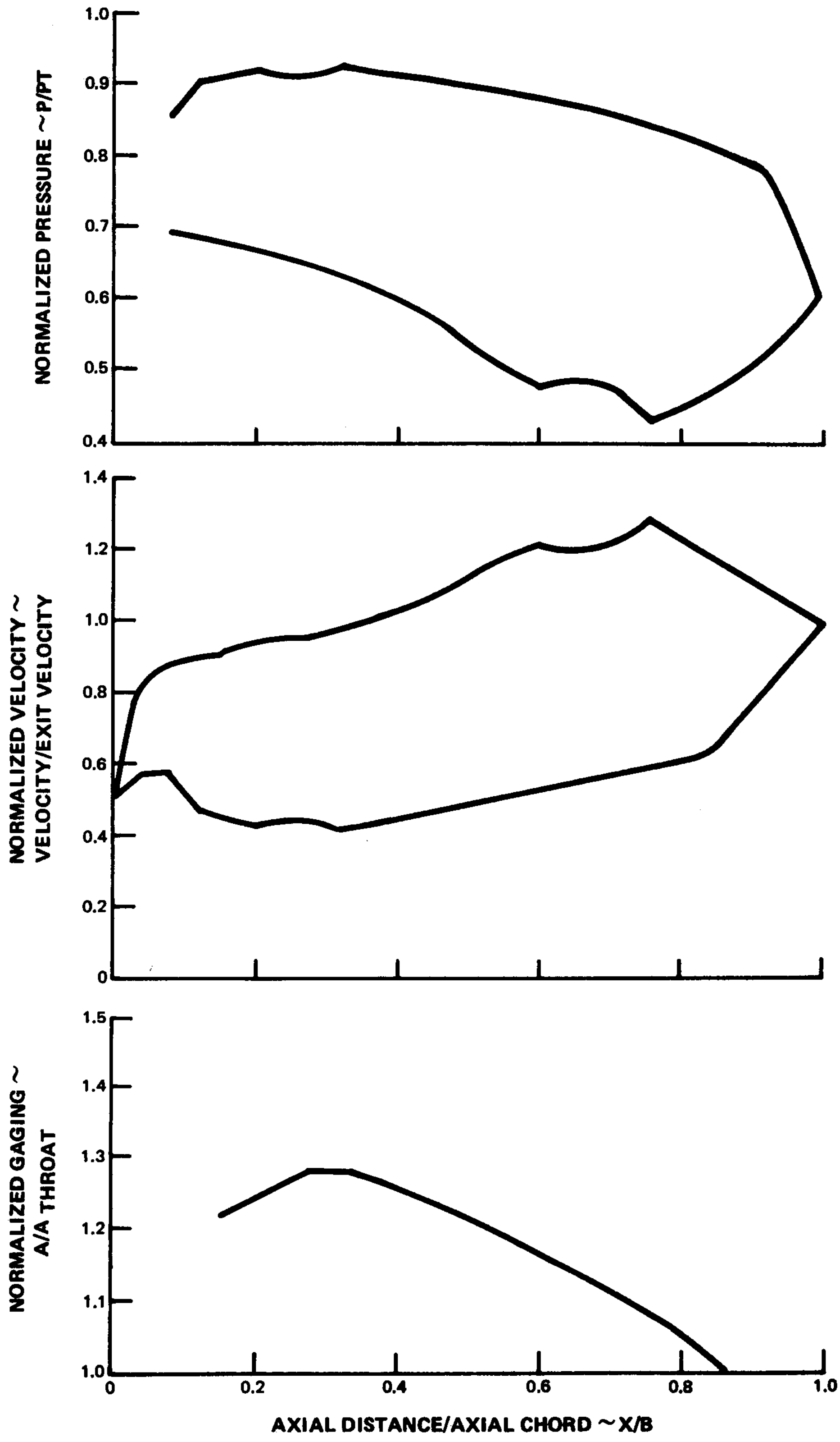

FIG. 18 FIRST STAGE BLADE ROOT NORMALIZED PRESSURE VELOCITY AND GAGING DIAGRAMS

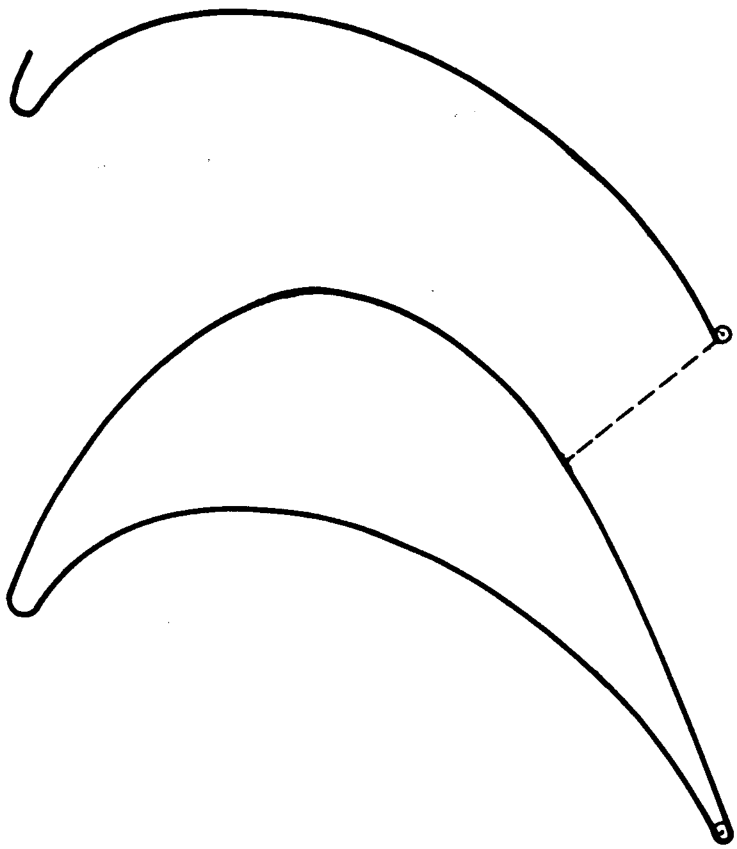

FIG. 19 FIRST STAGE BLADE QUARTER ROOT 5.0 SCALE

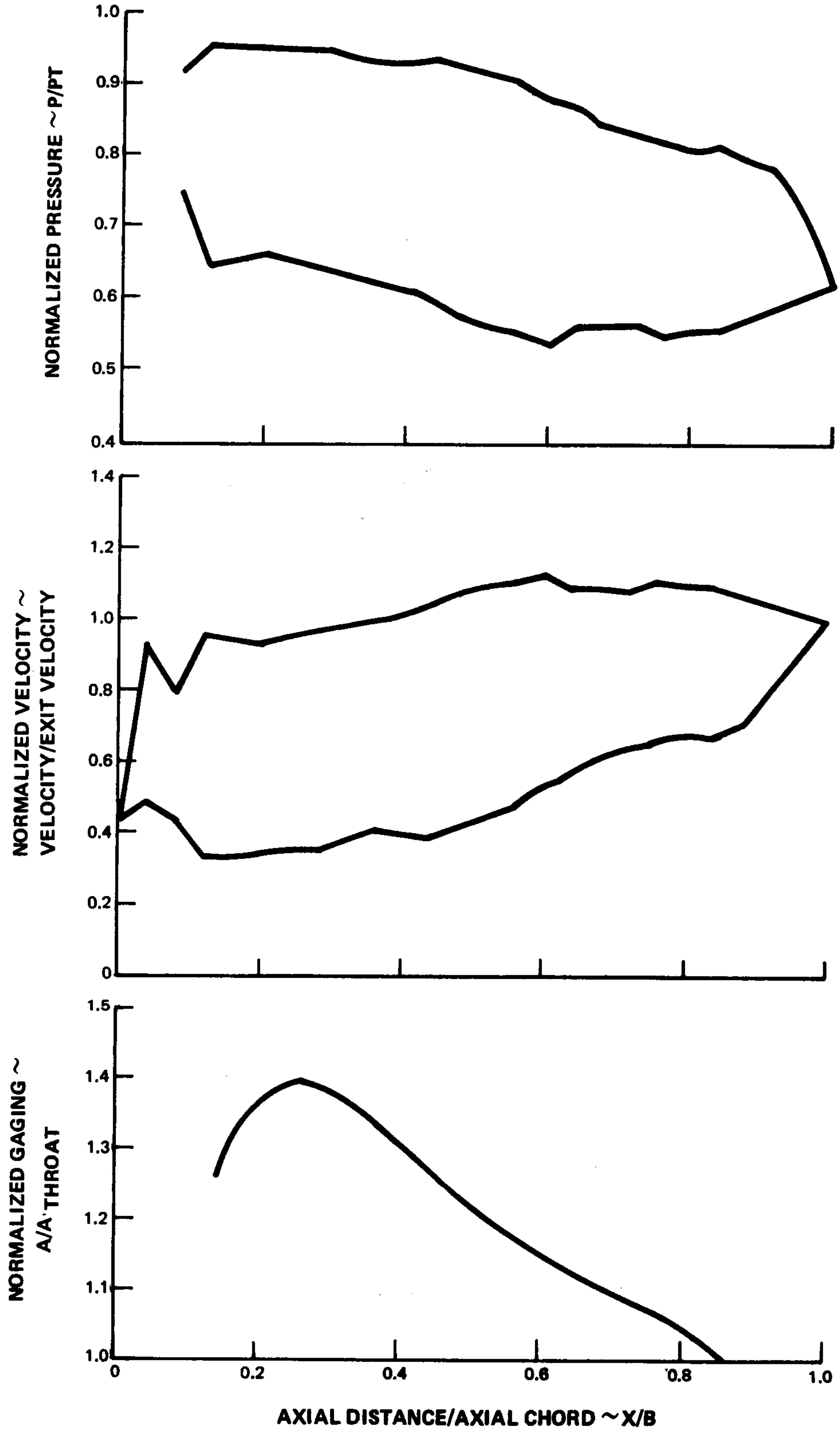

FIG. 20 FIRST STAGE BLADE QUARTER ROOT NORMALIZED PRESSURE VELOCITY AND GAGING DIAGRAMS

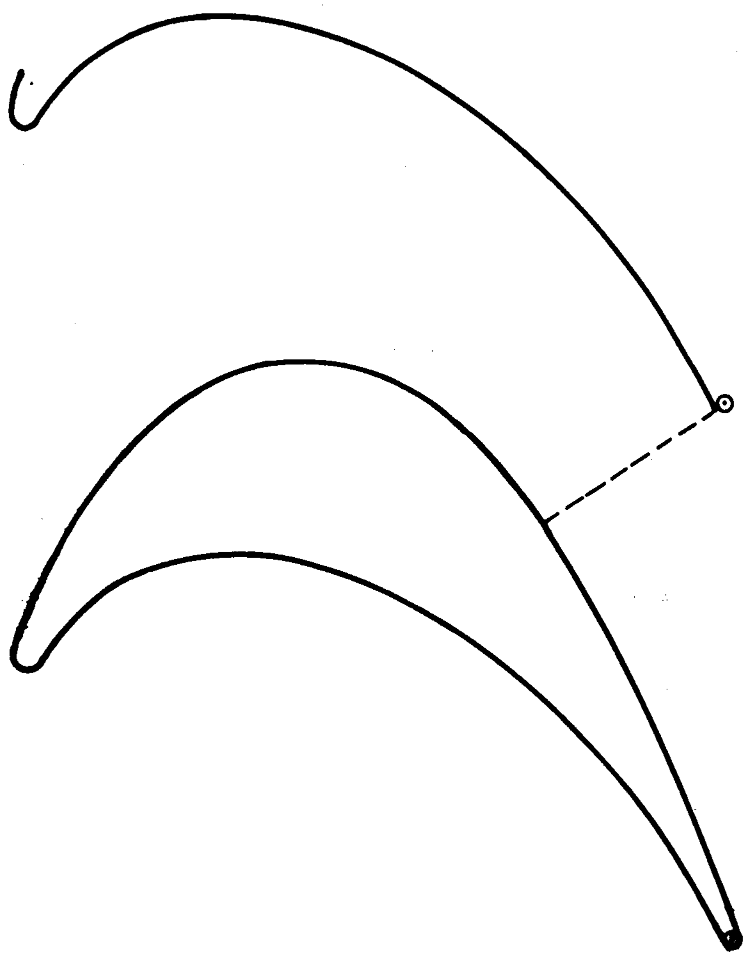

FIG. 21 FIRST STAGE BLADE MEAN 5.0 SCALE

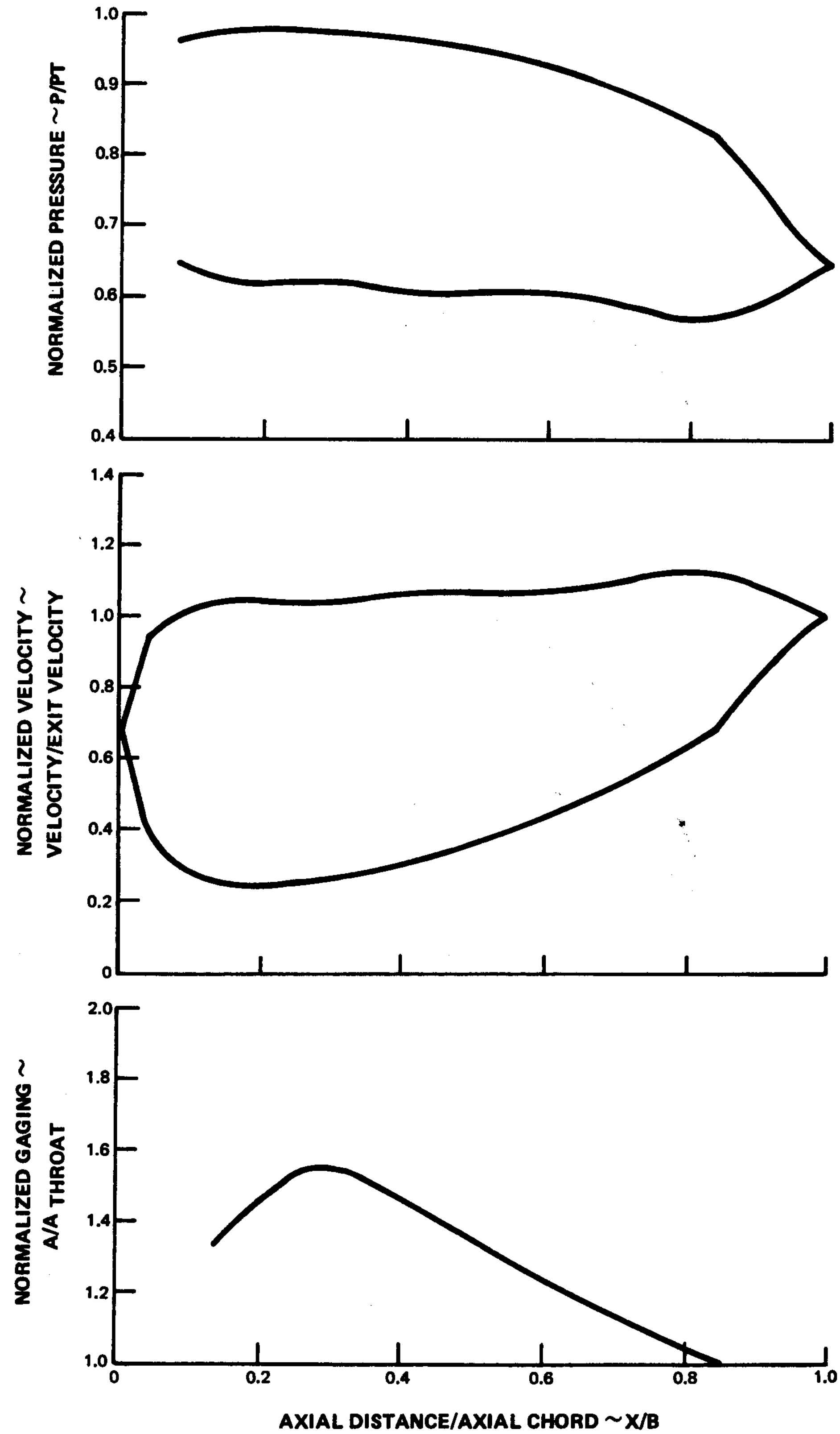

FIG. 22 FIRST STAGE BLADE MEAN NORMALIZED PRESSURE VELOCITY AND GAGING DIAGRAMS

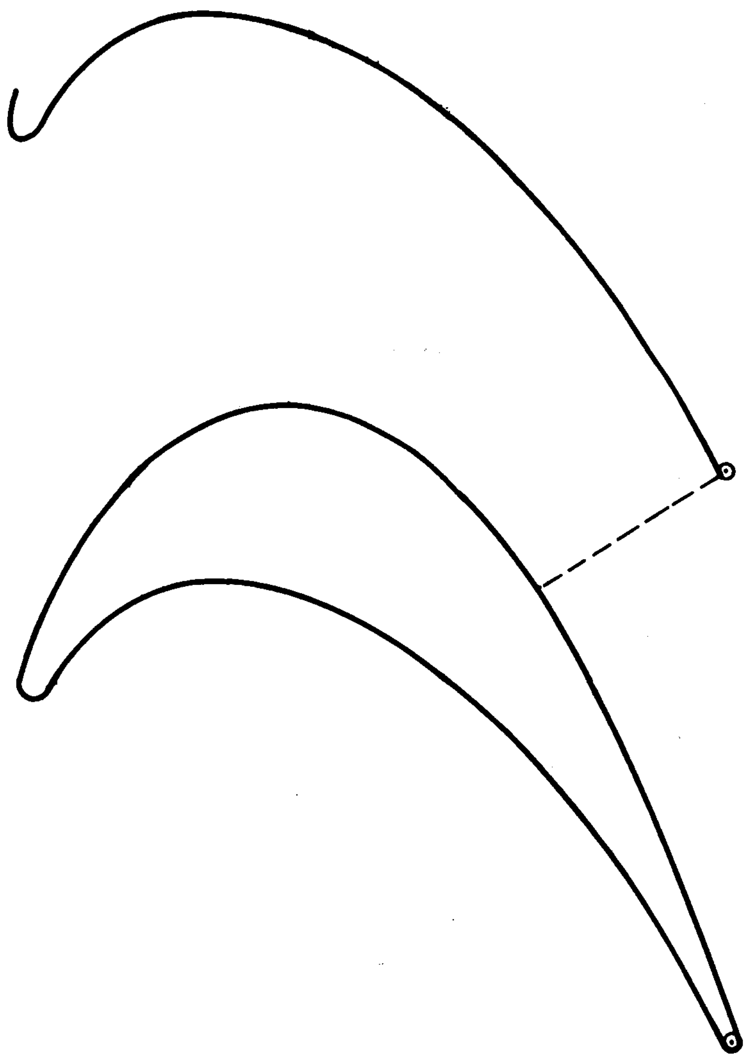

FIG. 23 FIRST STAGE BLADE QUARTER TIP 5.0 SCALE

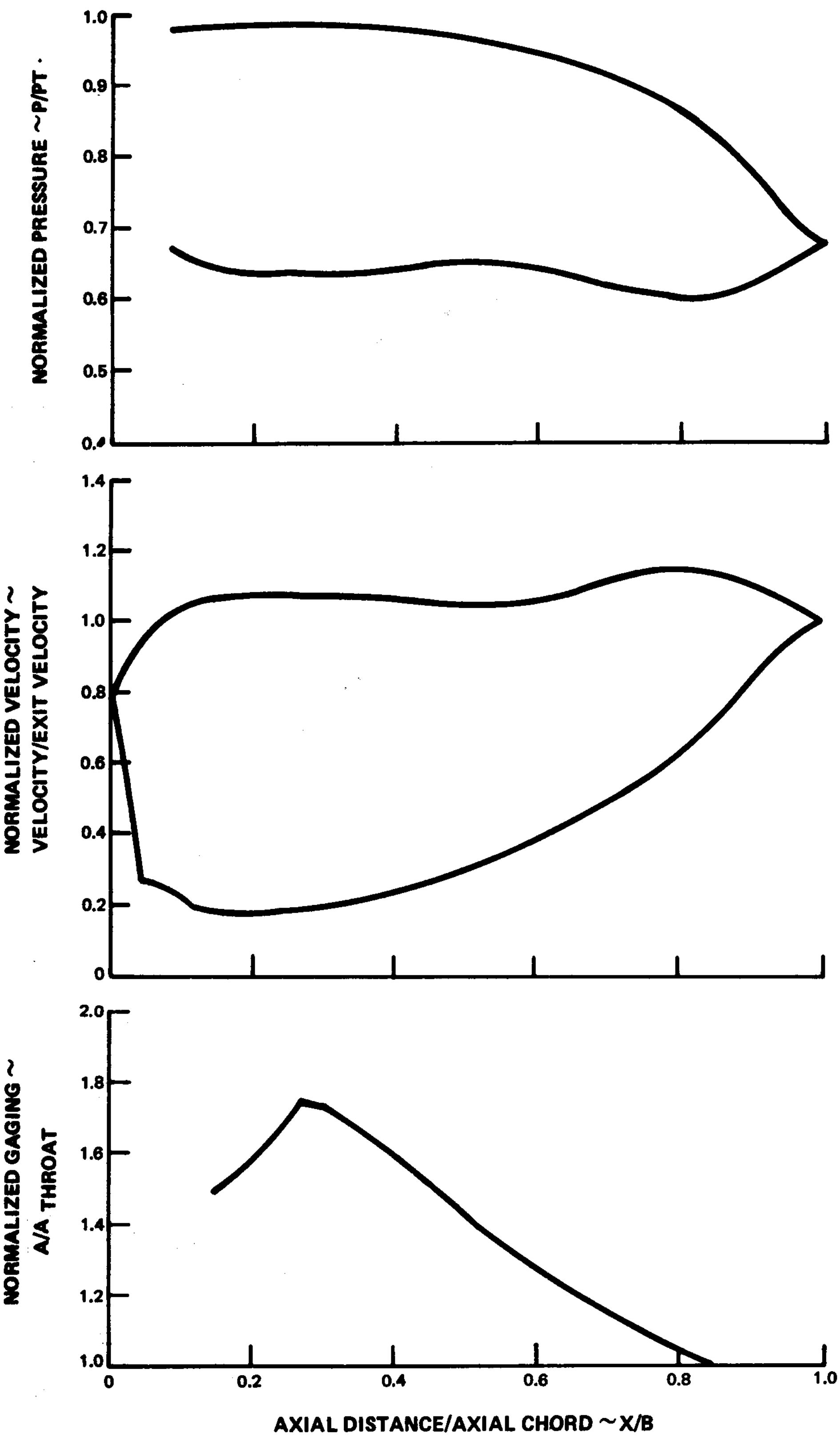

FIG. 24 FIRST STAGE BLADE QUARTER TIP NORMALIZED PRESSURE VELOCITY AND GAGING DIAGRAMS

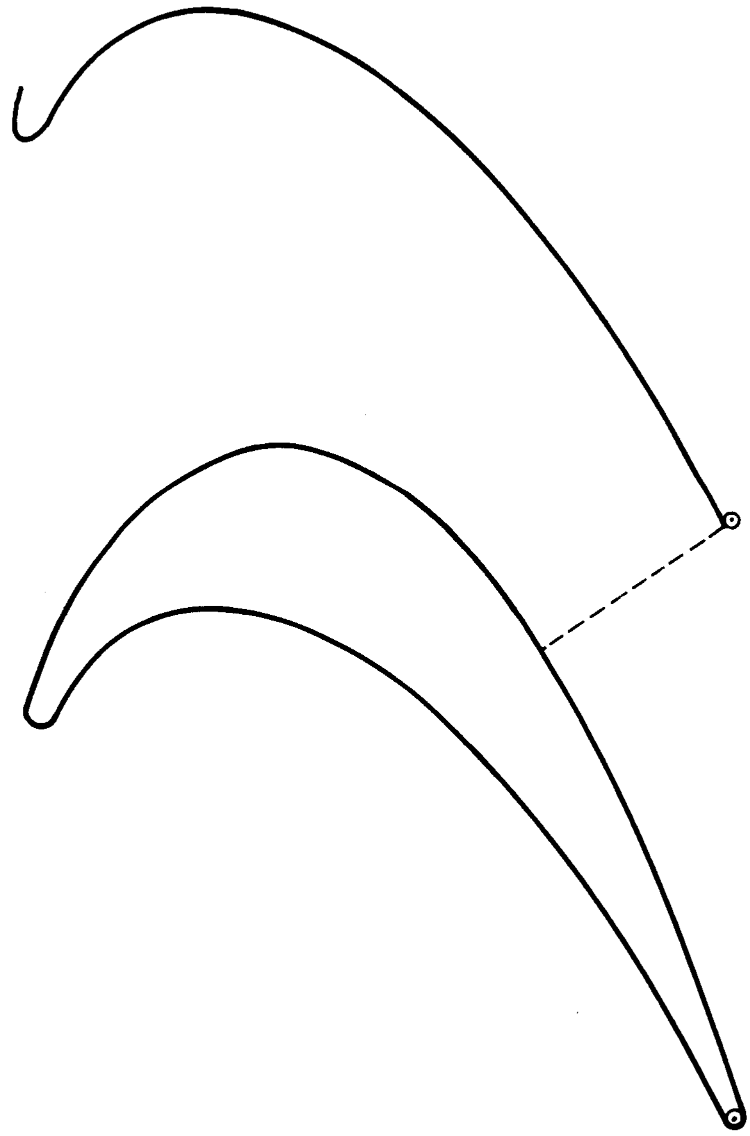

FIG. 25 FIRST STAGE BLADE TIP 5.0 SCALE

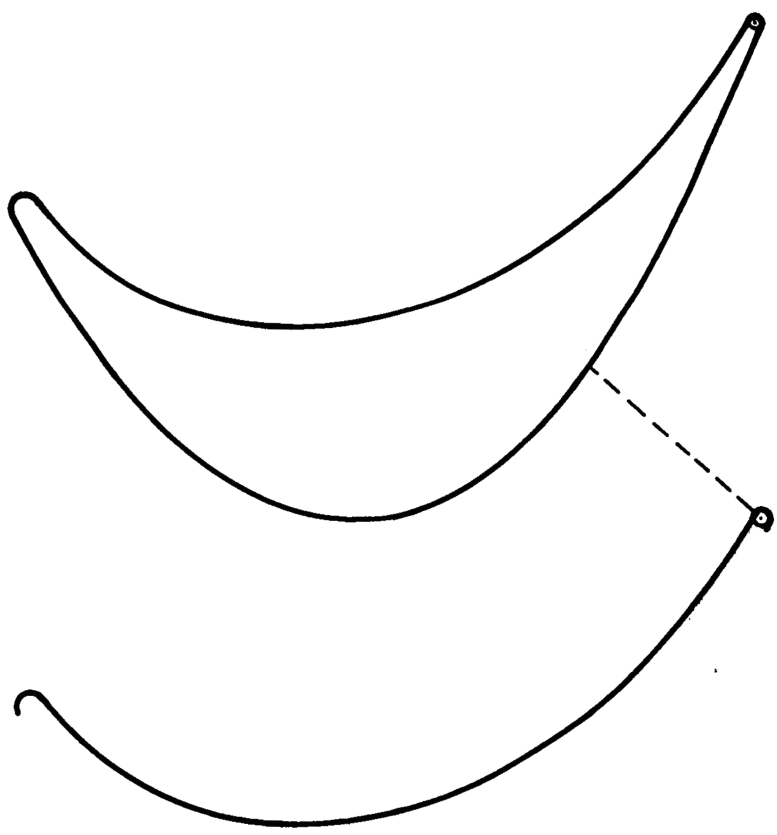

FIG. 27 SECOND STAGE VANE ROOT (5.0 SCALE)

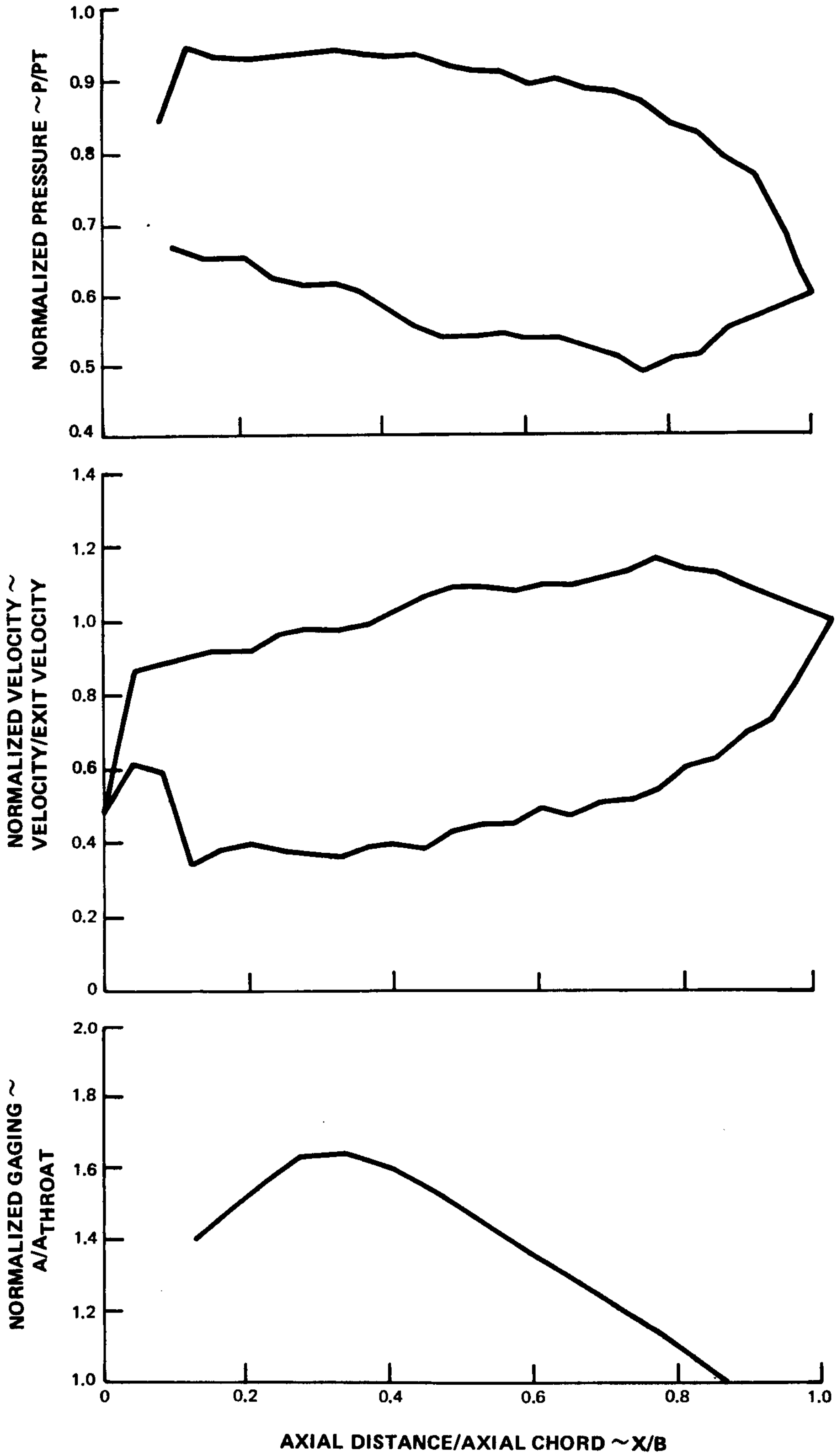

FIG. 28 SECOND STAGE VANE ROOT NORMALIZED PRESSURE VELOCITY AND GAGING DIAGRAMS

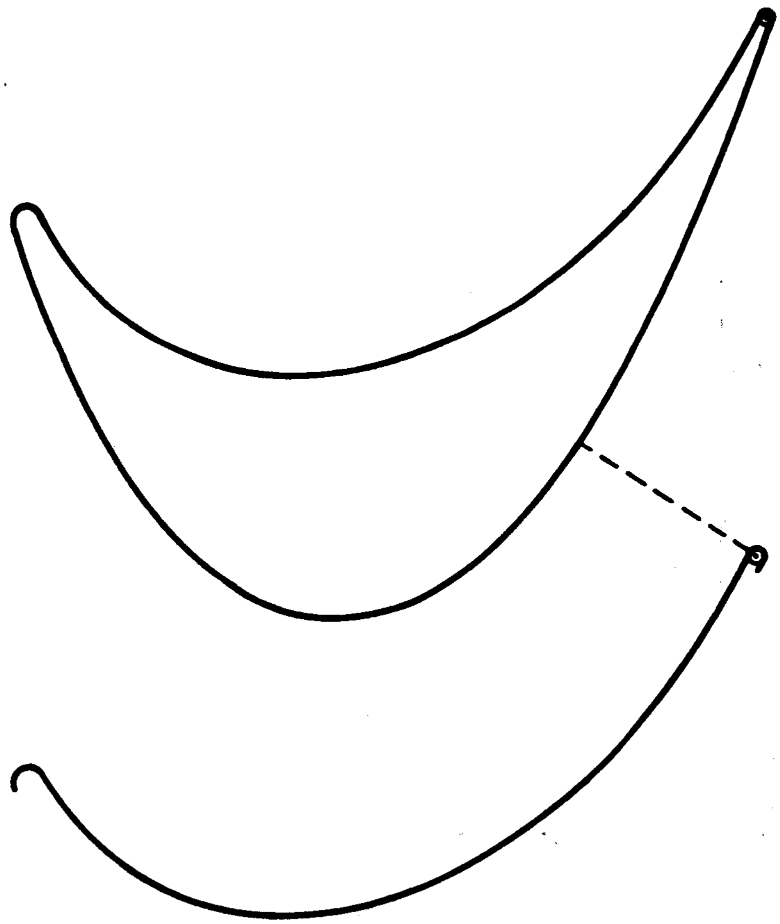

FIG. 29 SECOND STAGE VANE QUARTER ROOT (5.0 SCALE)

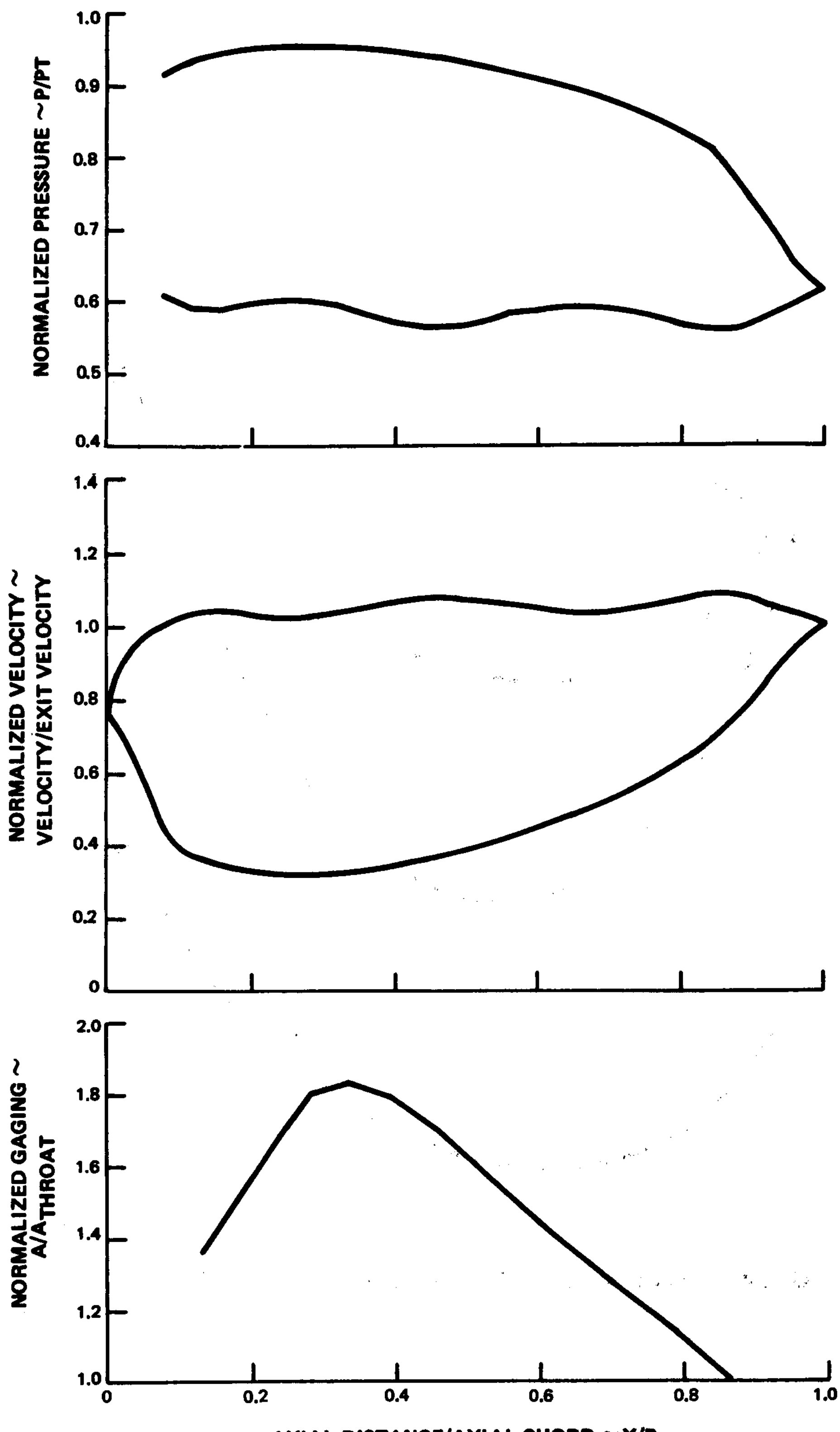

FIG.30 SECOND STAGE VANE QUARTER ROOT NORMALIZED PRESSURE VELOCITY AND GAGING DIAGRAMS

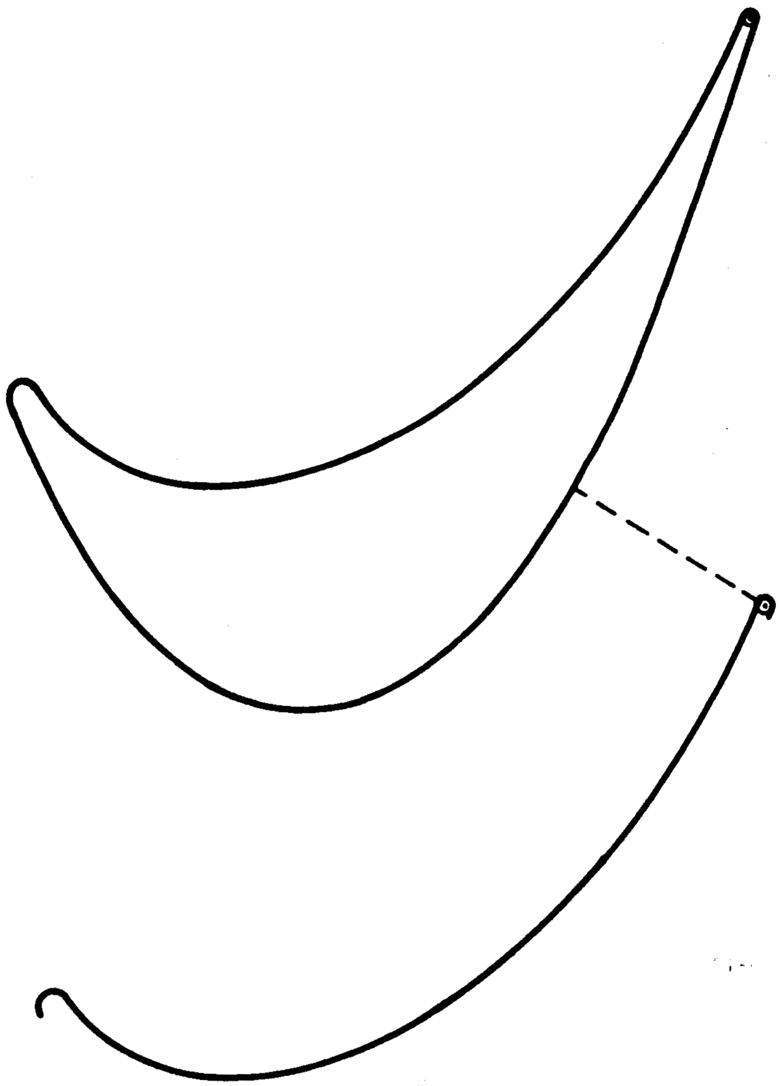

FIG. 31 SECOND STAGE VANE MEAN (5.0 SCALE)

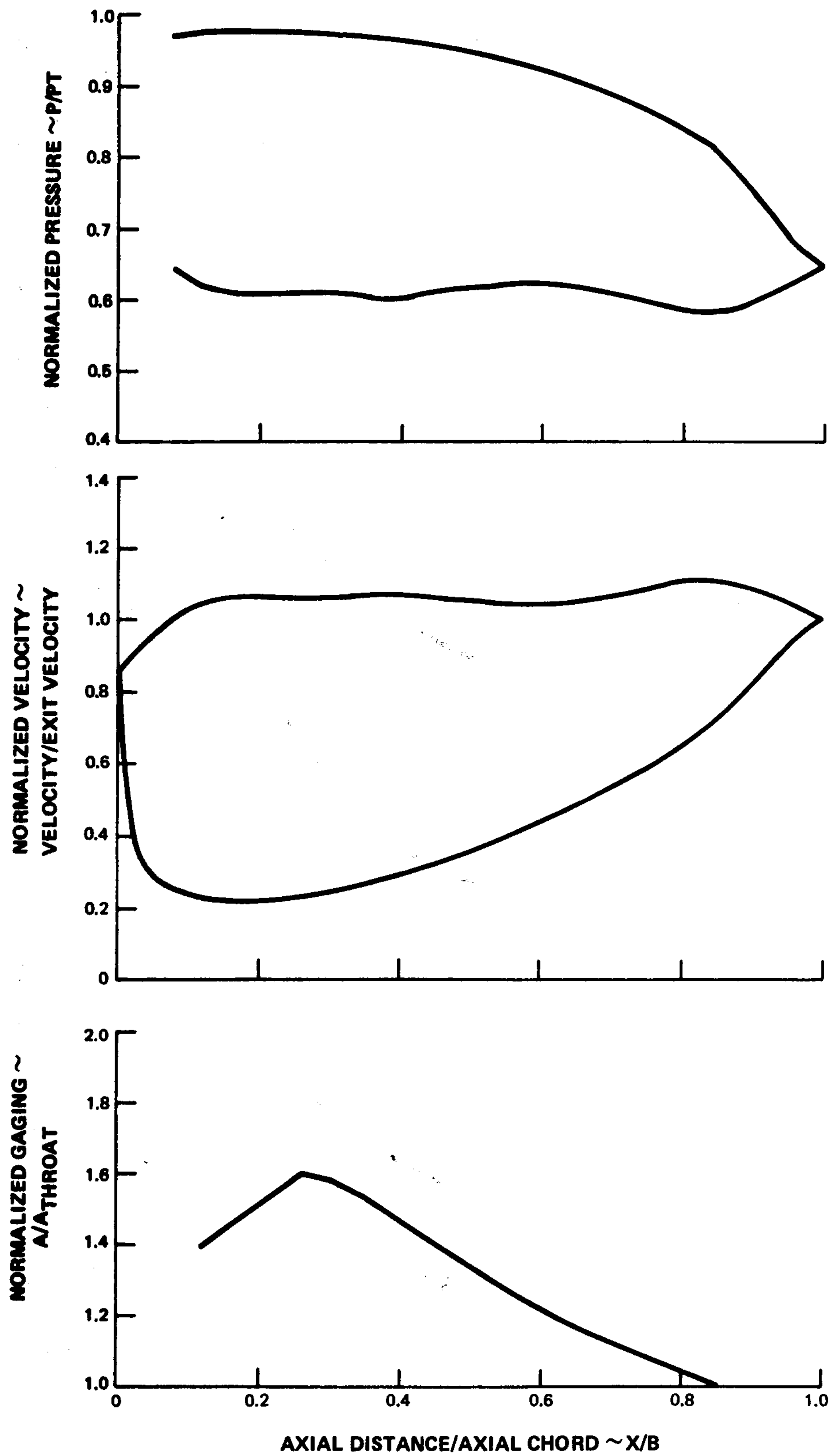

FIG. 32 SECOND STAGE VANE MEAN NORMALIZED PRESSURE VELOCITY AND GAGING DIAGRAMS

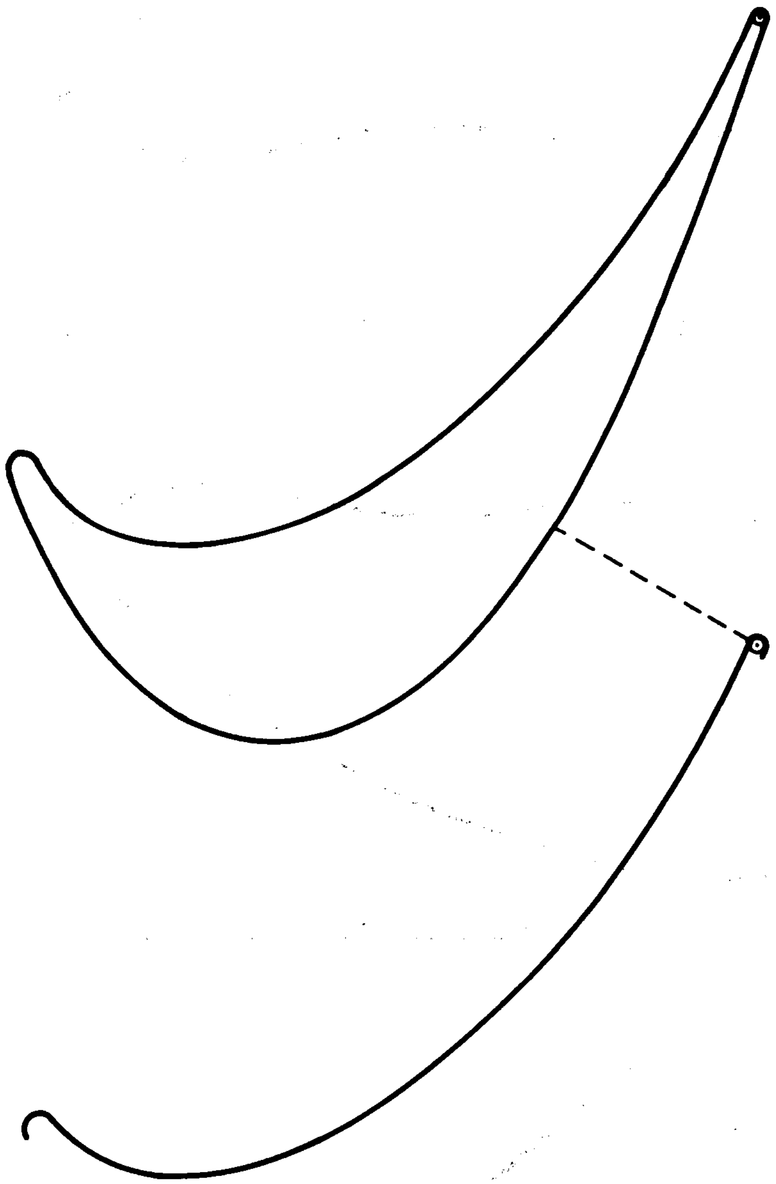

FIG. 33 SECOND STAGE VANE QUARTER TIP (5.0 SCALE)

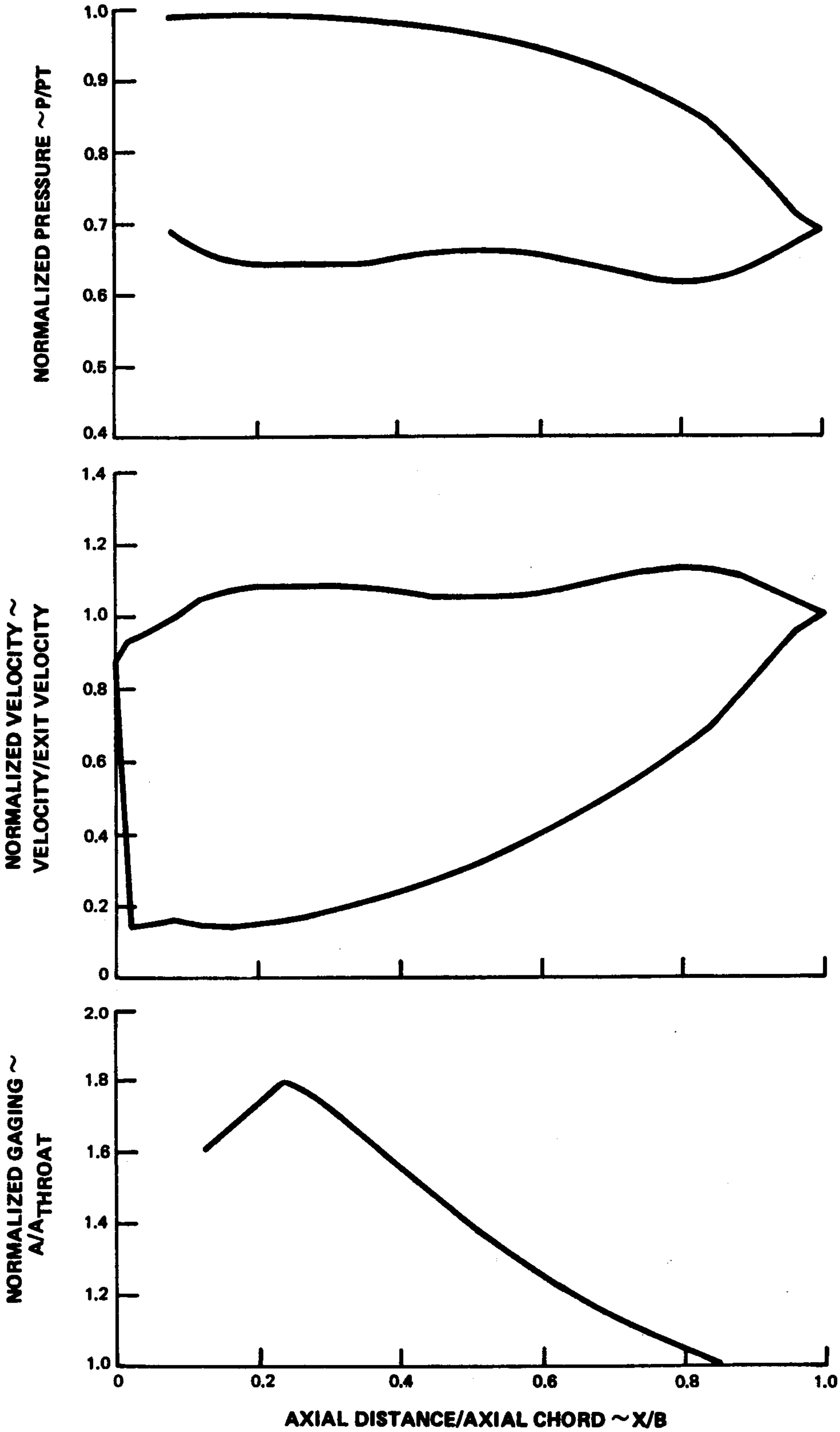

FIG. 34 SECOND STAGE VANE QUARTER TIP NORMALIZED PRESSURE VELOCITY AND GAGING DIAGRAMS

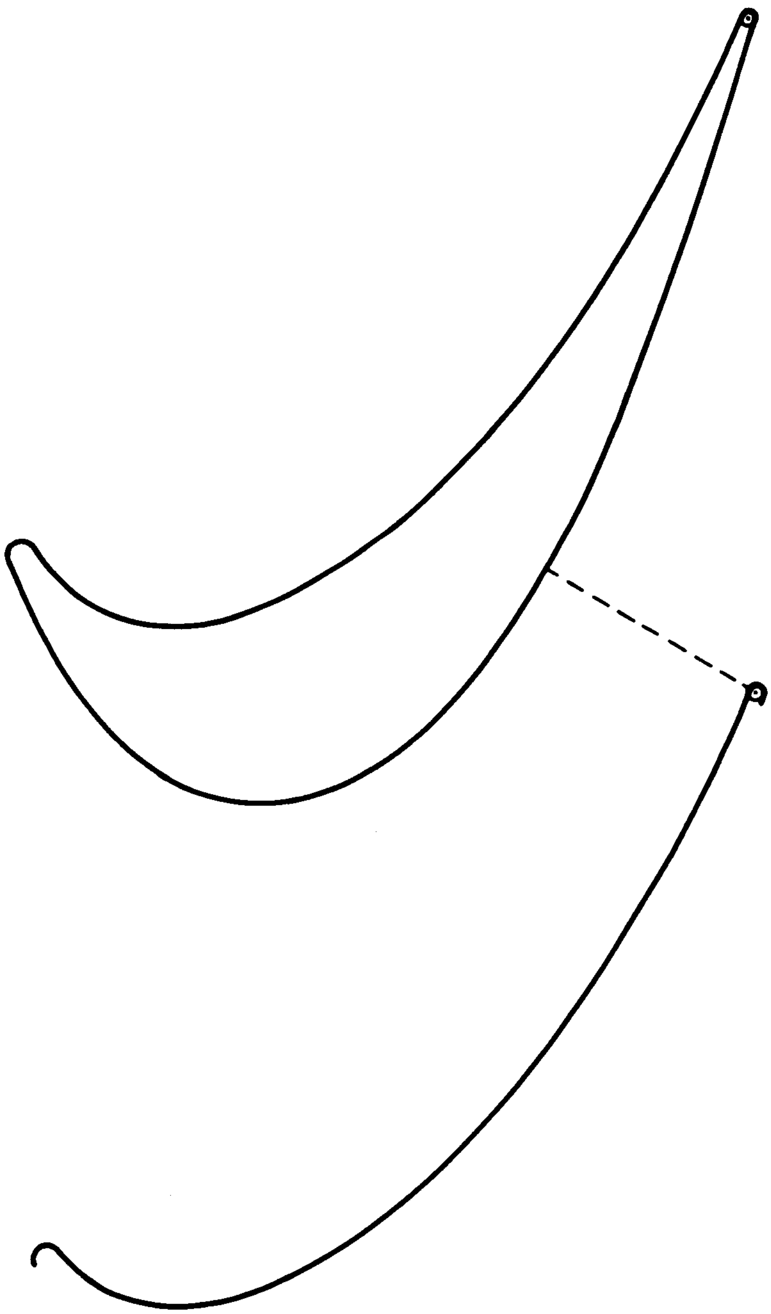

FIG. 35 SECOND STAGE VANE TIP (5.0 SCALE)

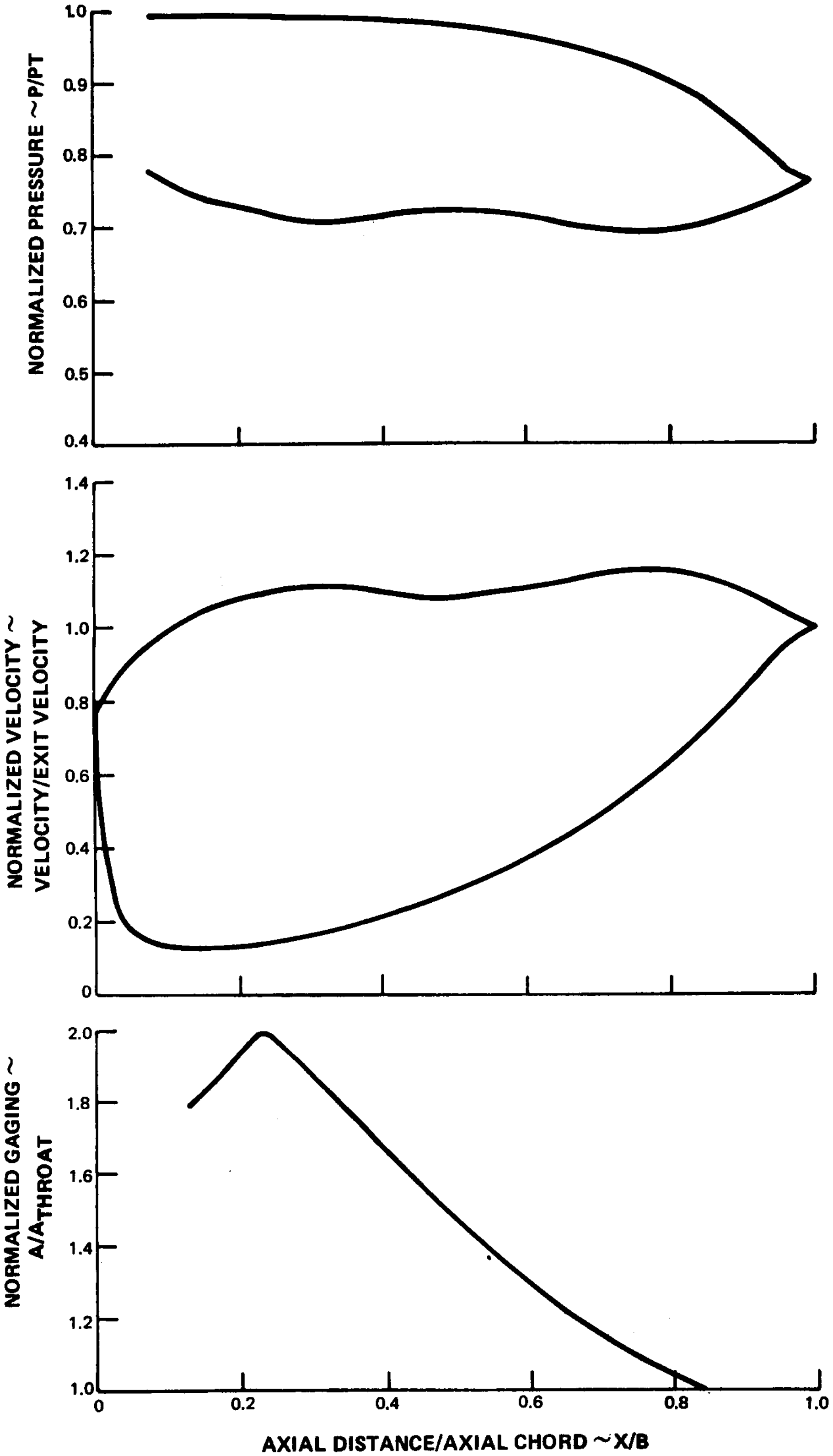

FIG. 36 SECOND STAGE VANE TIP NORMALIZED PRESSURE VELOCITY AND GAGING DIAGRAMS

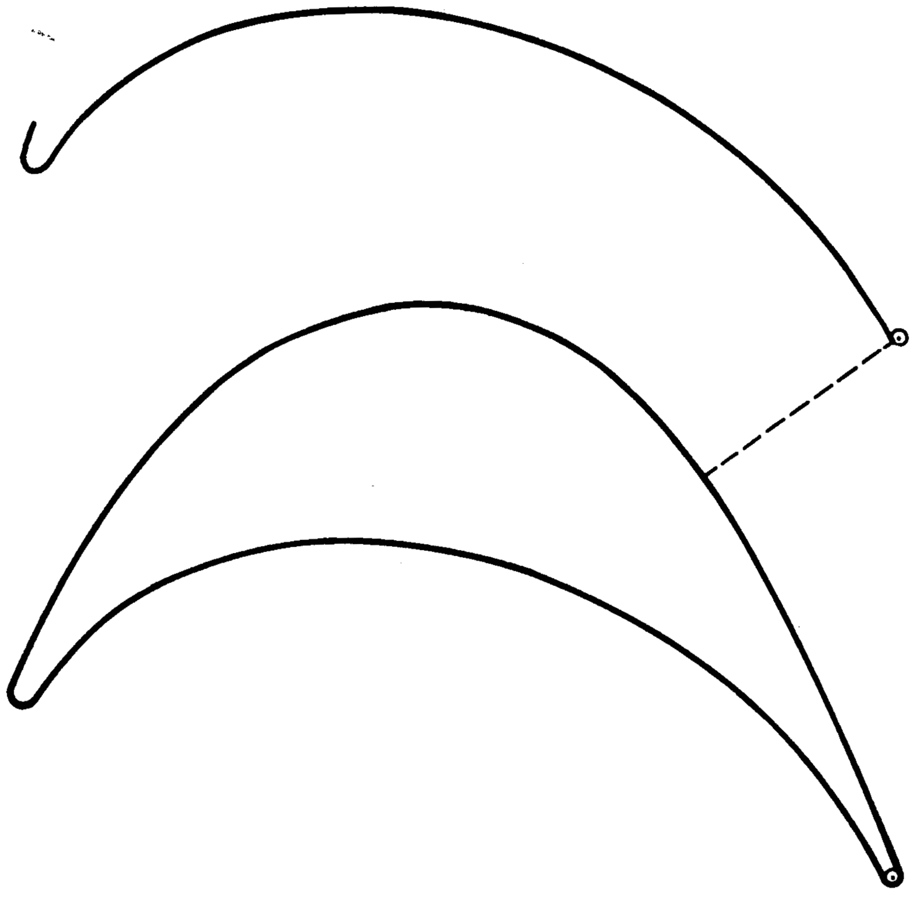

FIG. 37 SECOND STAGE BLADE ROOT 5.0 SCALE

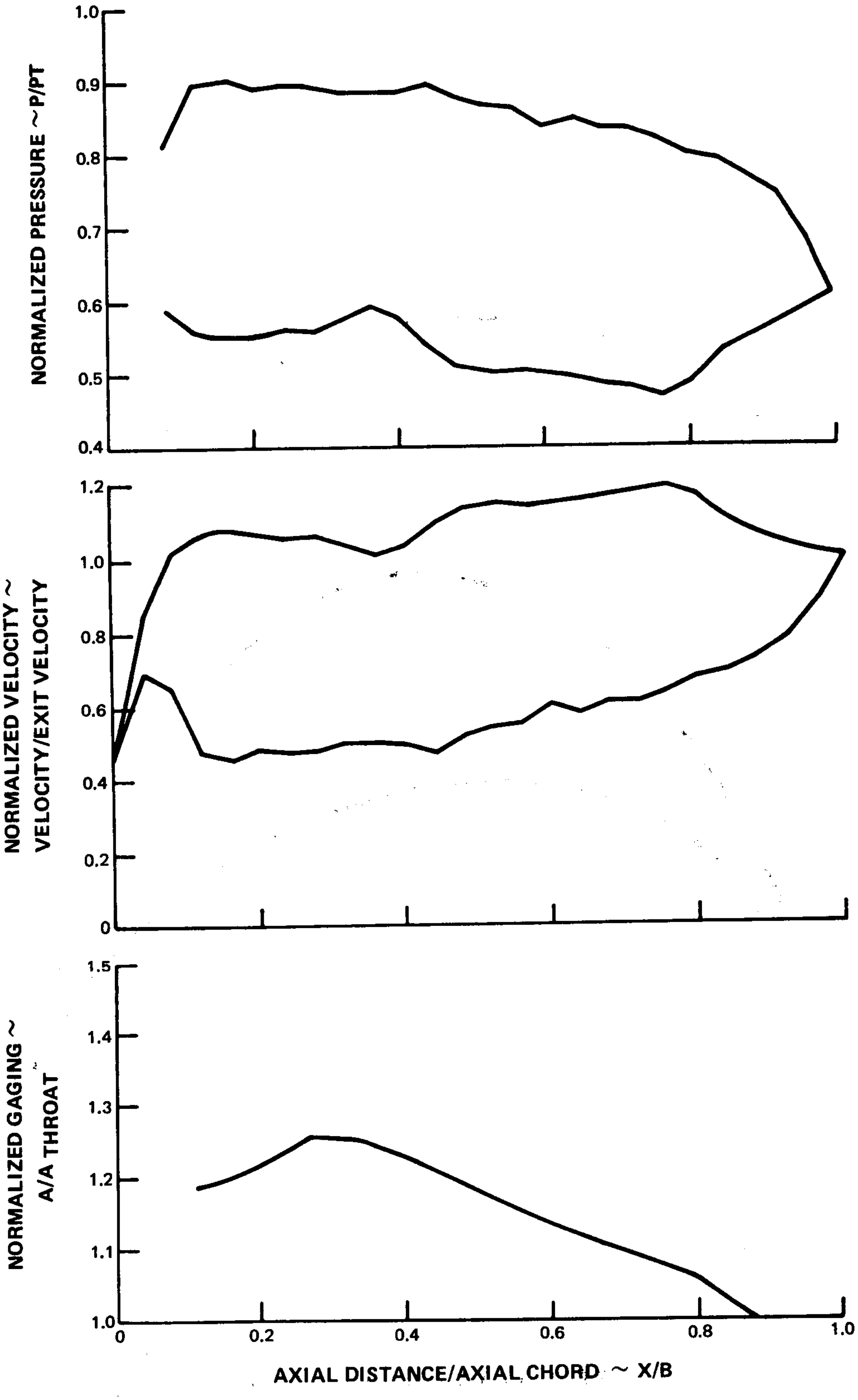

FIG. 38 SECOND STAGE BLADE ROOT NORMALIZED PRESSURE VELOCITY AND GAGING DIAGRAMS

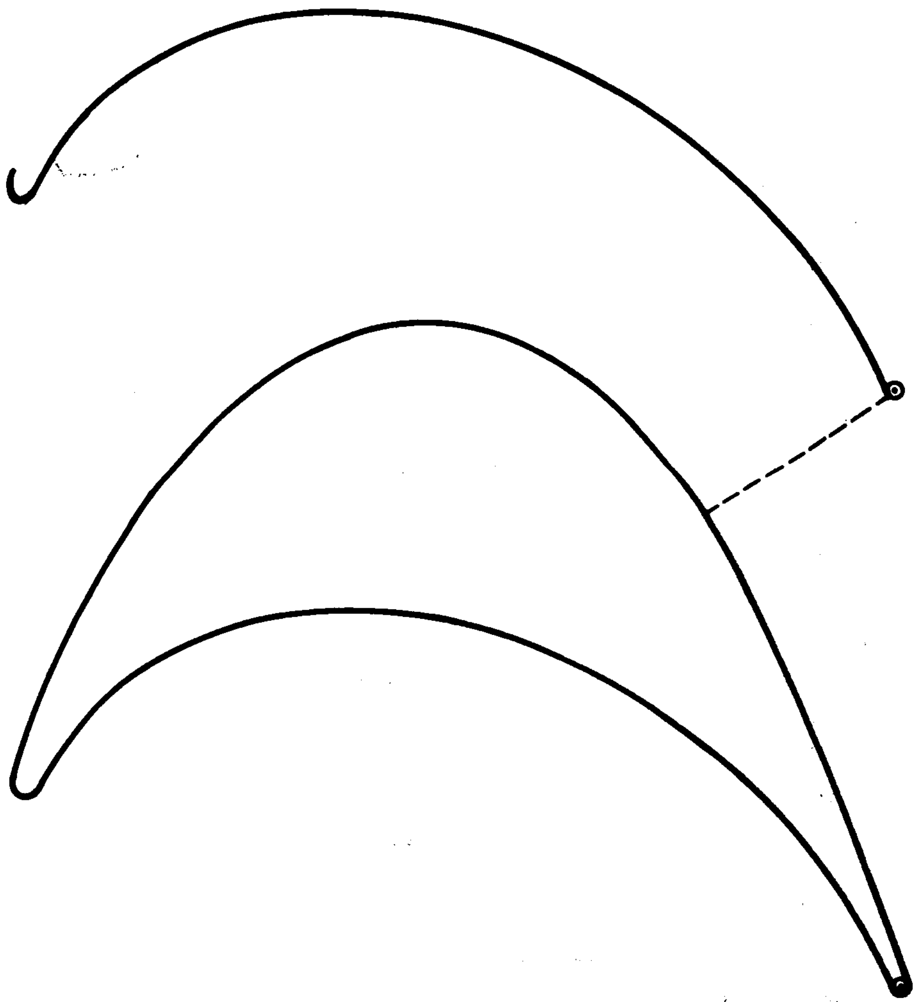

FIG. 39 SECOND STAGE BLADE QUARTER ROOT 5.0 SCALE

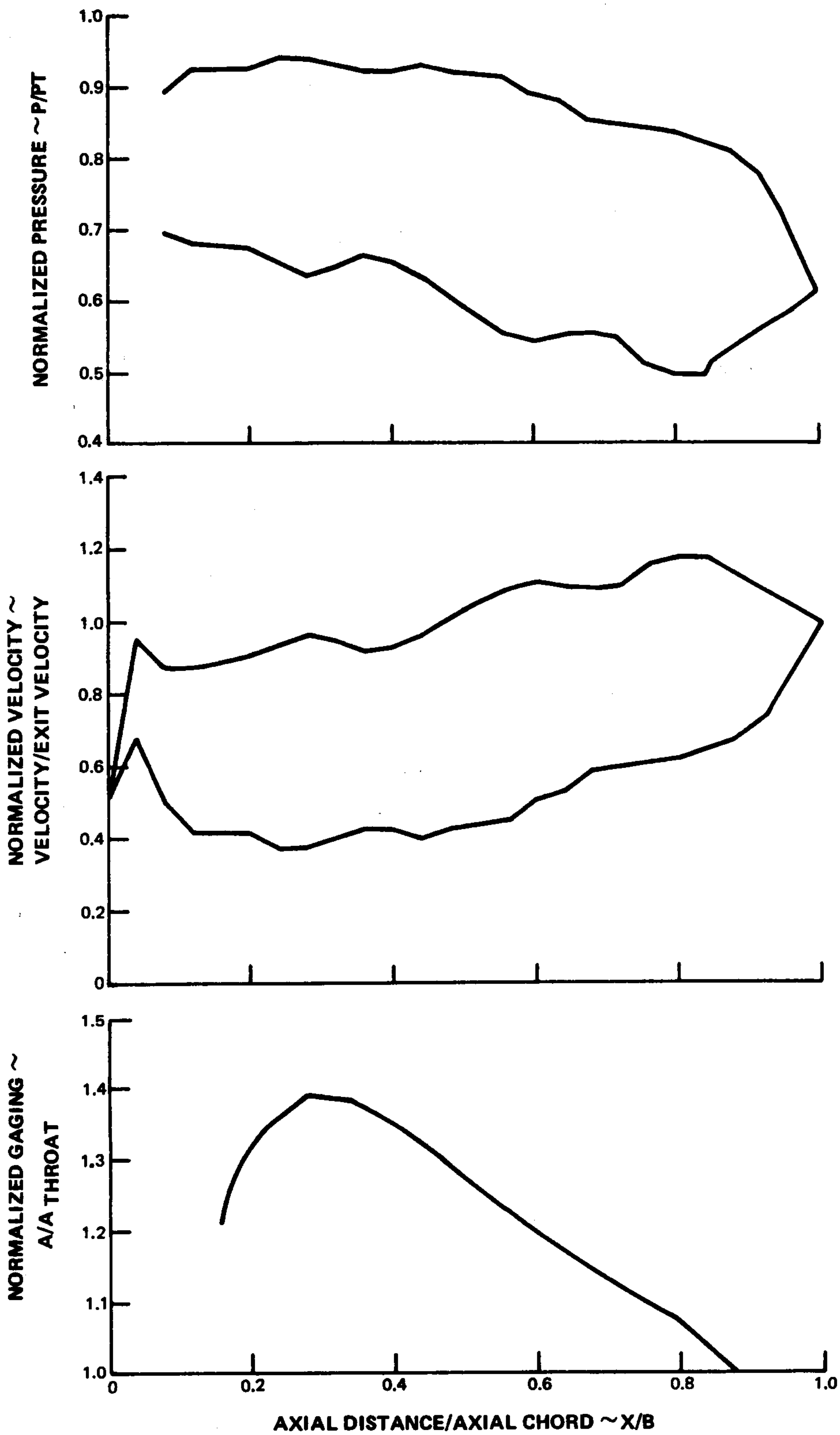

FIG. 40 SECOND STAGE BLADE QUARTER ROOT NORMALIZED PRESSURE VELOCITY AND GAGING DIAGRAMS

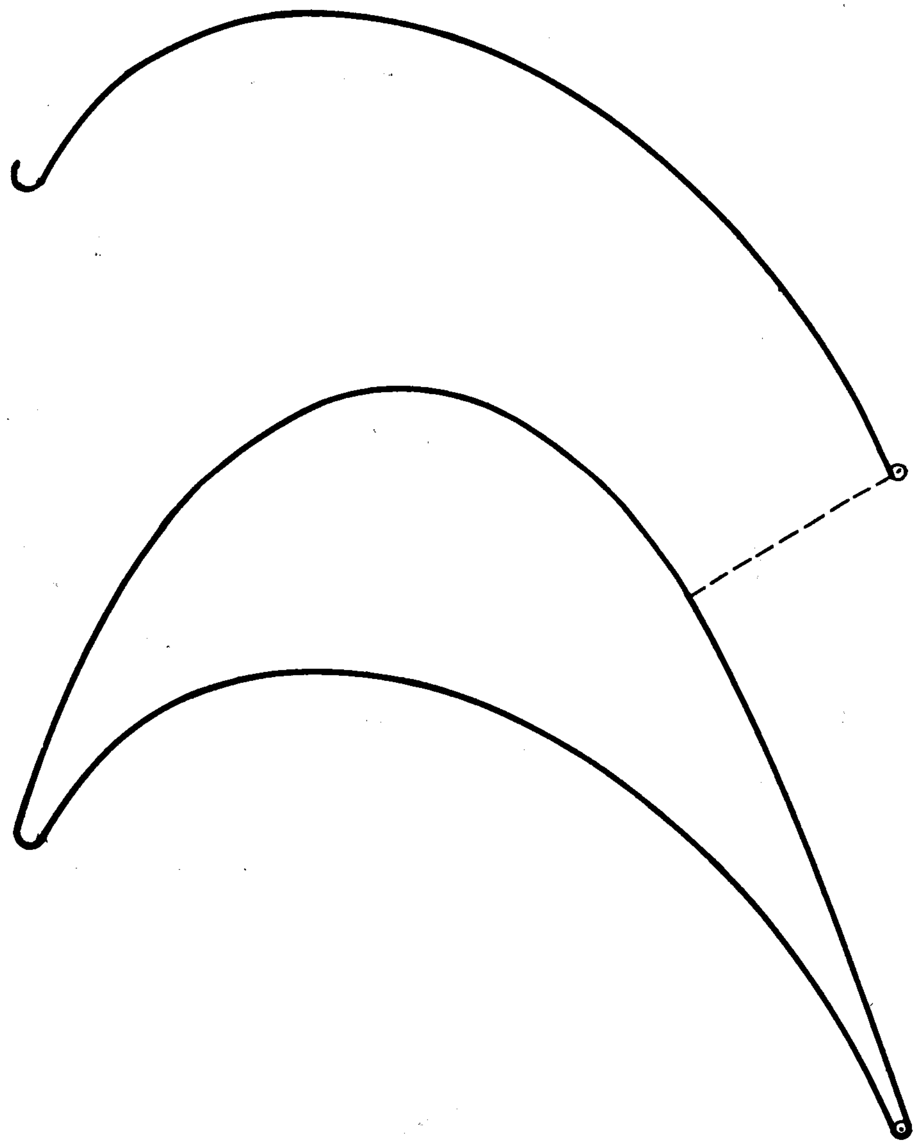

FIG. 41 SECOND STAGE BLADE MEAN 3.0 SCALE

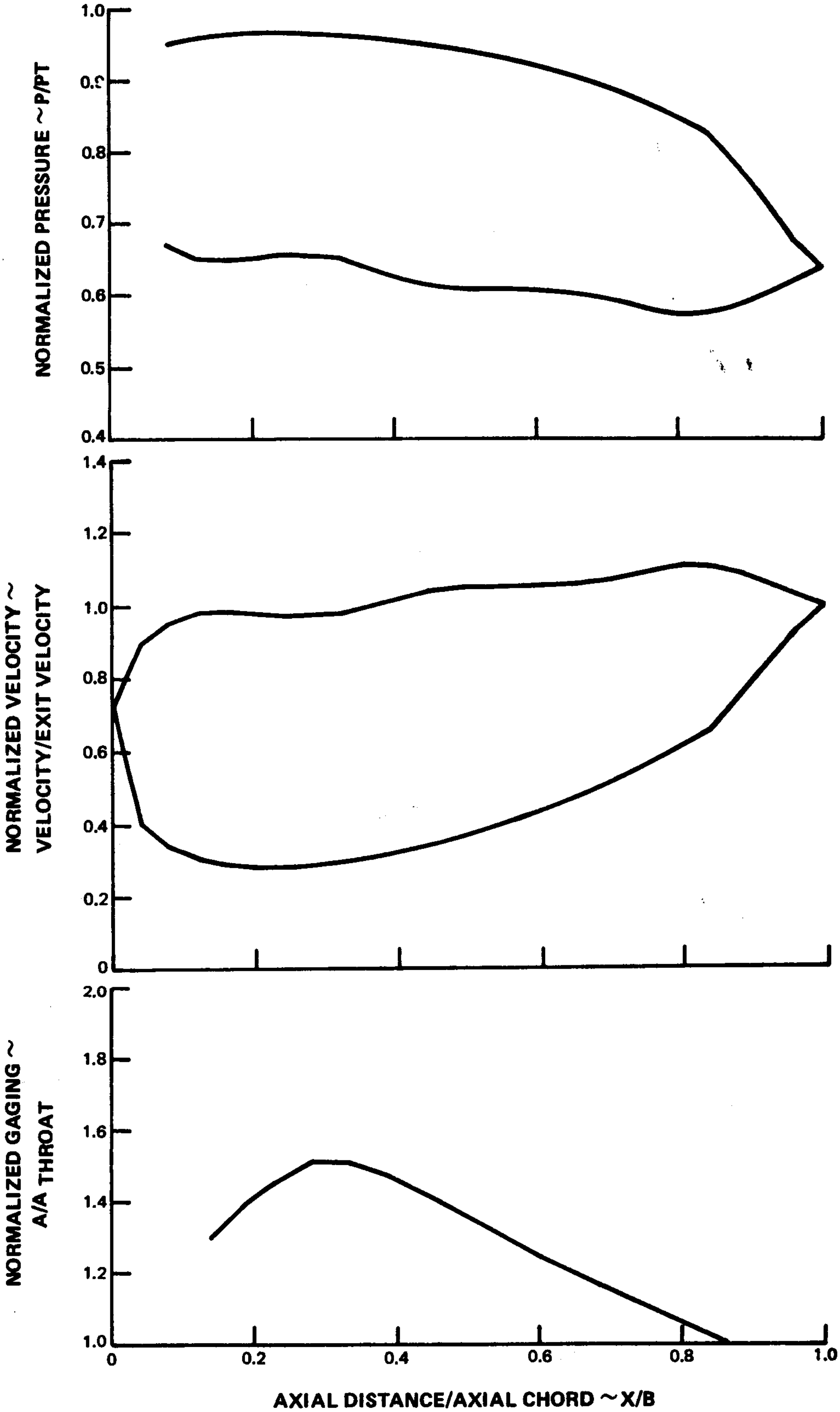

FIG. 42 SECOND STAGE BLADE MEAN NORMALIZED PRESSURE VELOCITY AND GAGING DIAGRAMS

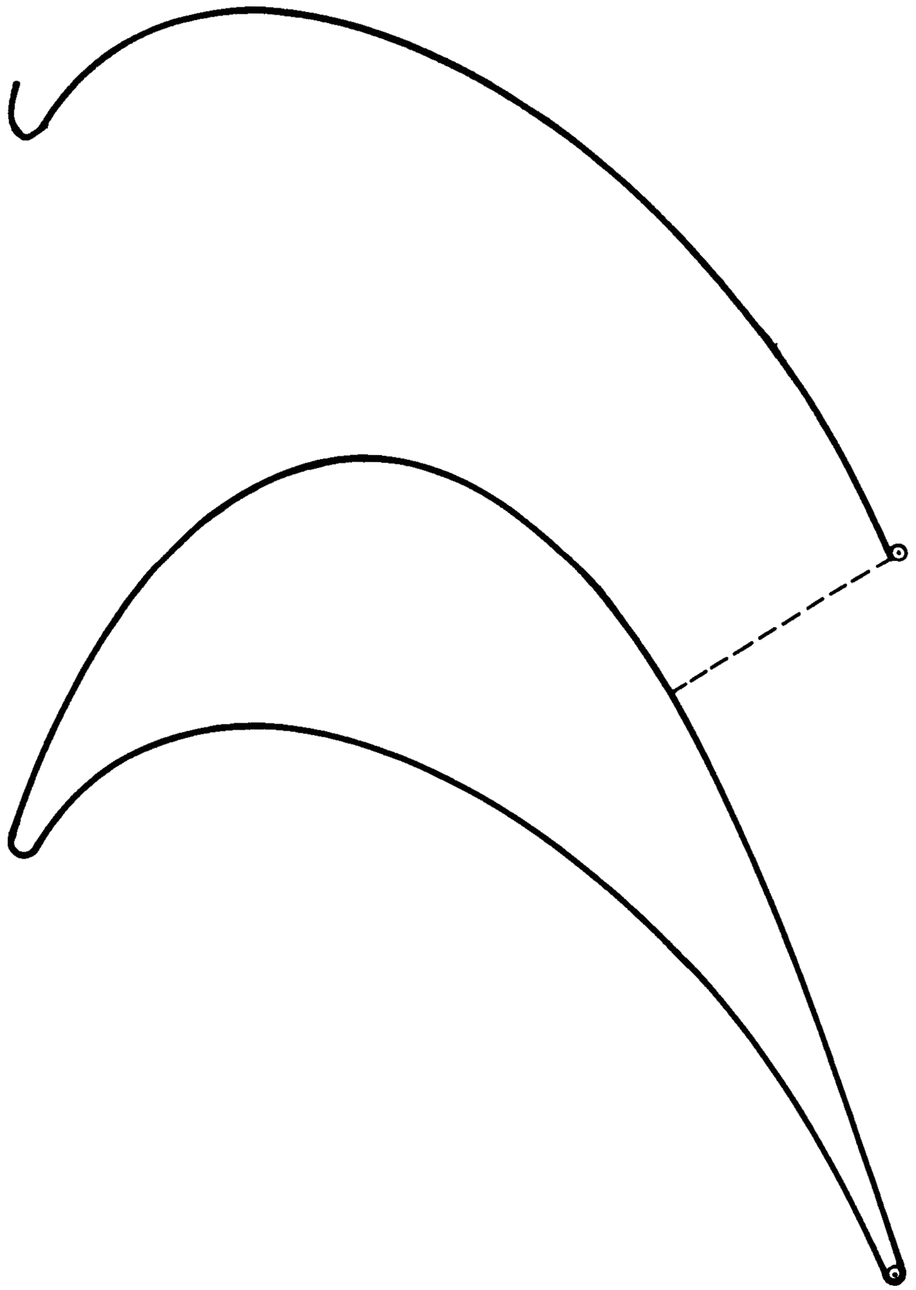

FIG. 43 SECOND STAGE BLADE QUARTER TIP 5.0 SCALE

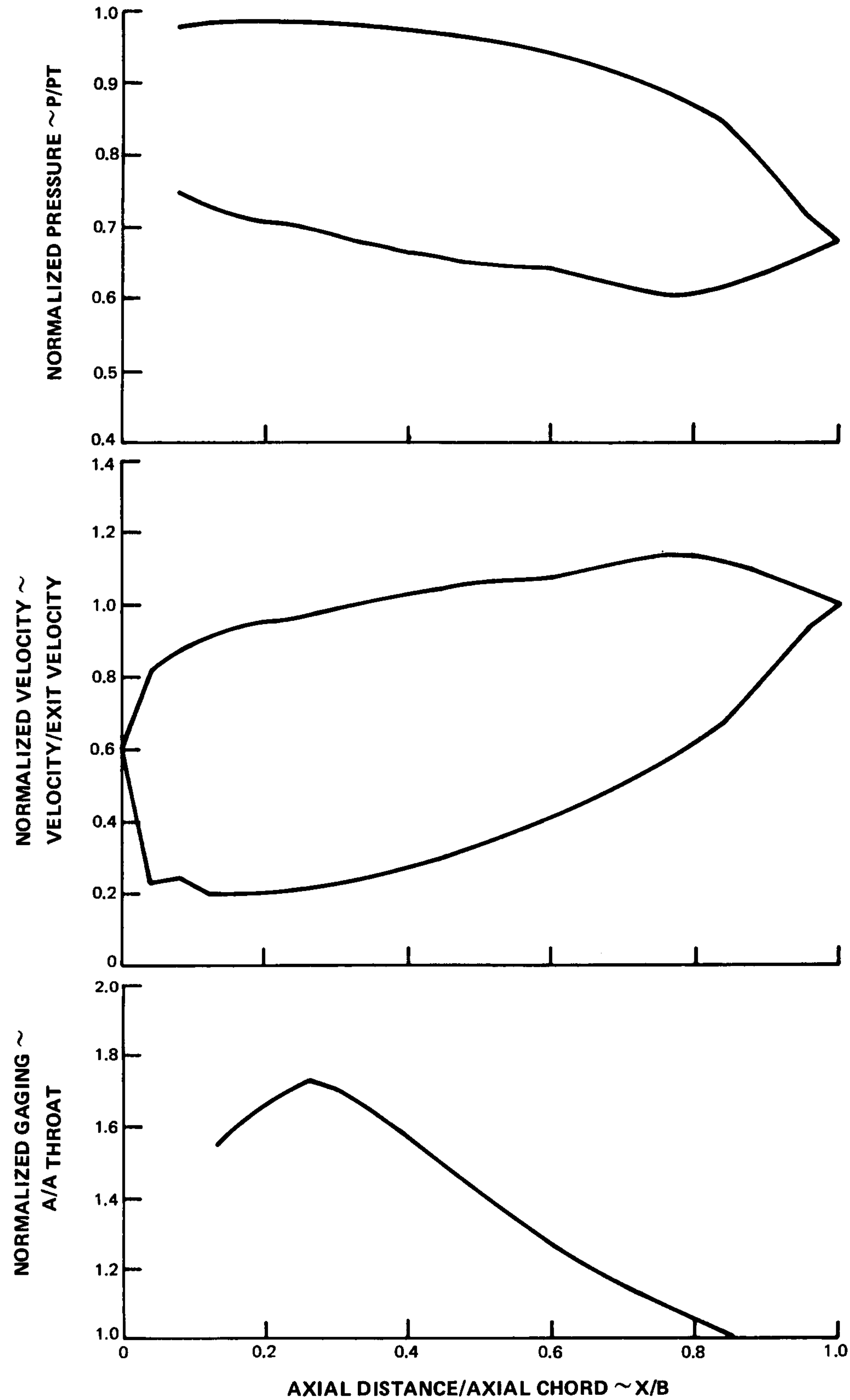

FIG. 44 SECOND STAGE BLADE QUARTER TIP NORMALIZED PRESSURE VELOCITY AND GAGING DIAGRAMS

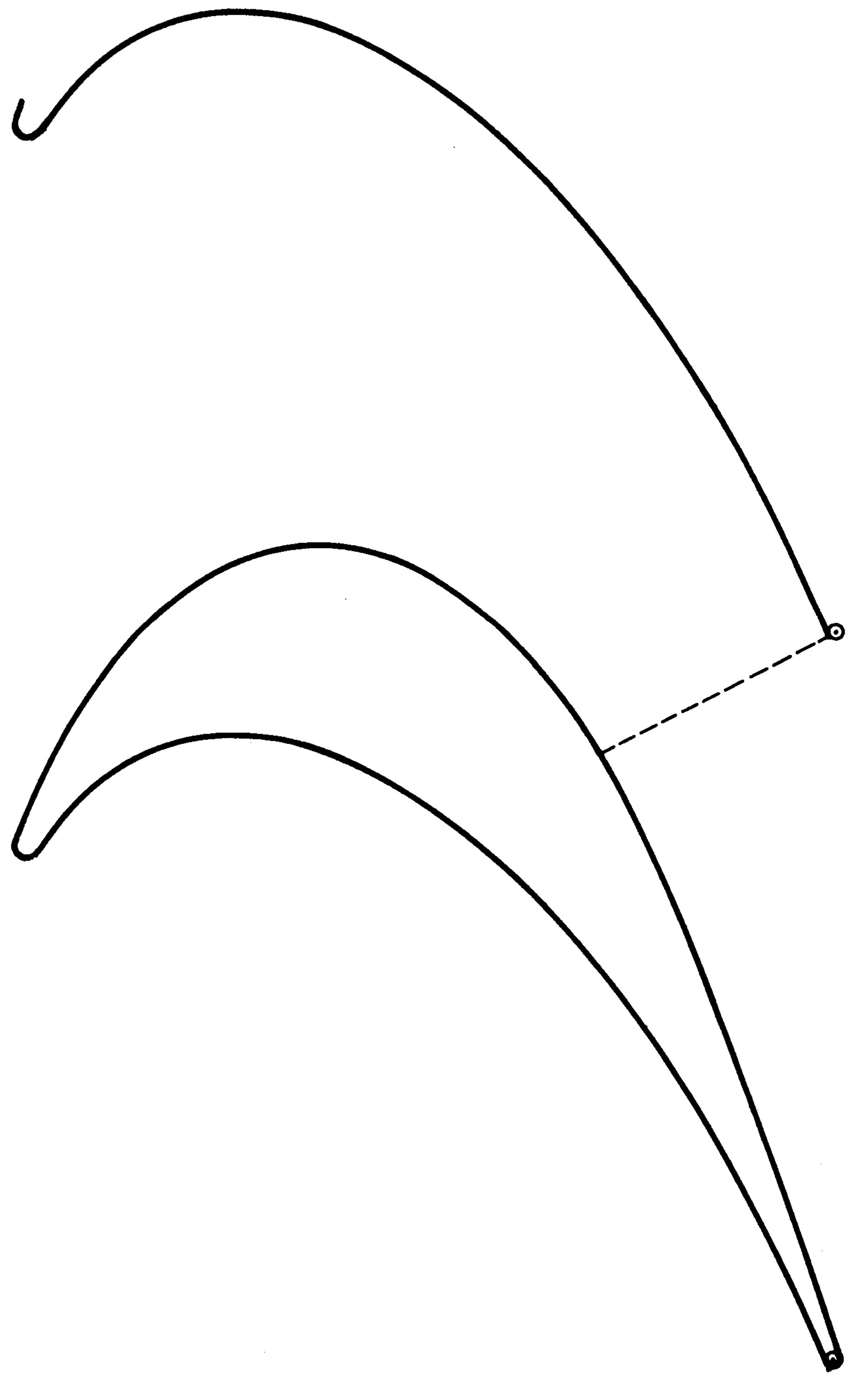

FIG. 45 SECOND STAGE BLADE TIP 5.0 SCALE

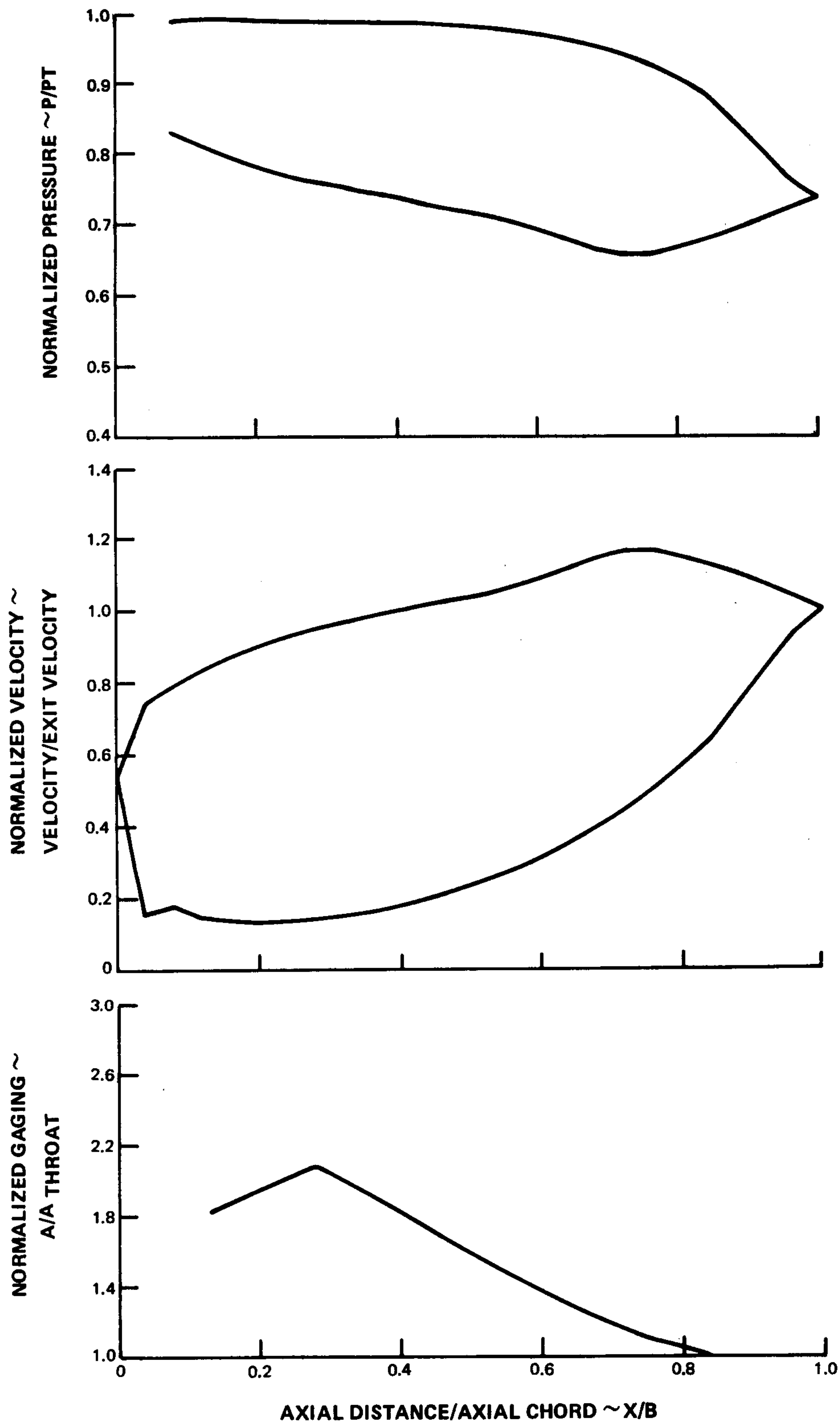

FIG. 46 SECOND STAGE BLADE TIP NORMALIZED PRESSURE VELOCITY AND GAGING DIAGRAMS

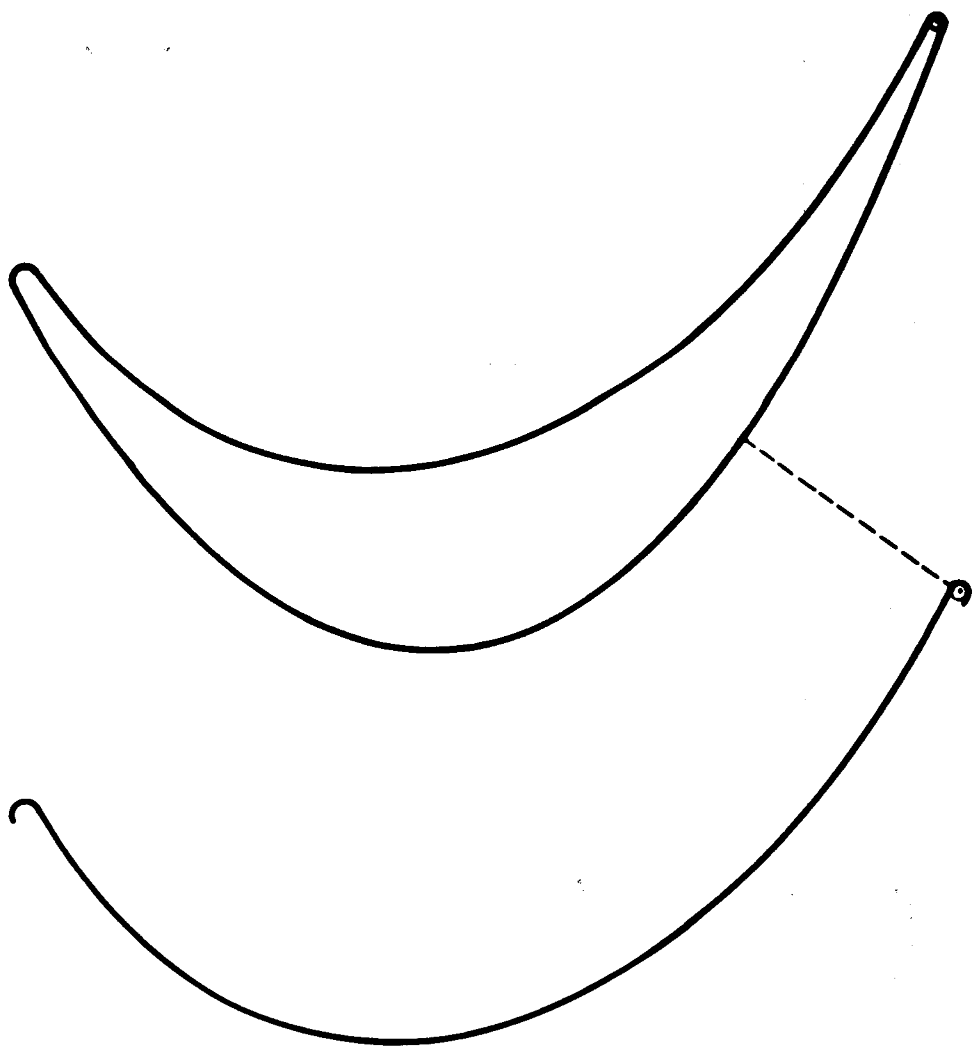

FIG. 47 THIRD STAGE VANE ROOT (5.0 SCALE)

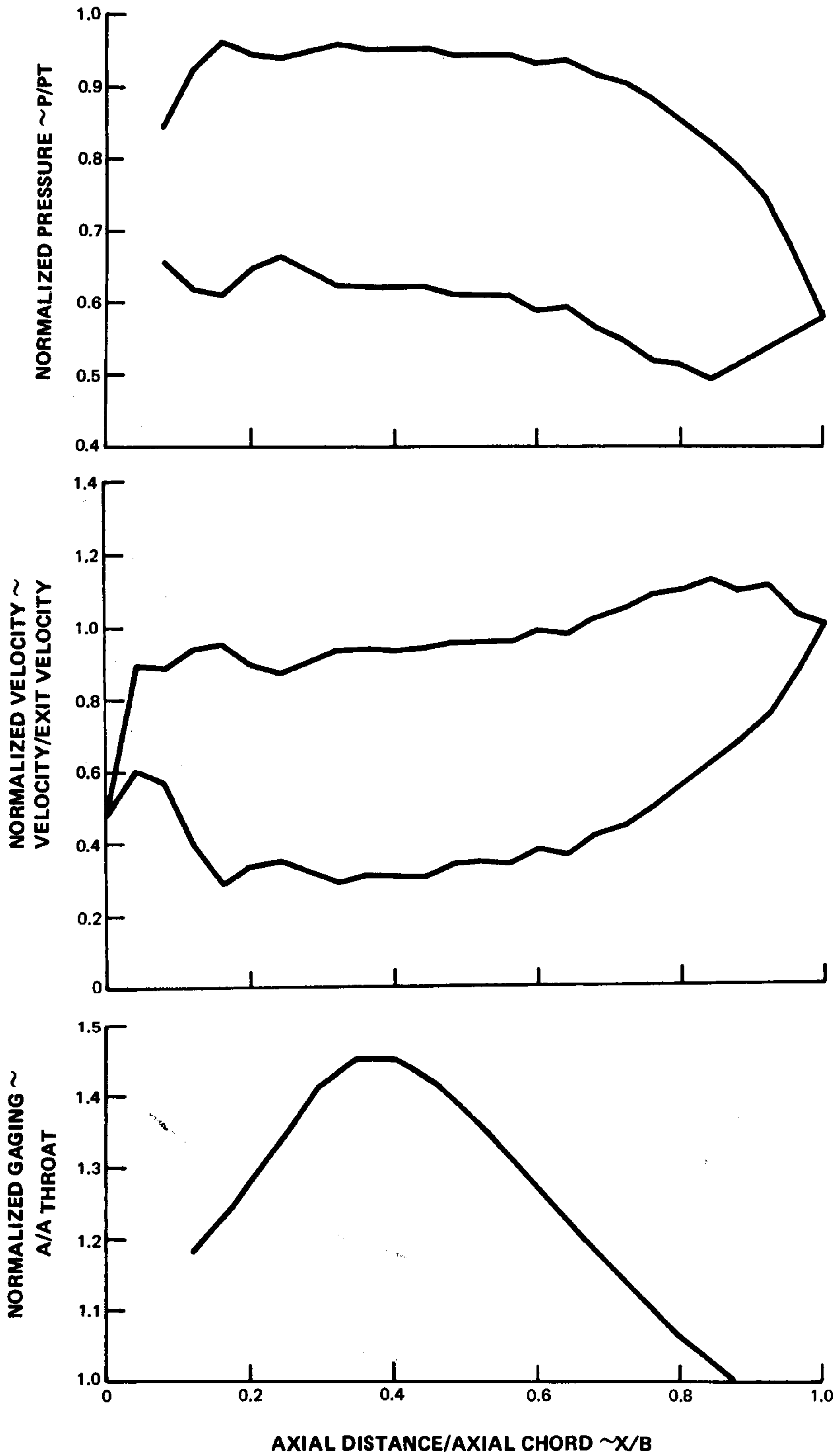

FIG. 48 THIRD STAGE VANE ROOT NORMALIZED PRESSURE VELOCITY AND GAGING DIAGRAMS

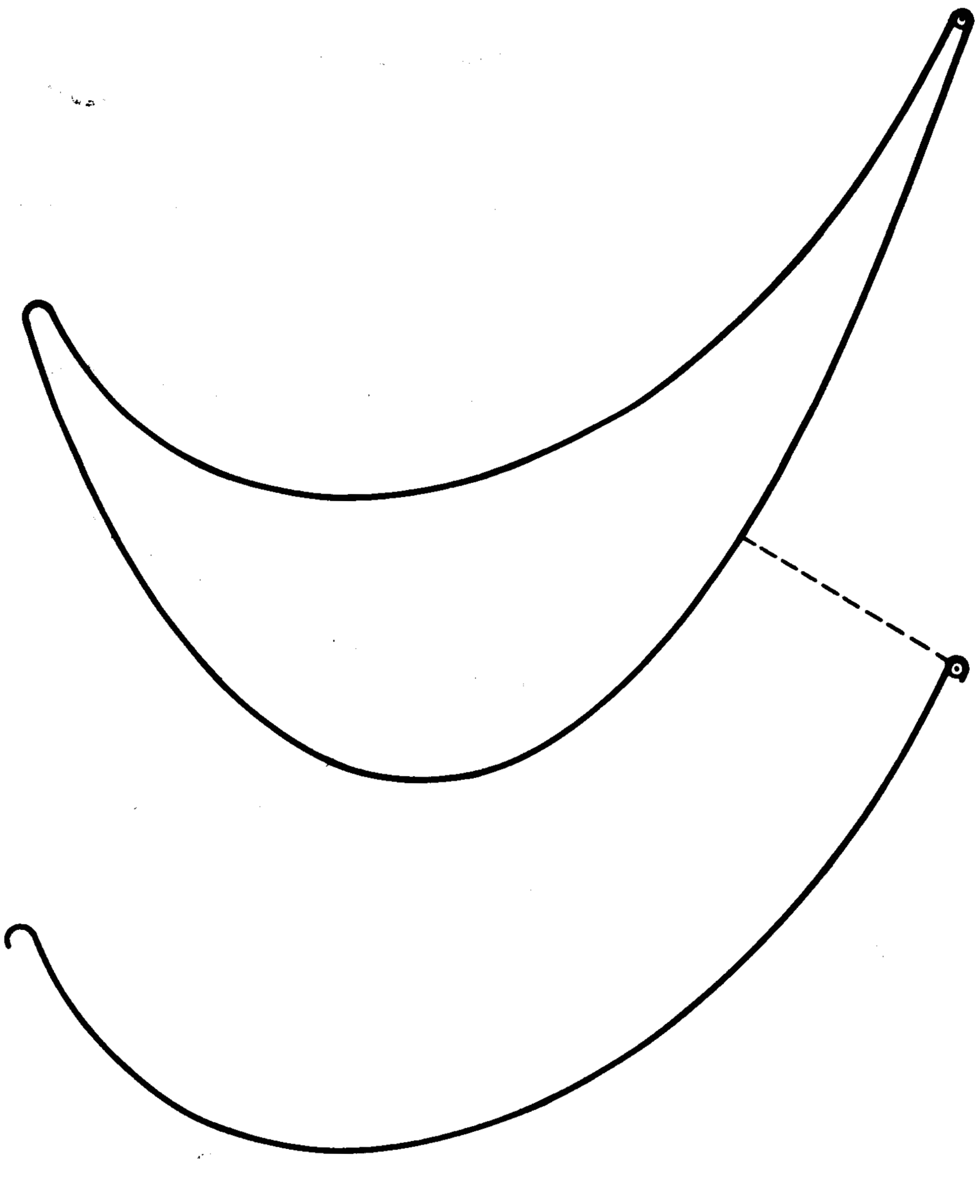

FIG. 49 THIRD STAGE VANE QUARTER ROOT (5.0 SCALE)

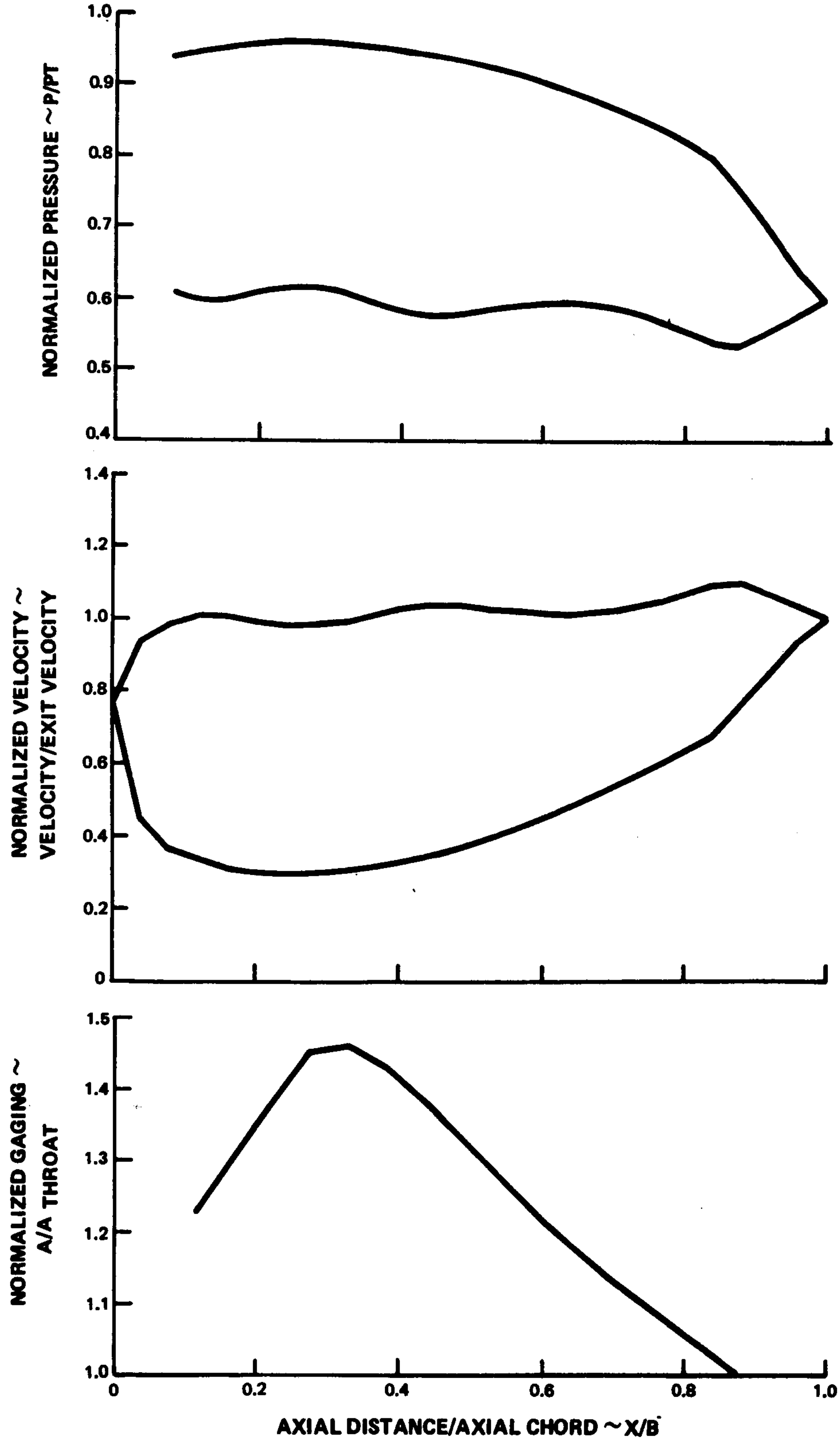

FIG. 50 THIRD STAGE VANE QUARTER ROOT NORMALIZED PRESSURE VELOCITY AND GAGING DIAGRAMS

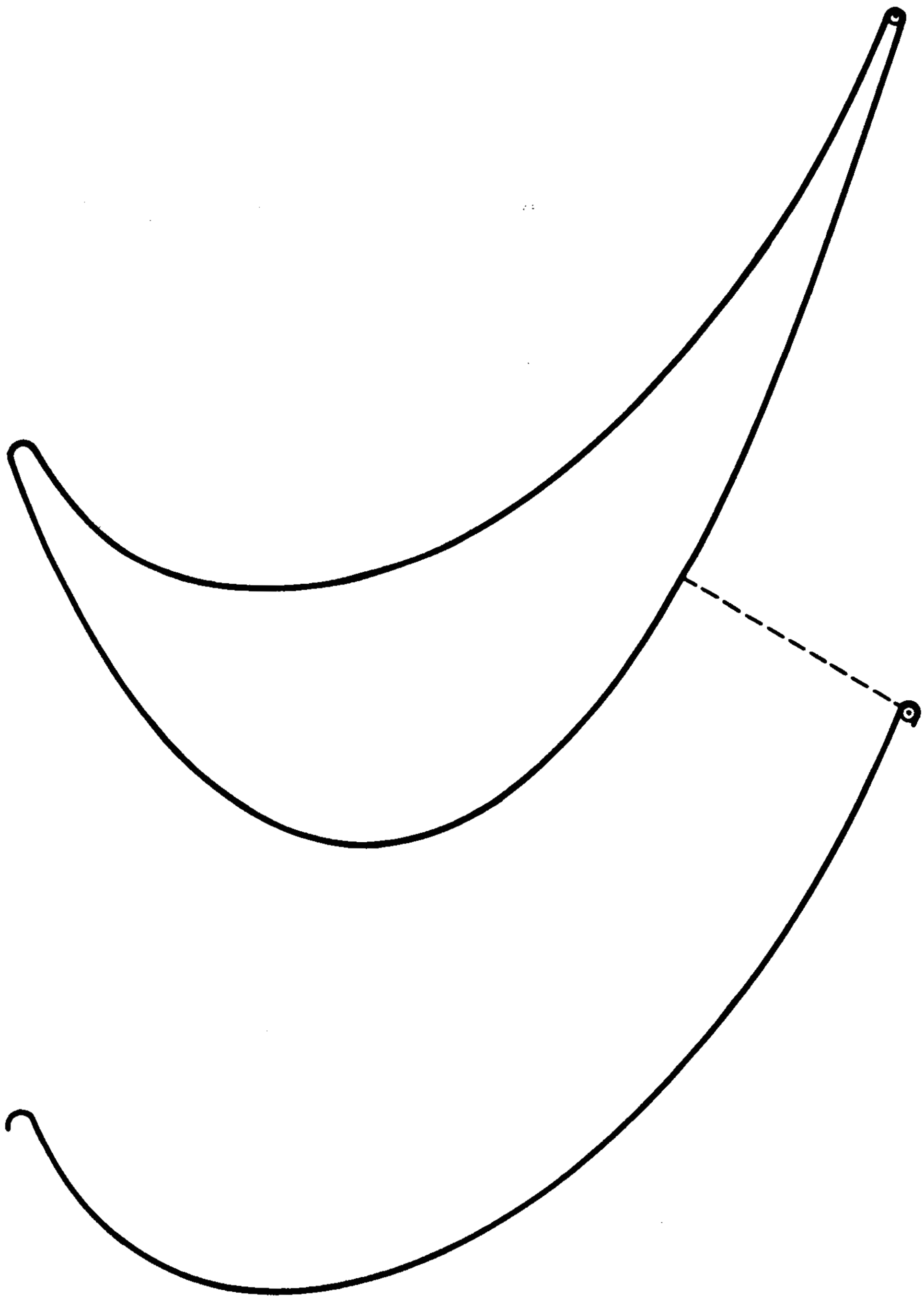

FIG. 51 THIRD STAGE VANE MEAN (5.0 SCALE)

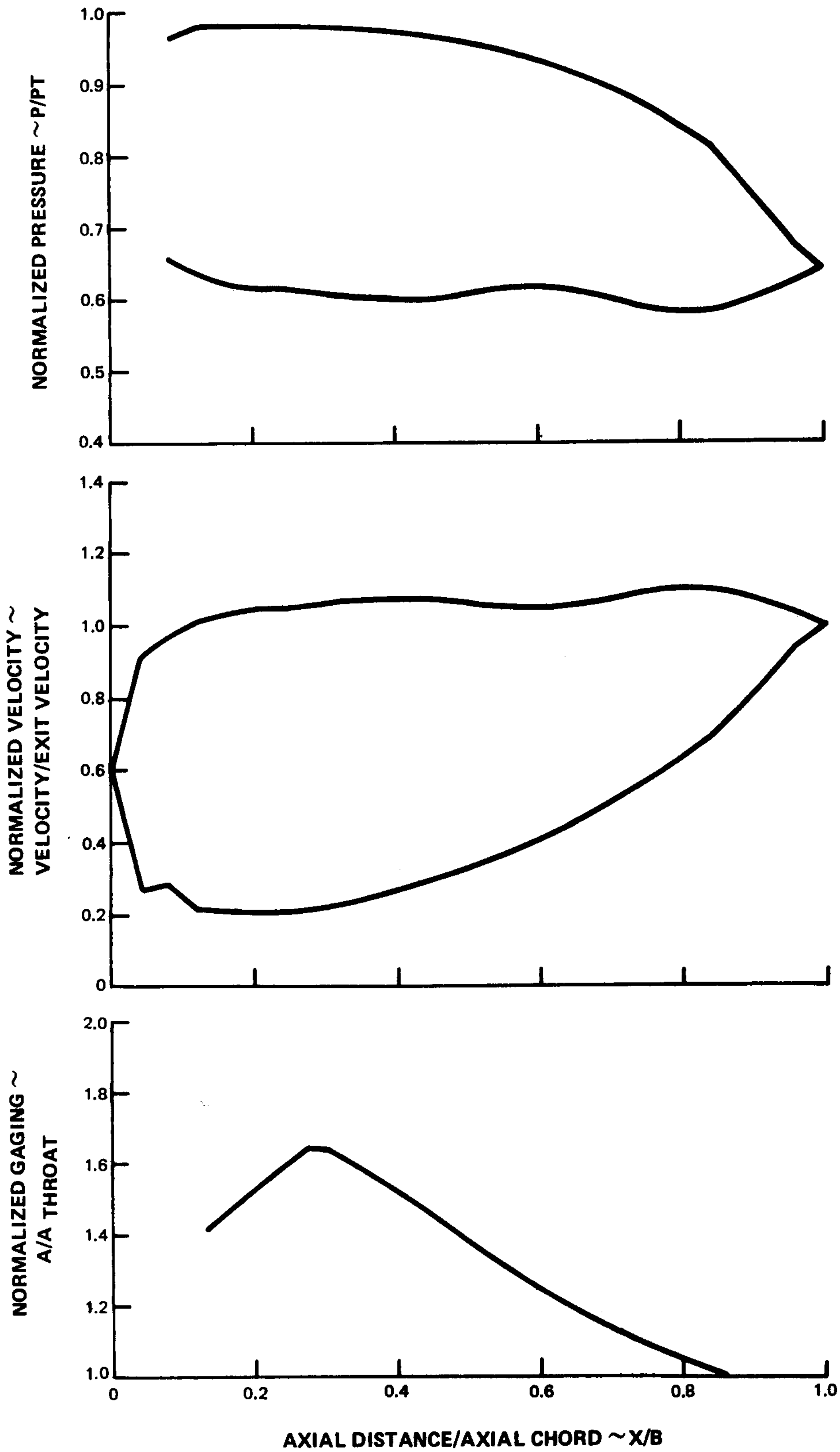

FIG. 52 THIRD STAGE VANE MEAN NORMALIZED PRESSURE VELOCITY AND GAGING DIAGRAMS

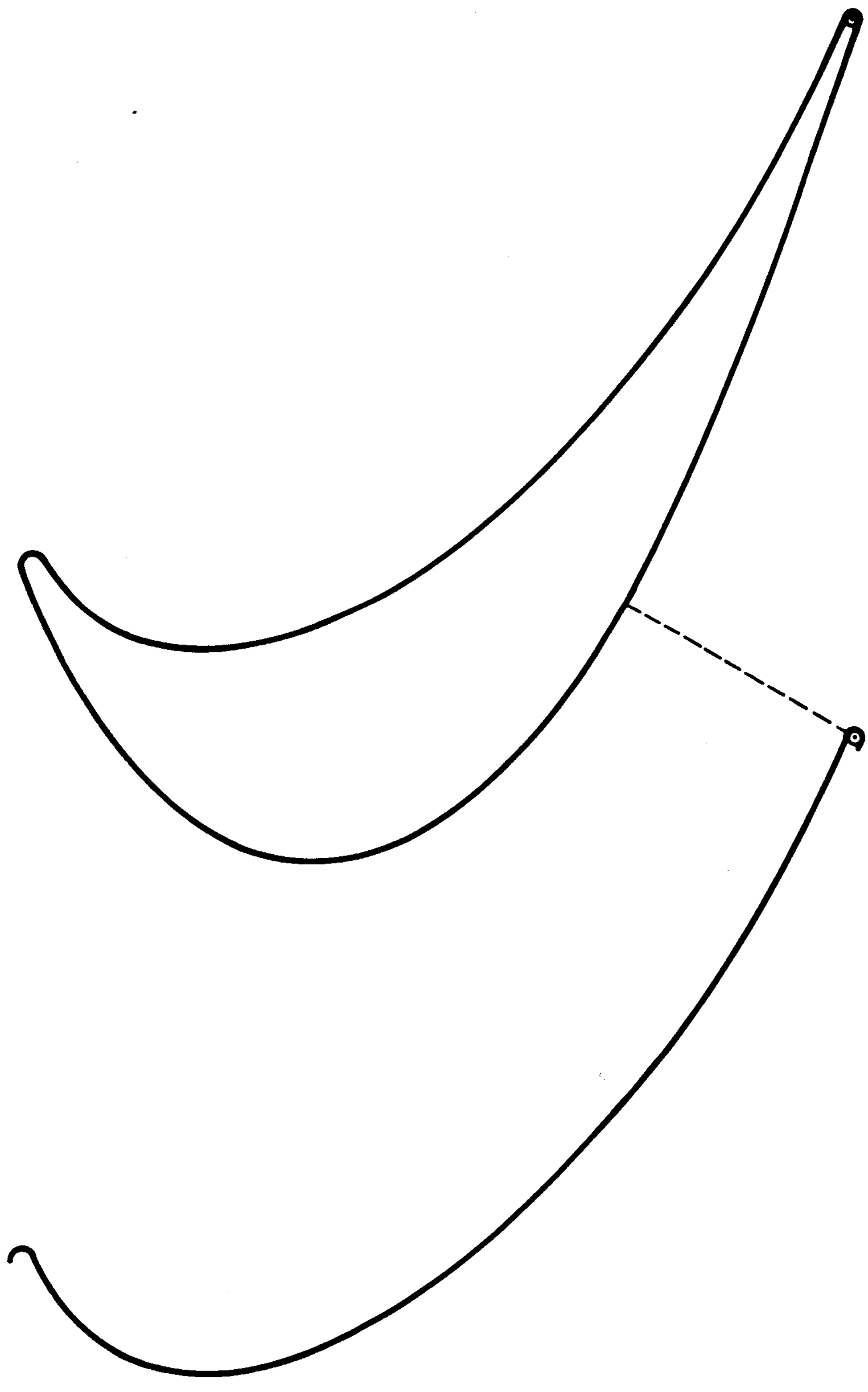

FIG. 53 THIRD STAGE VANE QUARTER TIP (5.0 SCALE)

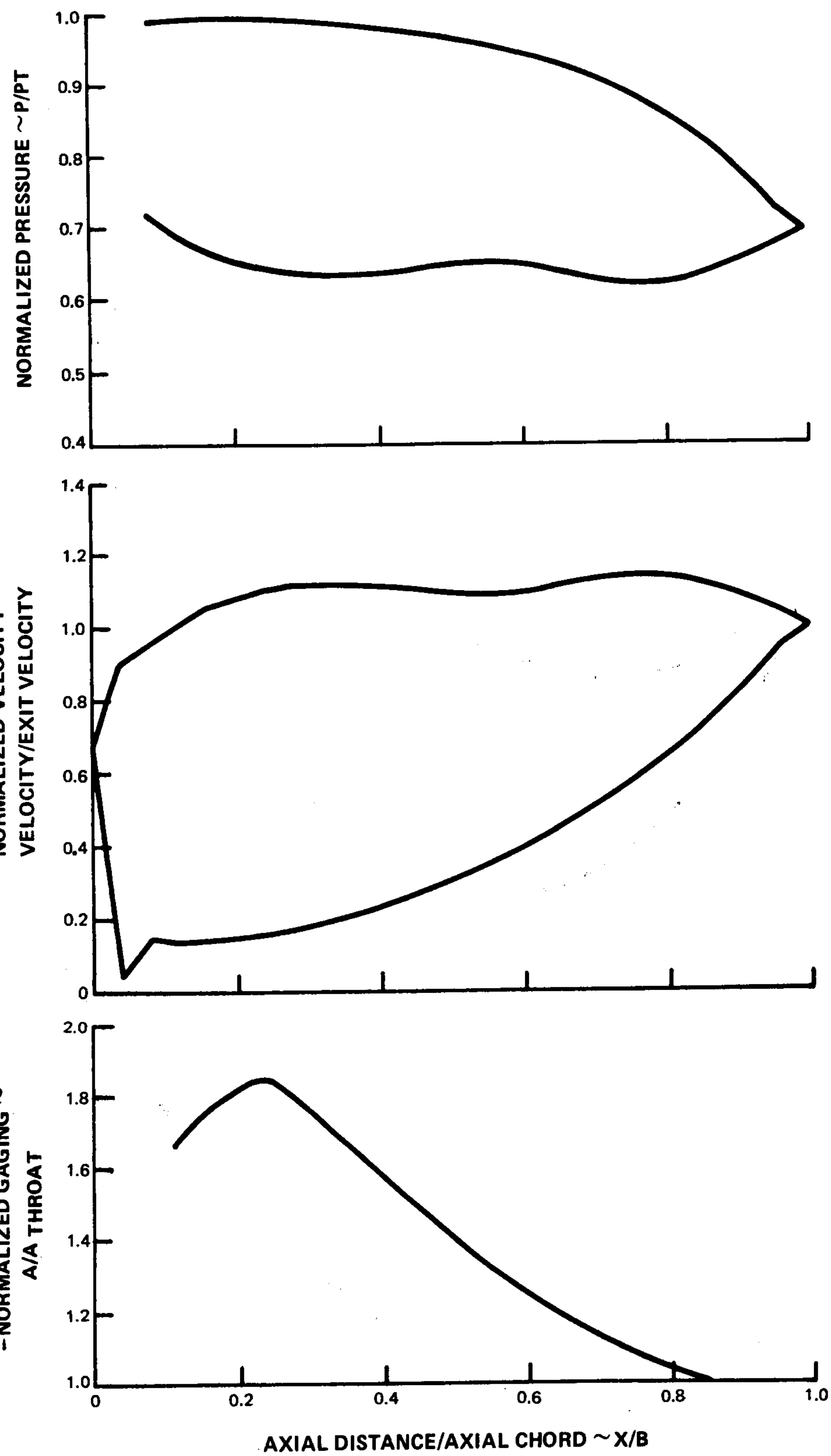

FIG. 54 THIRD STAGE VANE QUARTER TIP NORMALIZED PRESSURE VELOCITY AND GAGING DIAGRAMS

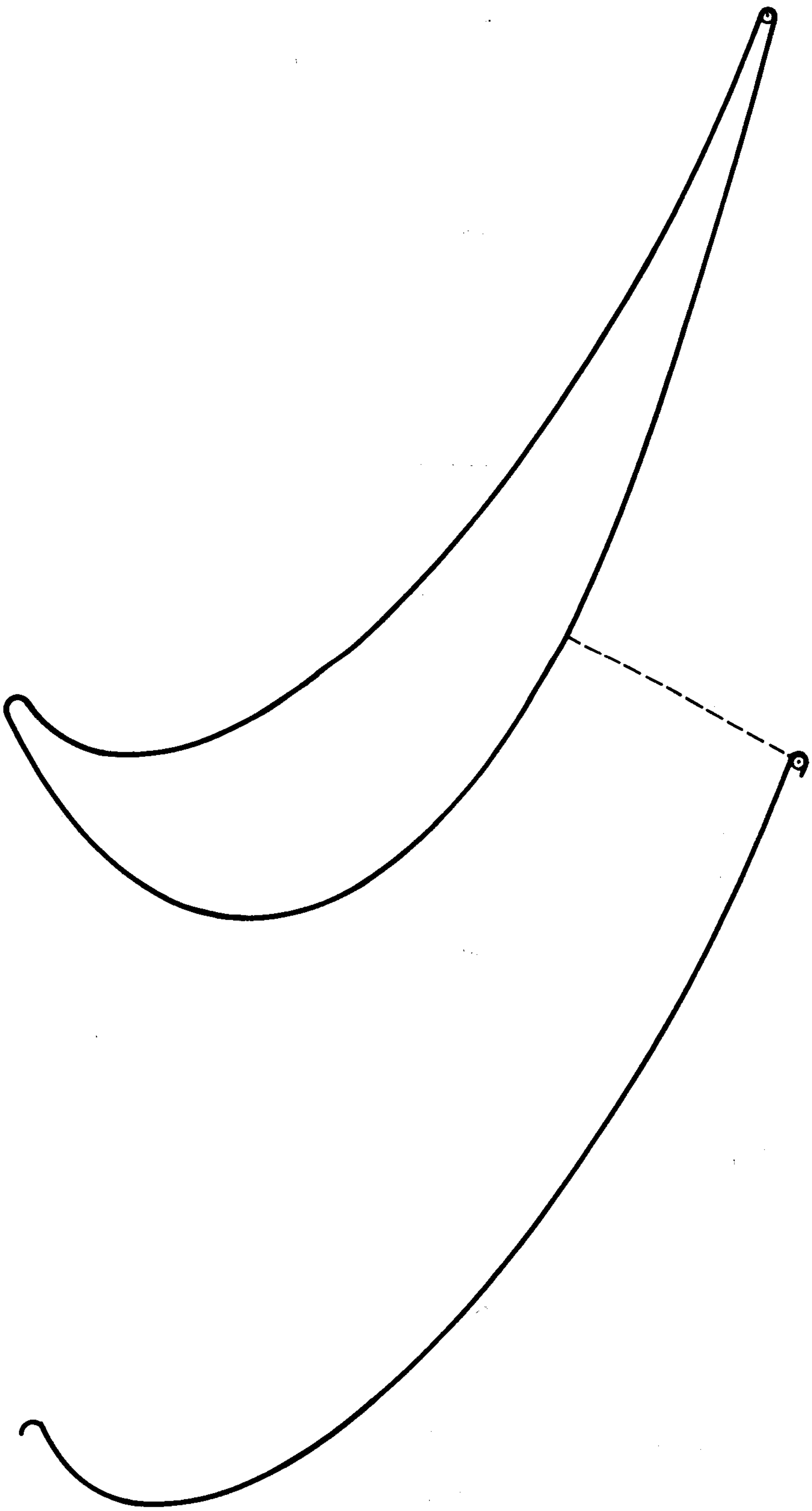

FIG. 55 THIRD STAGE VANE TIP (5.0 SCALE)

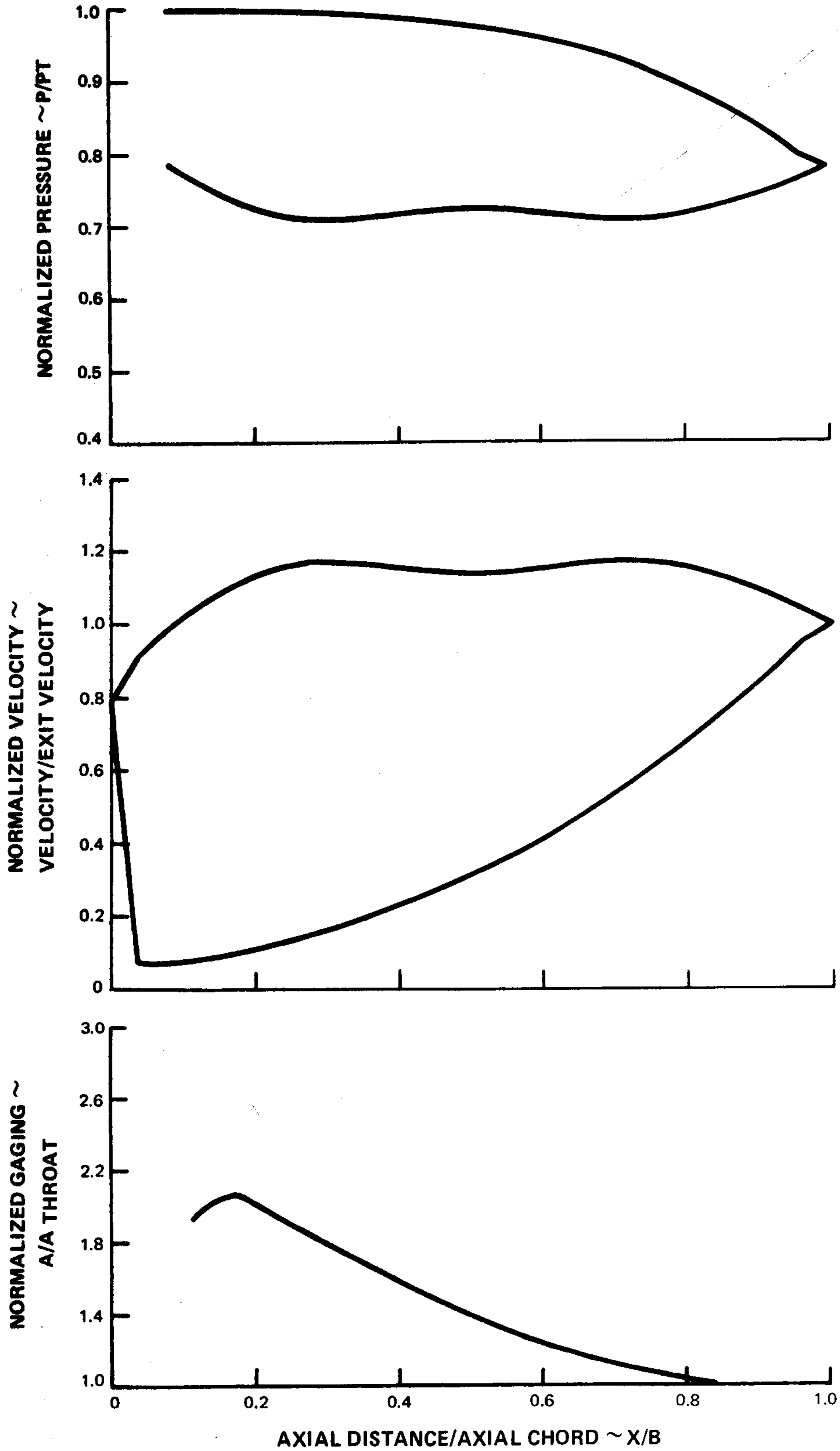

FIG. 56 THIRD STAGE VANE TIP NORMALIZED PRESSURE VELOCITY AND GAGING DIAGRAMS

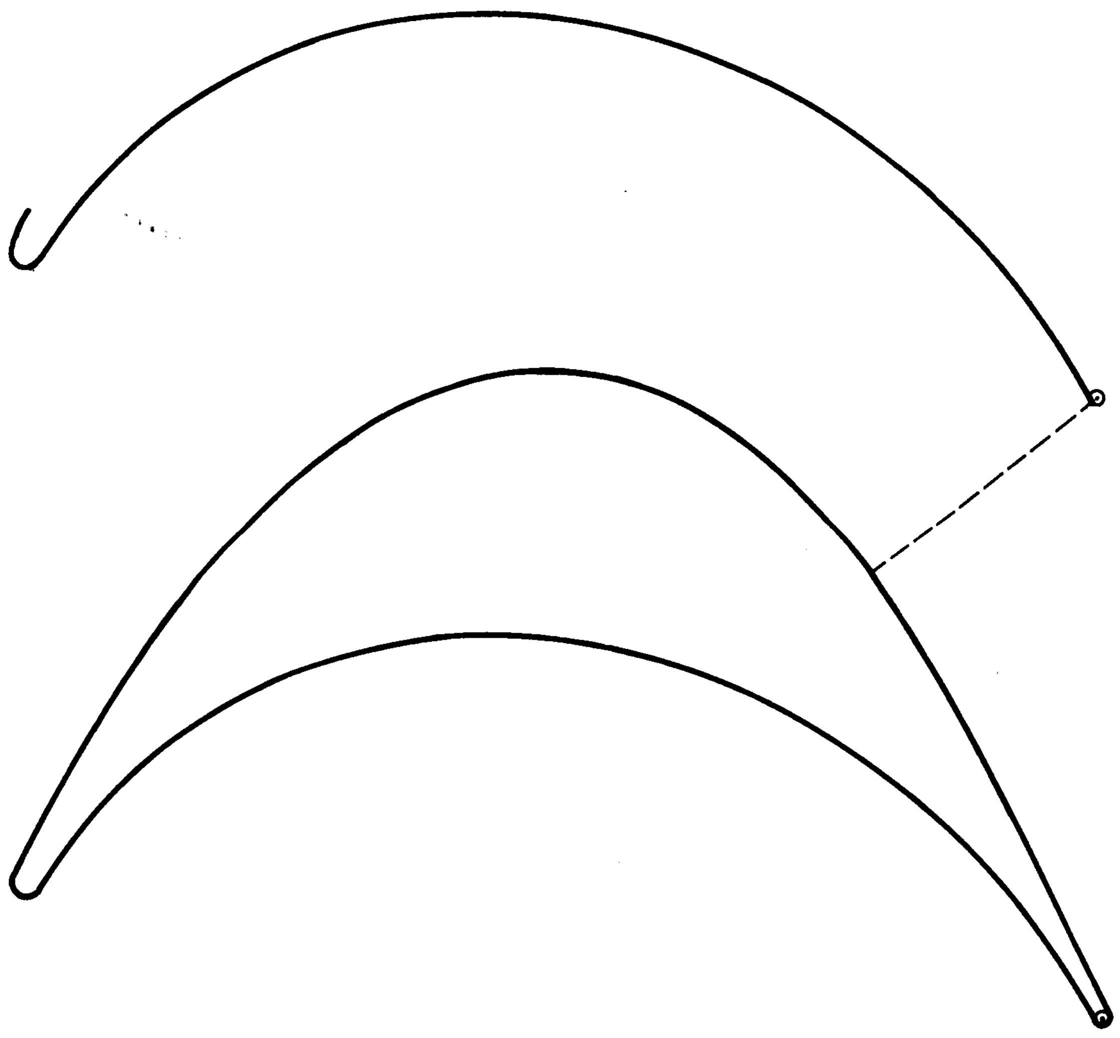

FIG. 57 THIRD STAGE BLADE ROOT 5.0 SCALE

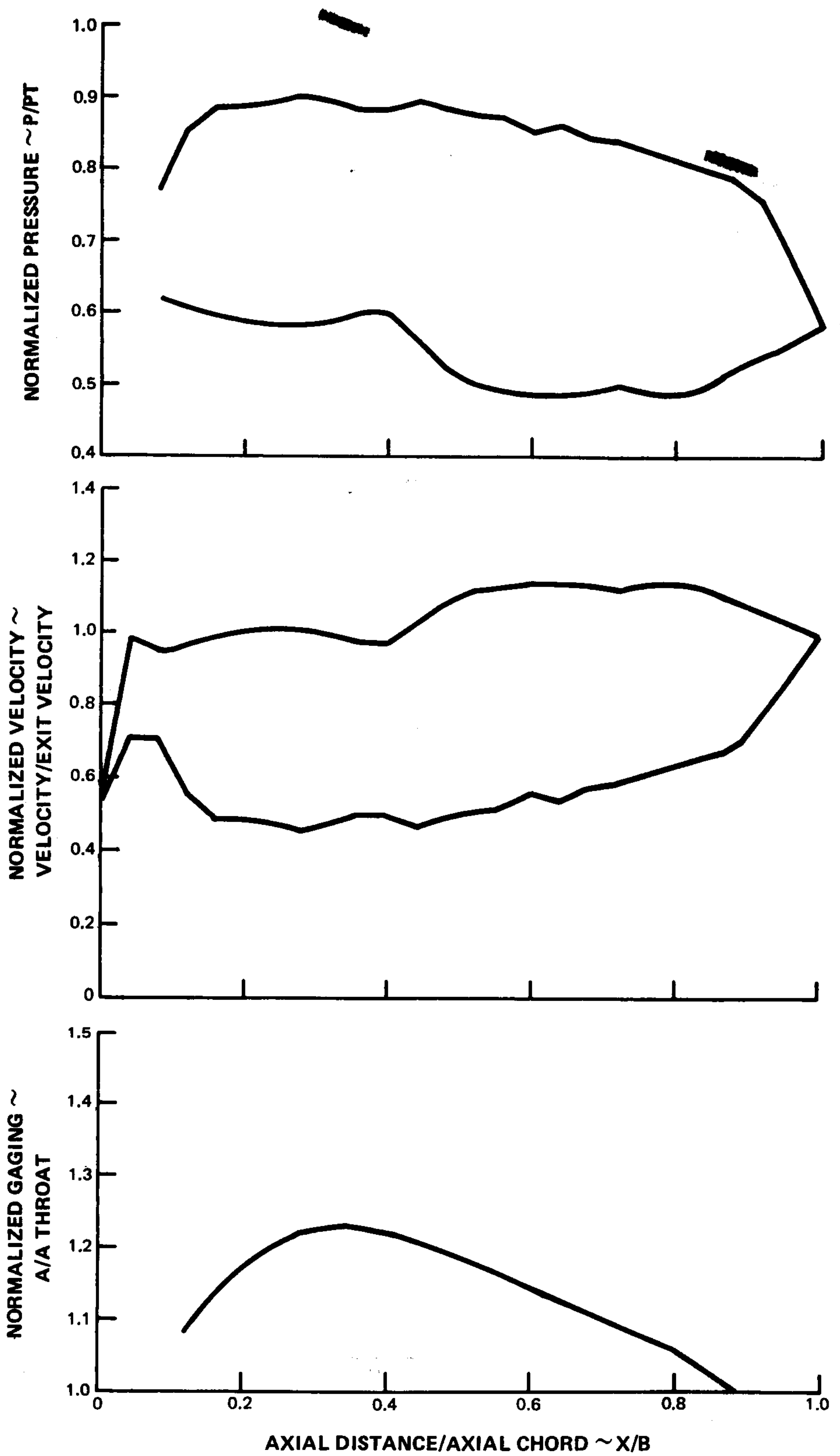

FIG. 58 THIRD STAGE BLADE ROOT NORMALIZED PRESSURE VELOCITY AND GAGING DIAGRAMS

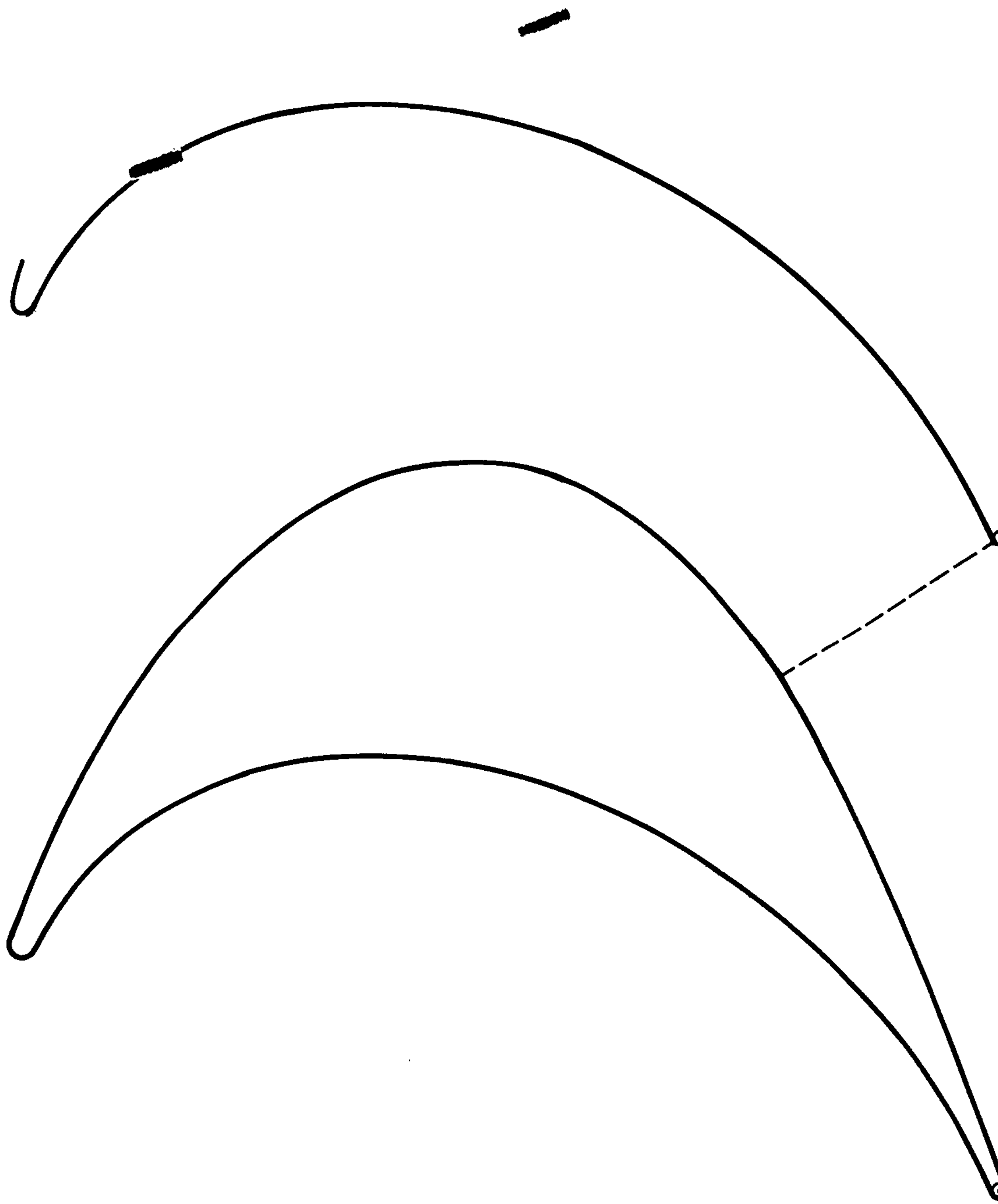

FIG. 59 THIRD STAGE BLADE QUARTER ROOT (5.0 SCALE)

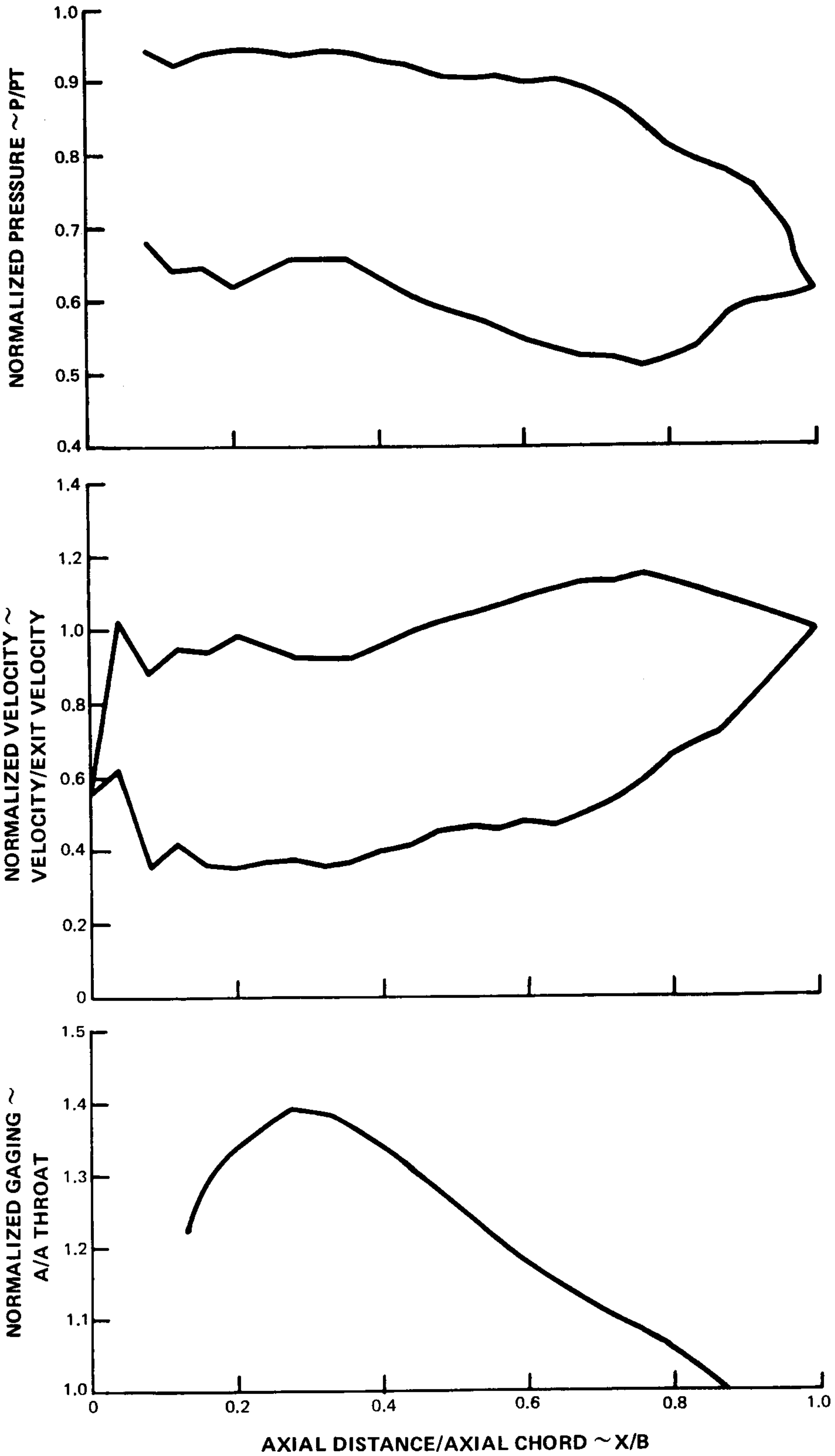

FIG. 60 THIRD STAGE BLADE QUARTER ROOT NORMALIZED PRESSURE VELOCITY AND GAGING DIAGRAMS

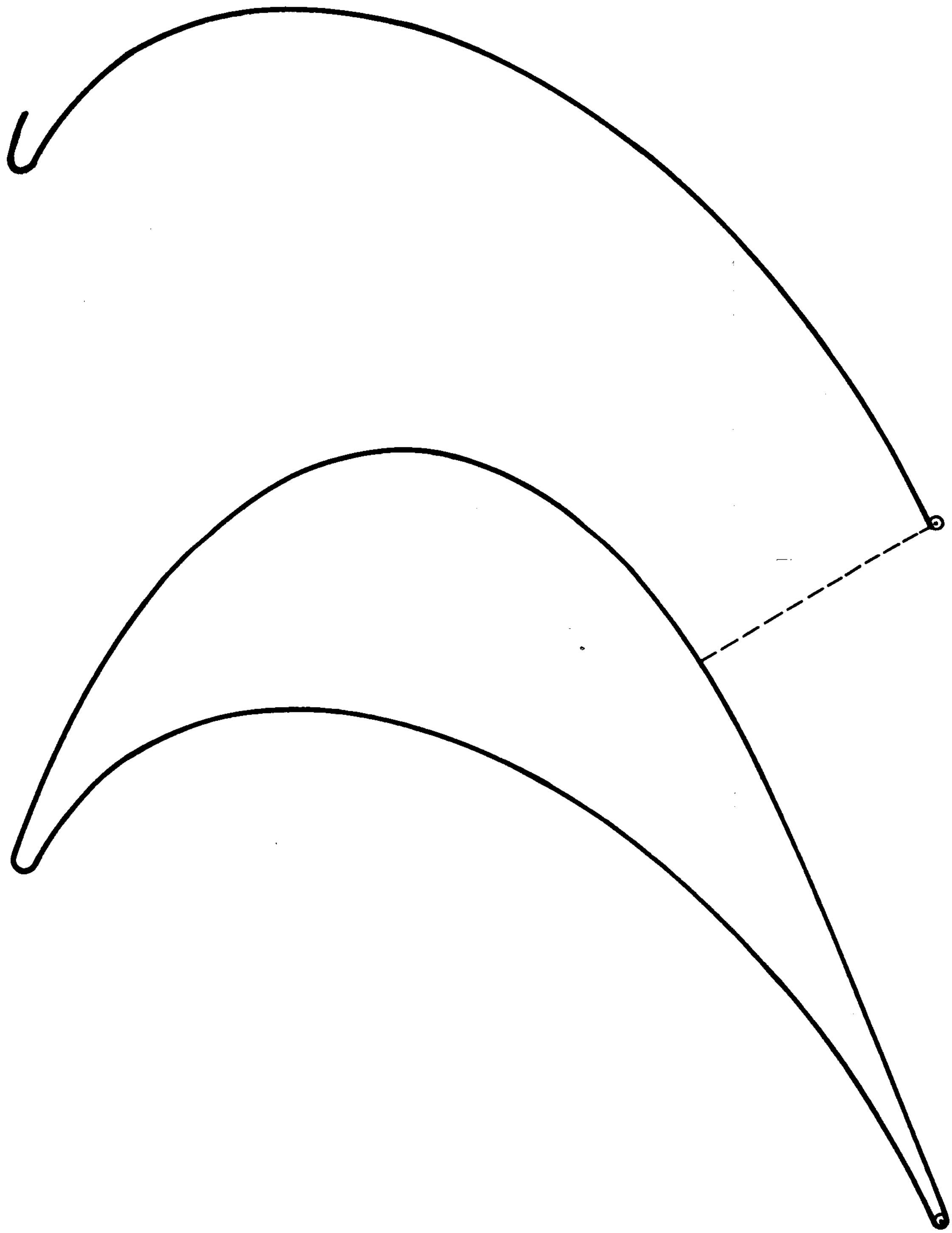

FIG. 61 THIRD STAGE BLADE MEAN **5.0 SCALE**

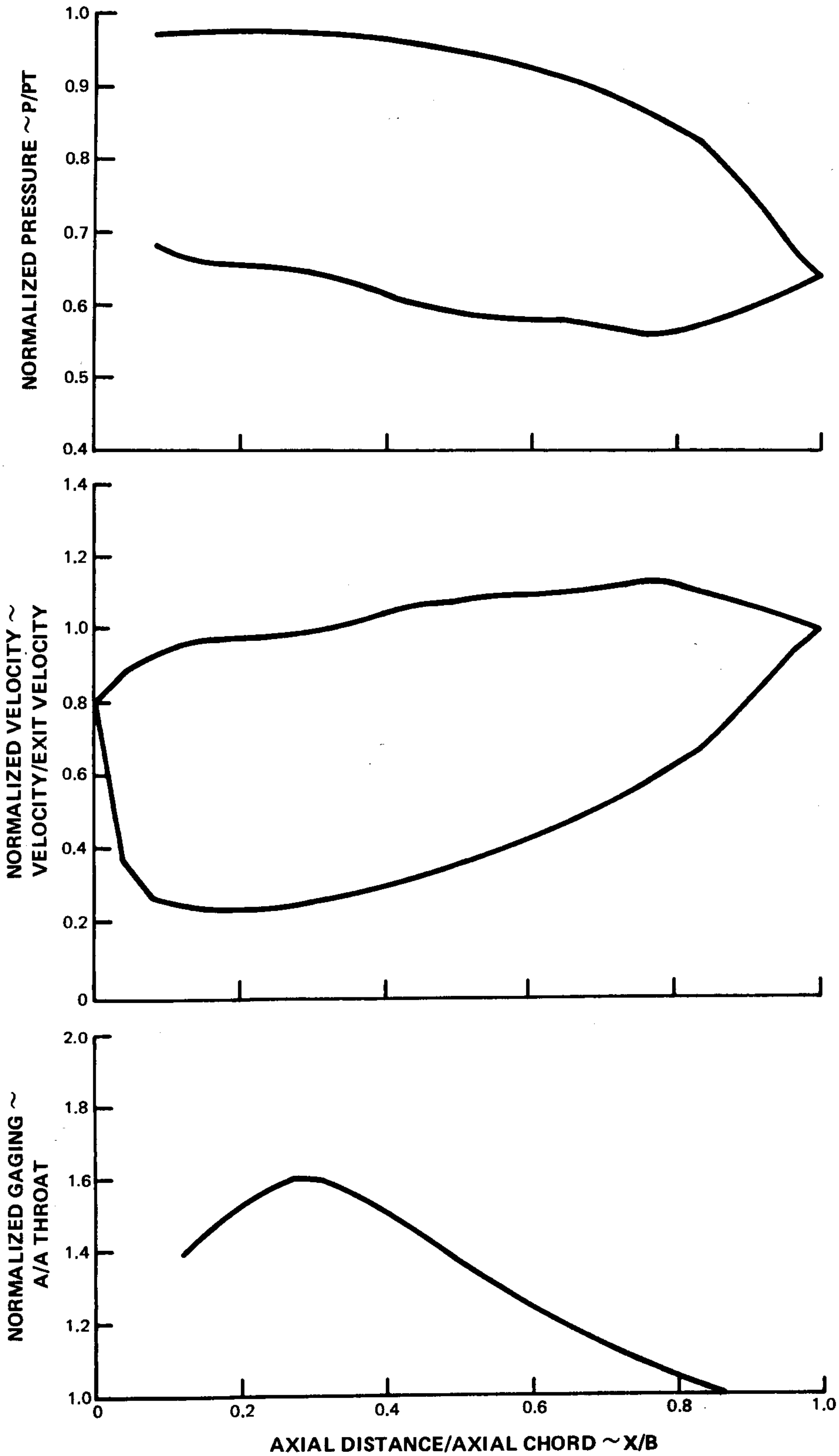

FIG. 62 THIRD STAGE BLADE MEAN NORMALIZED PRESSURE VELOCITY AND GAGING DIAGRAMS

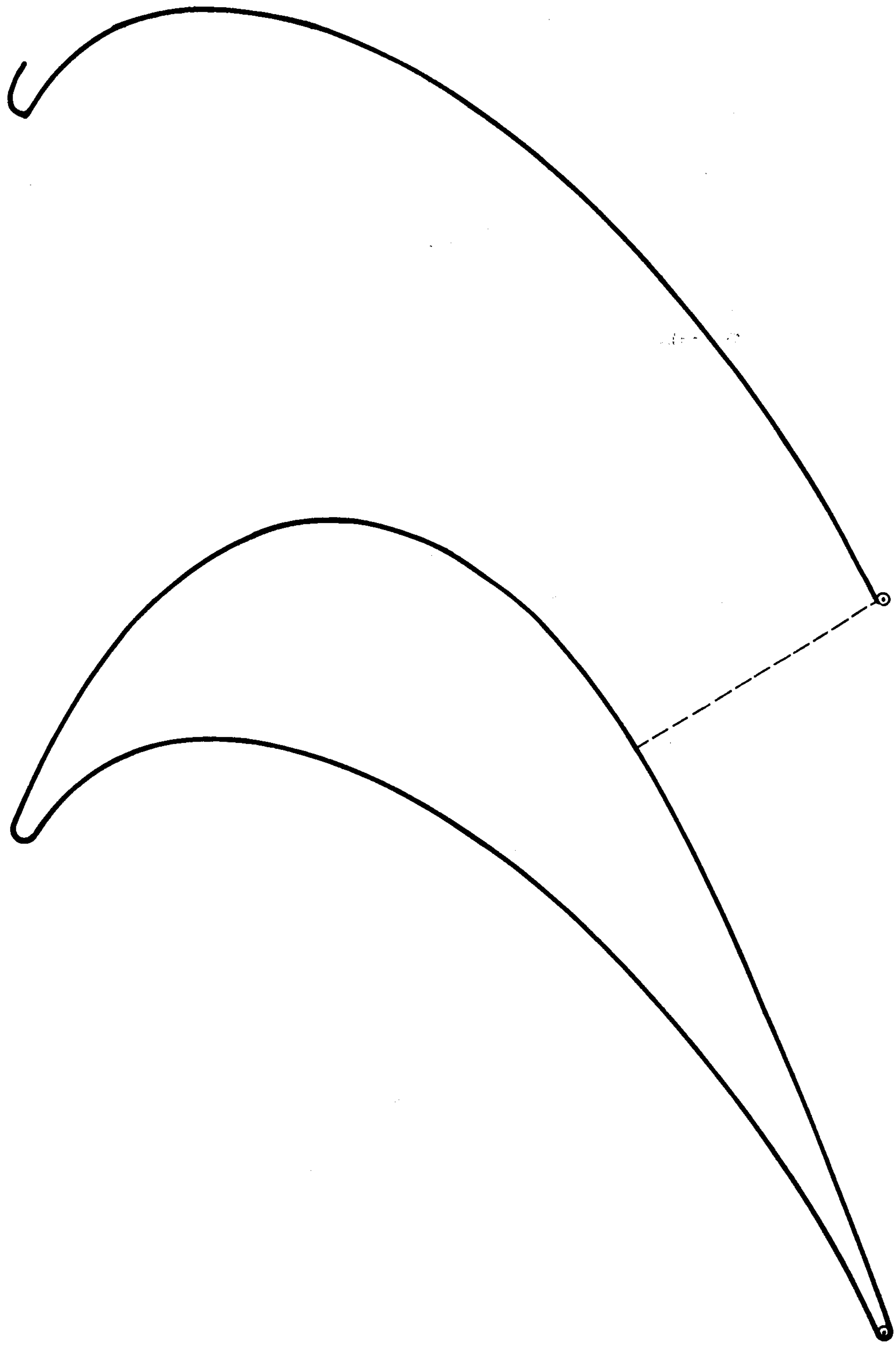

FIG. 63 THIRD STAGE BLADE QUARTER TIP **5.0 SCALE**

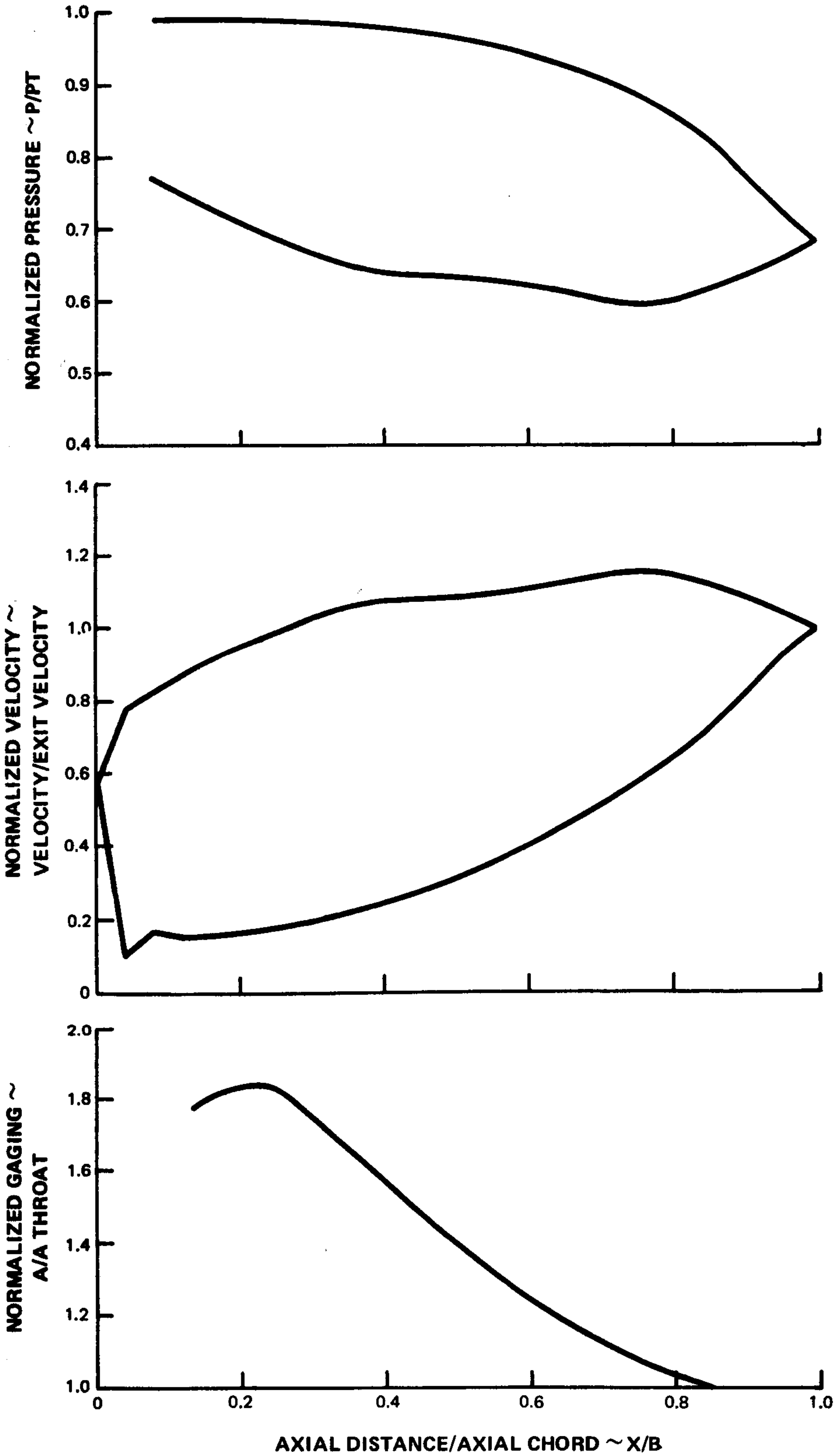

FIG. 64 THIRD STAGE BLADE QUARTER TIP NORMALIZED PRESSURE VELOCITY AND GAGING DIAGRAMS

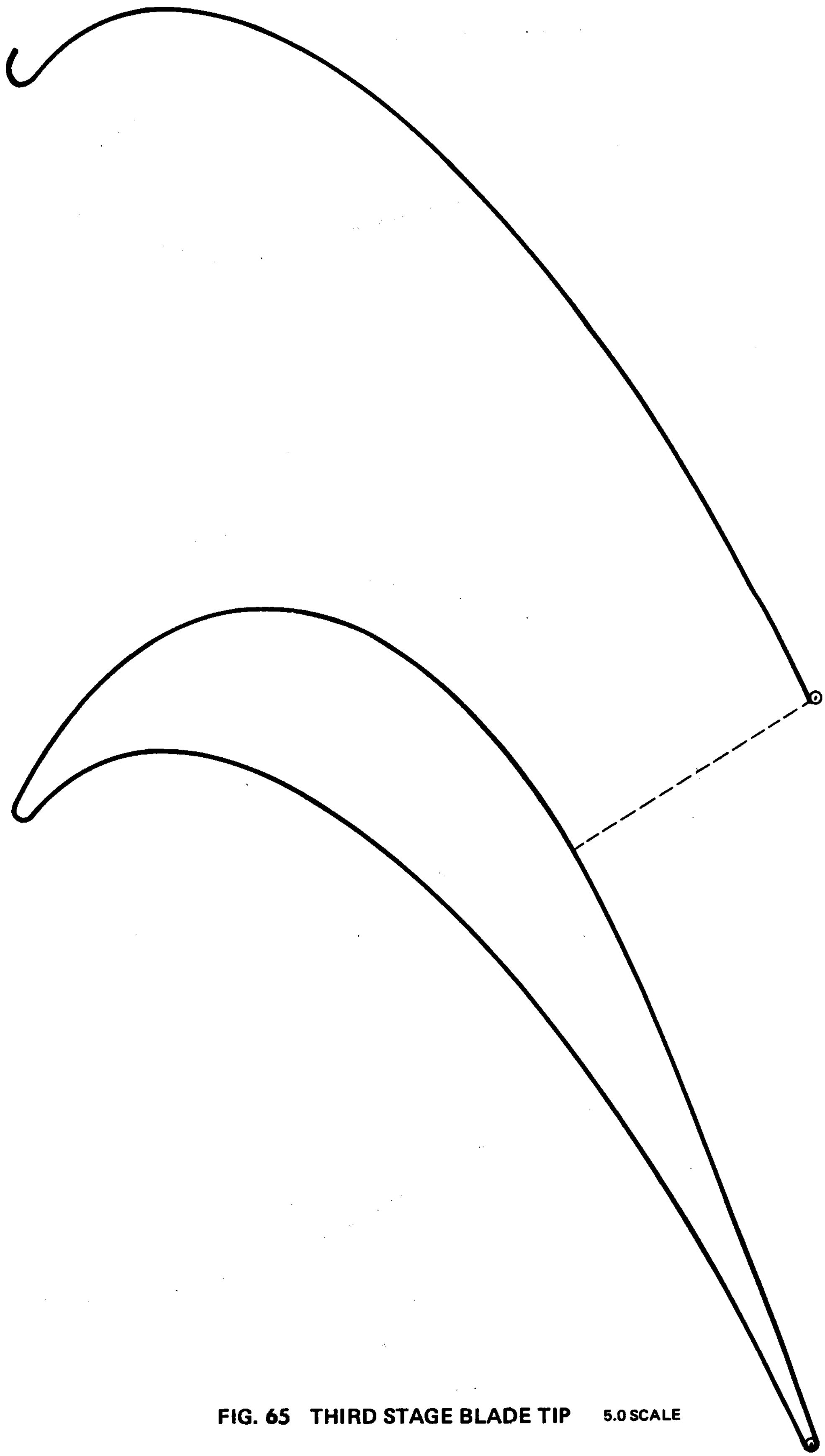

FIG. 65 THIRD STAGE BLADE TIP 5.0 SCALE

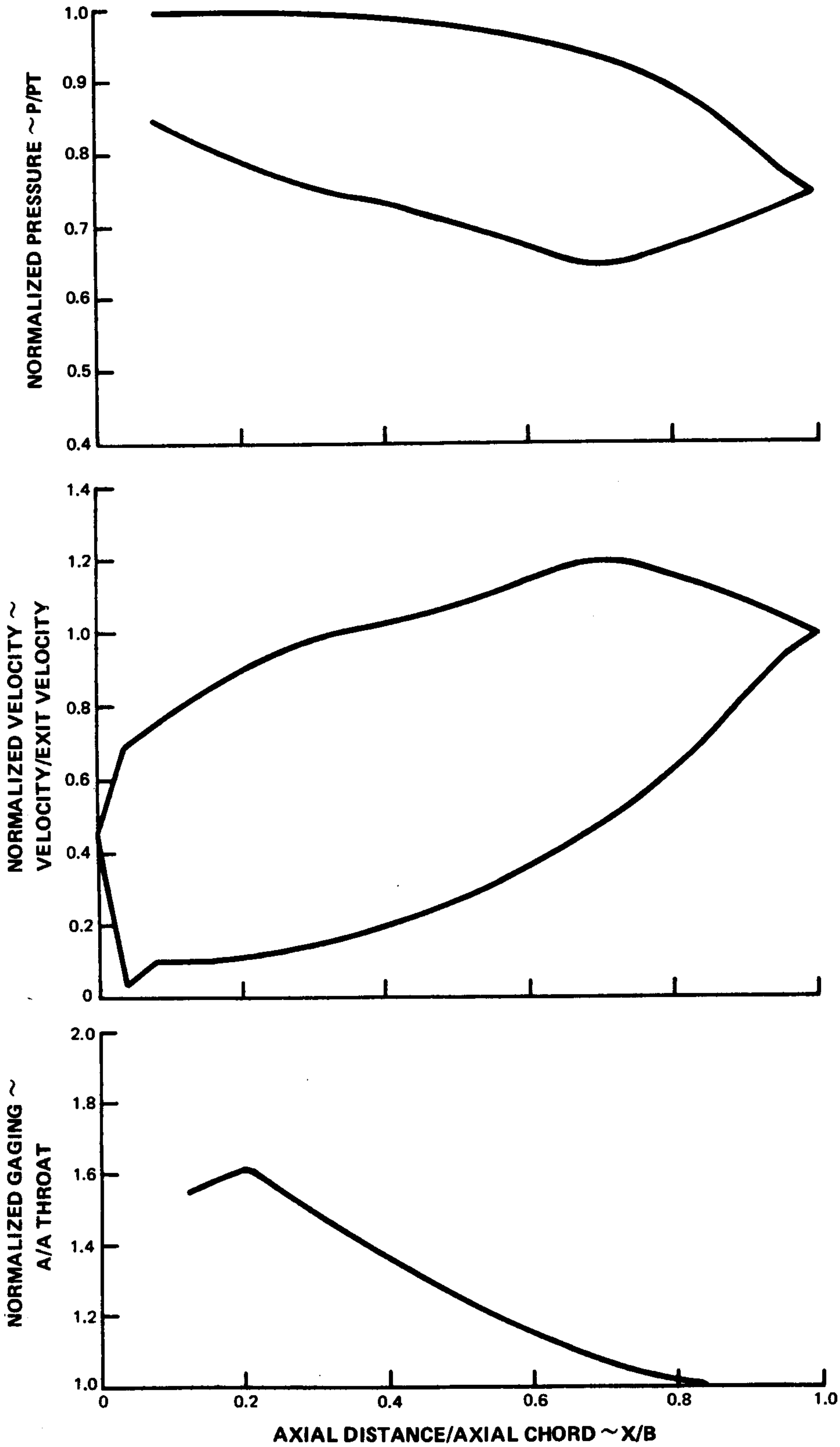

FIG. 66 THIRD STAGE BLADE TIP NORMALIZED PRESSURE VELOCITY AND GAGING DIAGRAMS

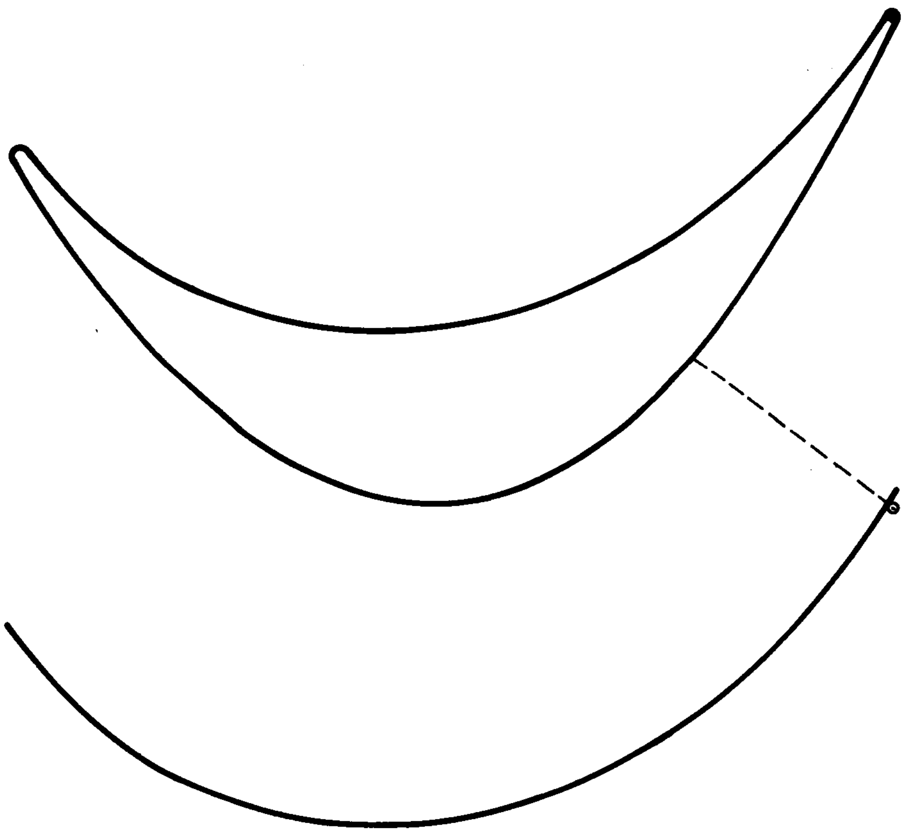

FIG. 67 FOURTH STAGE VANE ROOT (2.5 SCALE)

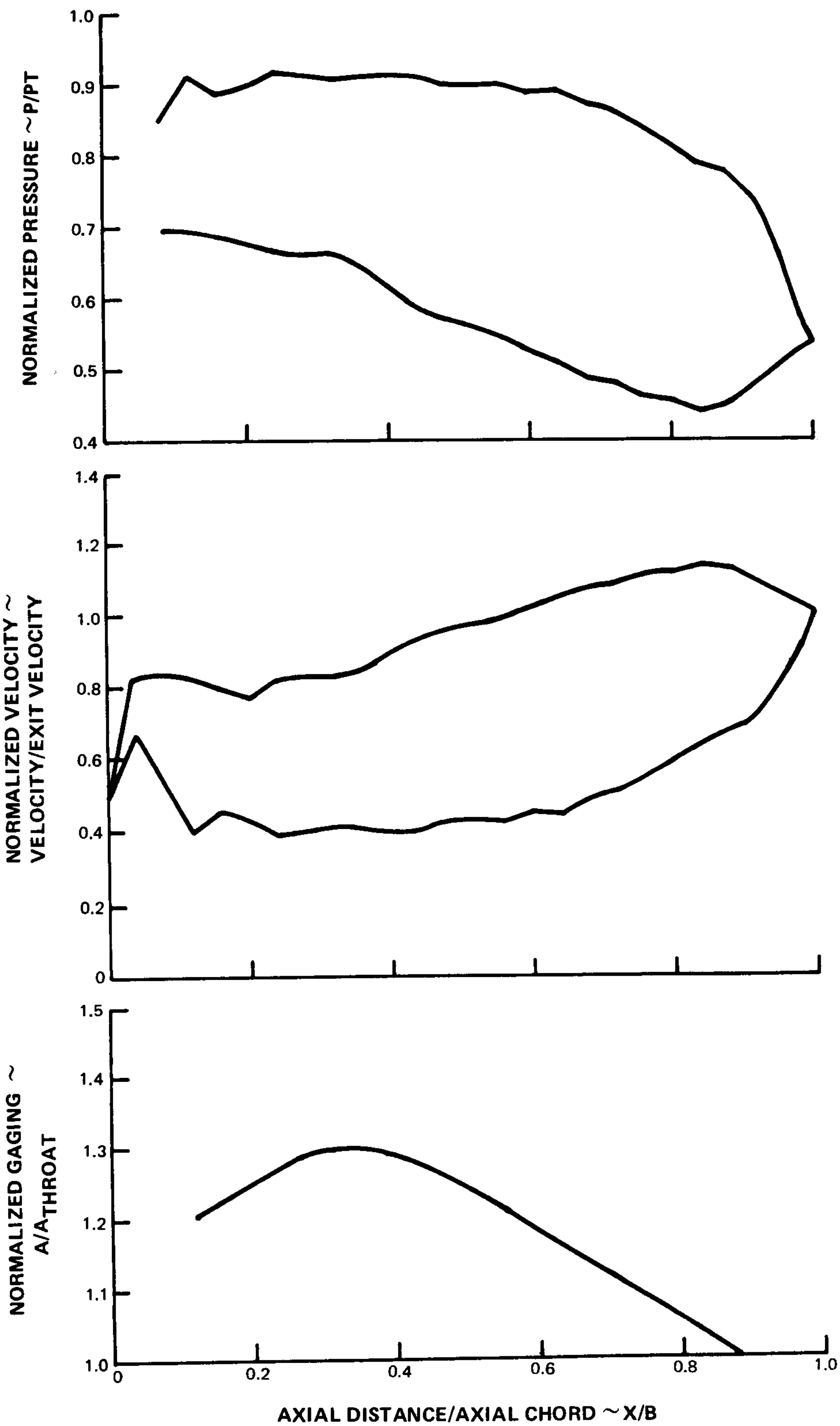

FIG. 68 FOURTH STAGE VANE ROOT NORMALIZED PRESSURE VELOCITY AND GAGING DIAGRAMS

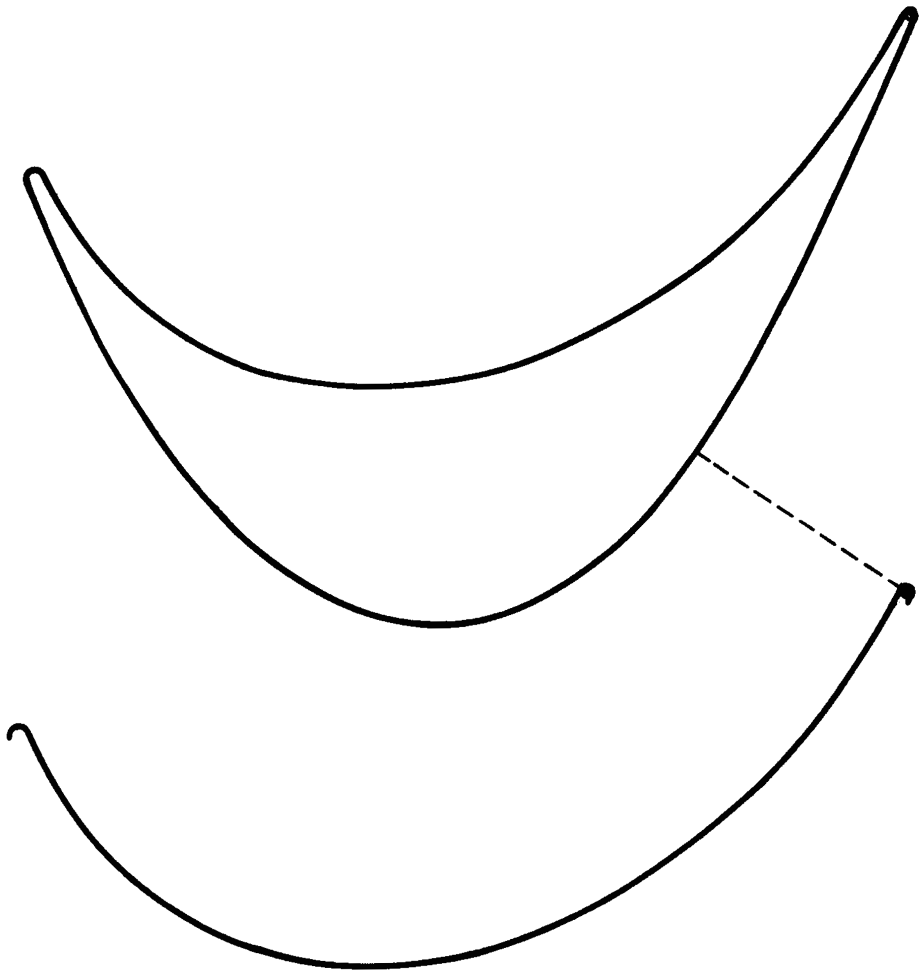

FIG. 69 FOURTH STAGE VANE QUARTER ROOT (2.5 SCALE)

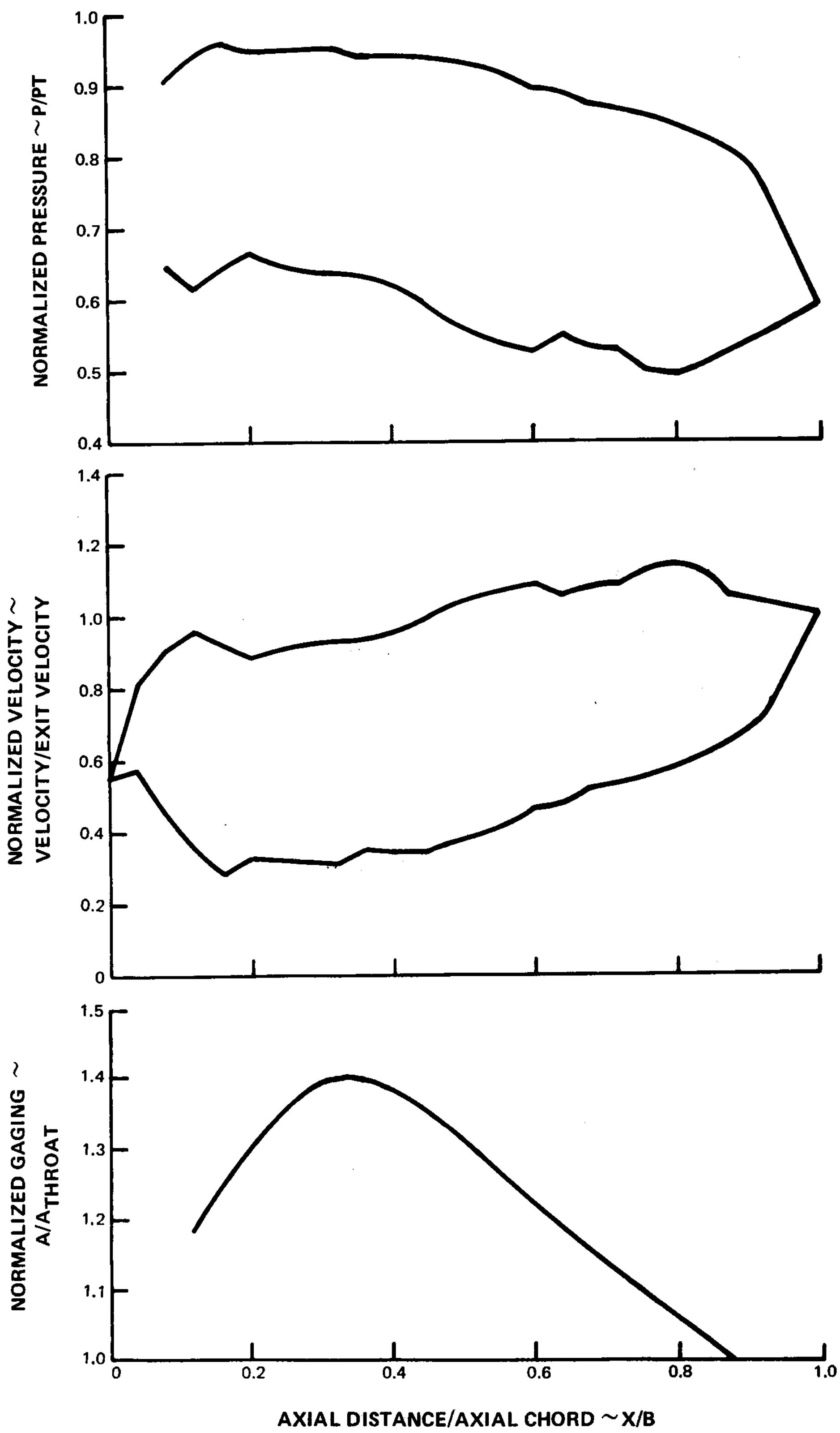

FIG. 70 FOURTH STAGE VANE QUARTER ROOT NORMALIZED PRESSURE VELOCITY AND GAGING DIAGRAMS

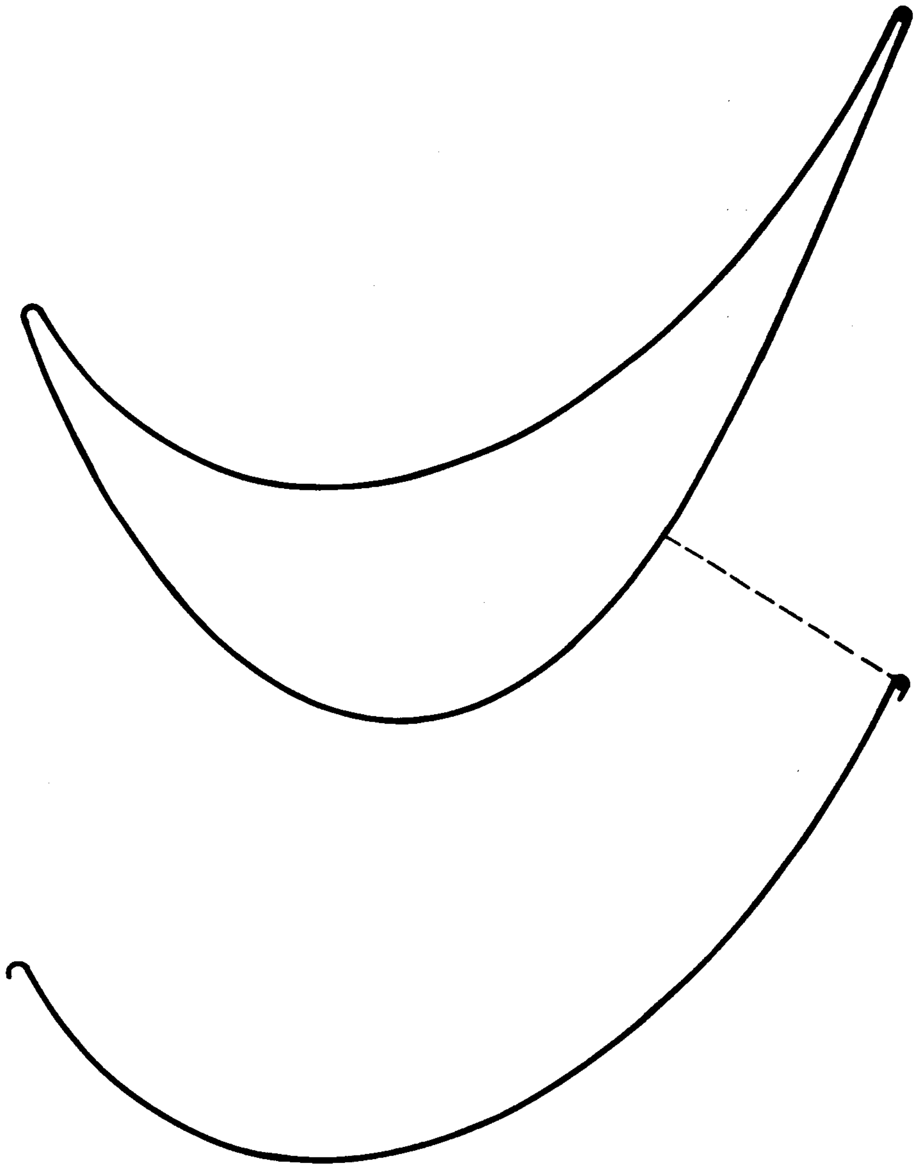

FIG. 71 FOURTH STAGE VANE MEAN (2.5 SCALE)

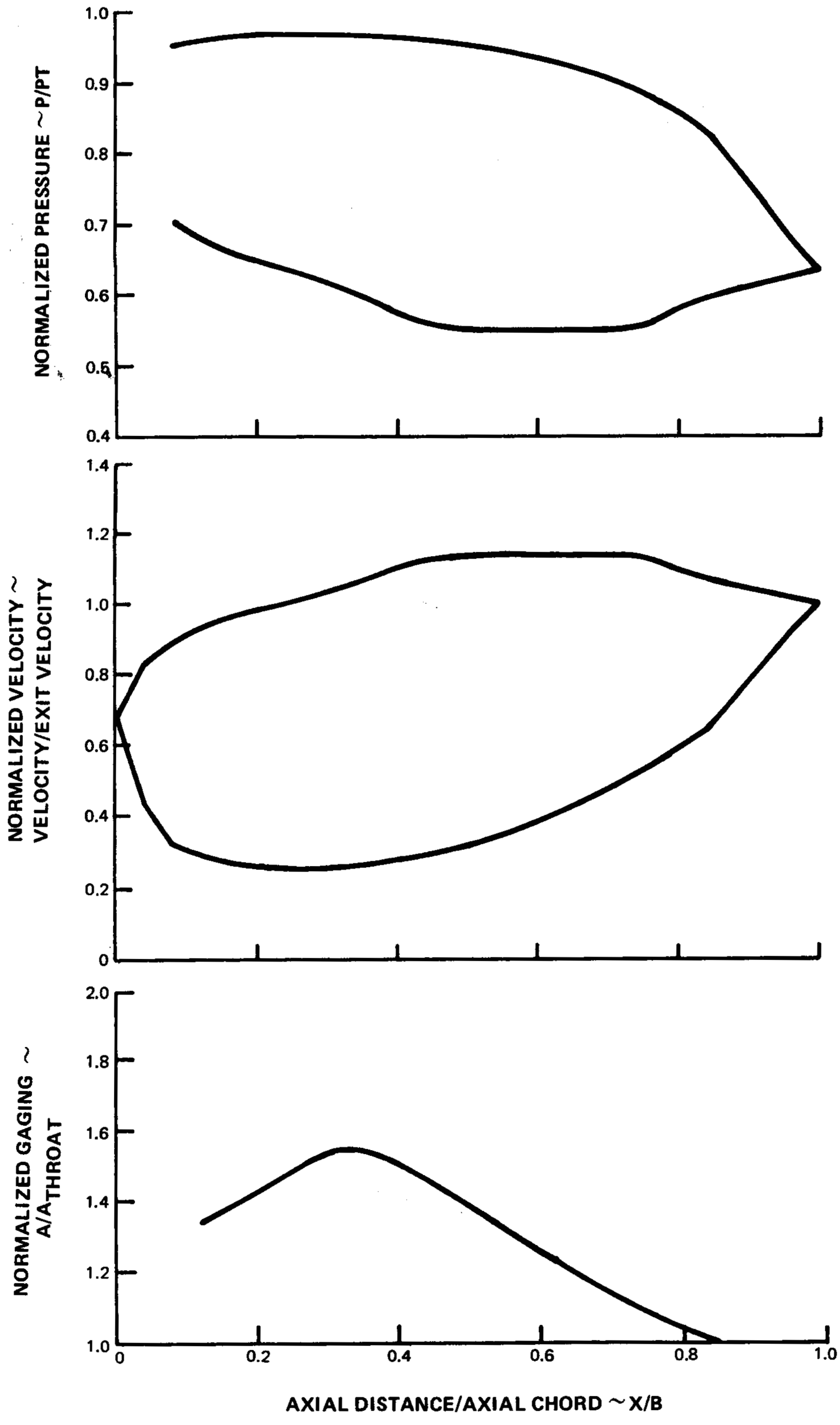

FIG. 72 FOURTH STAGE VANE MEAN NORMALIZED PRESSURE VELOCITY AND GAGING DIAGRAMS

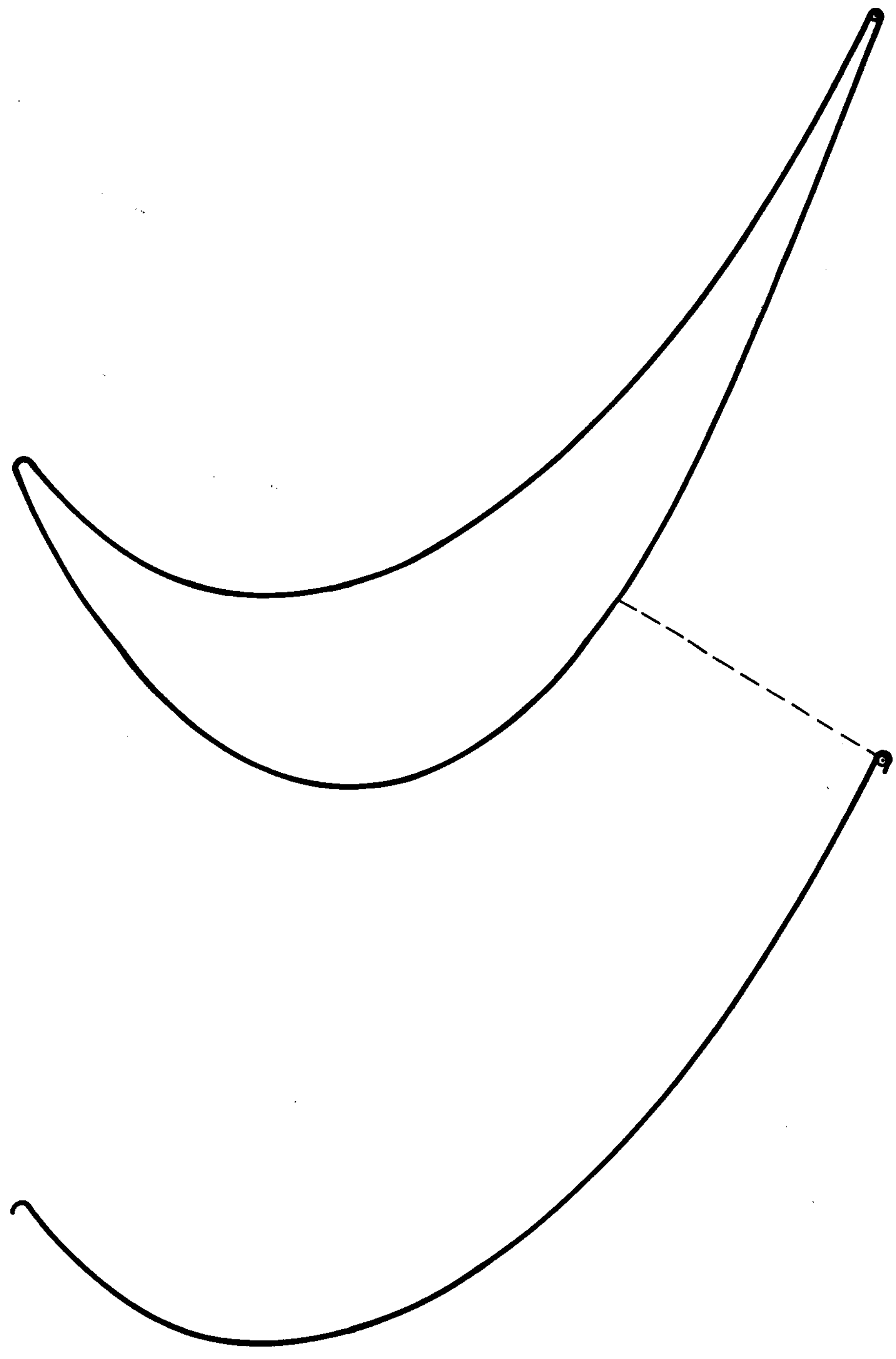

FIG. 73 FOURTH STAGE VANE QUARTER TIP (2.5 SCALE)

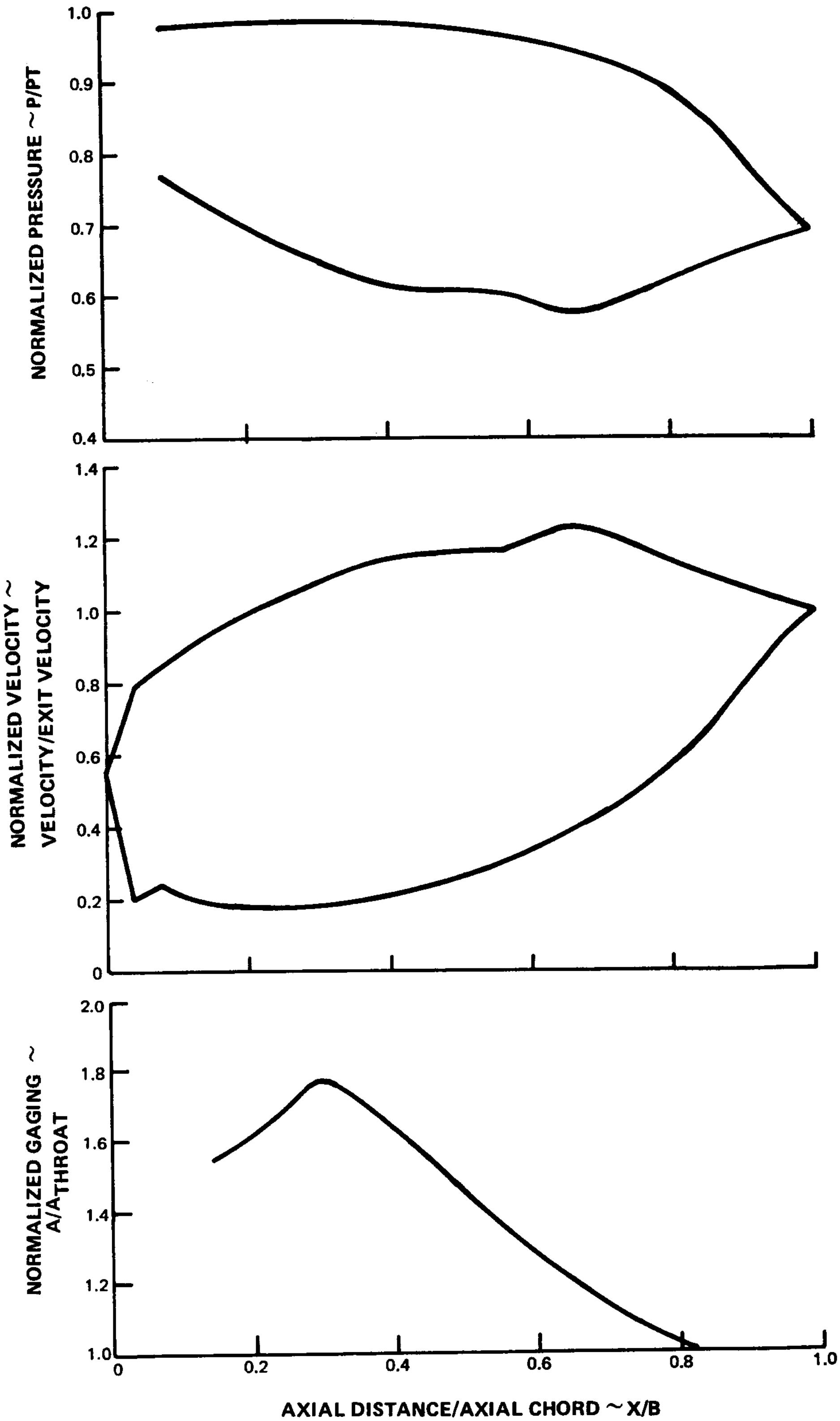

FIG. 74 FOURTH STAGE VANE QUARTER TIP NORMALIZED PRESSURE VELOCITY AND GAGING DIAGRAMS

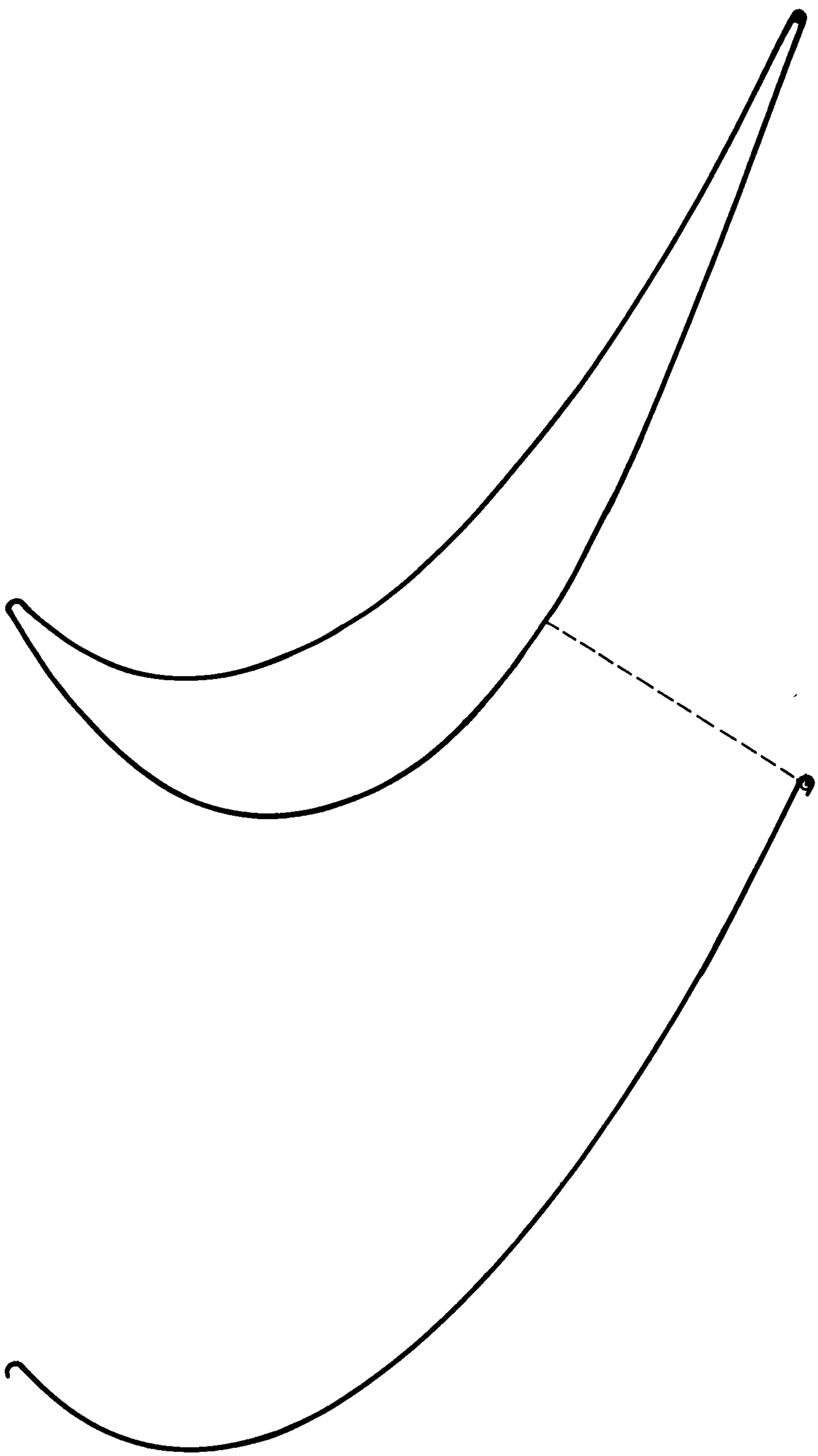

FIG. 75 FOURTH STAGE VANE TIP (2.5 SCALE)

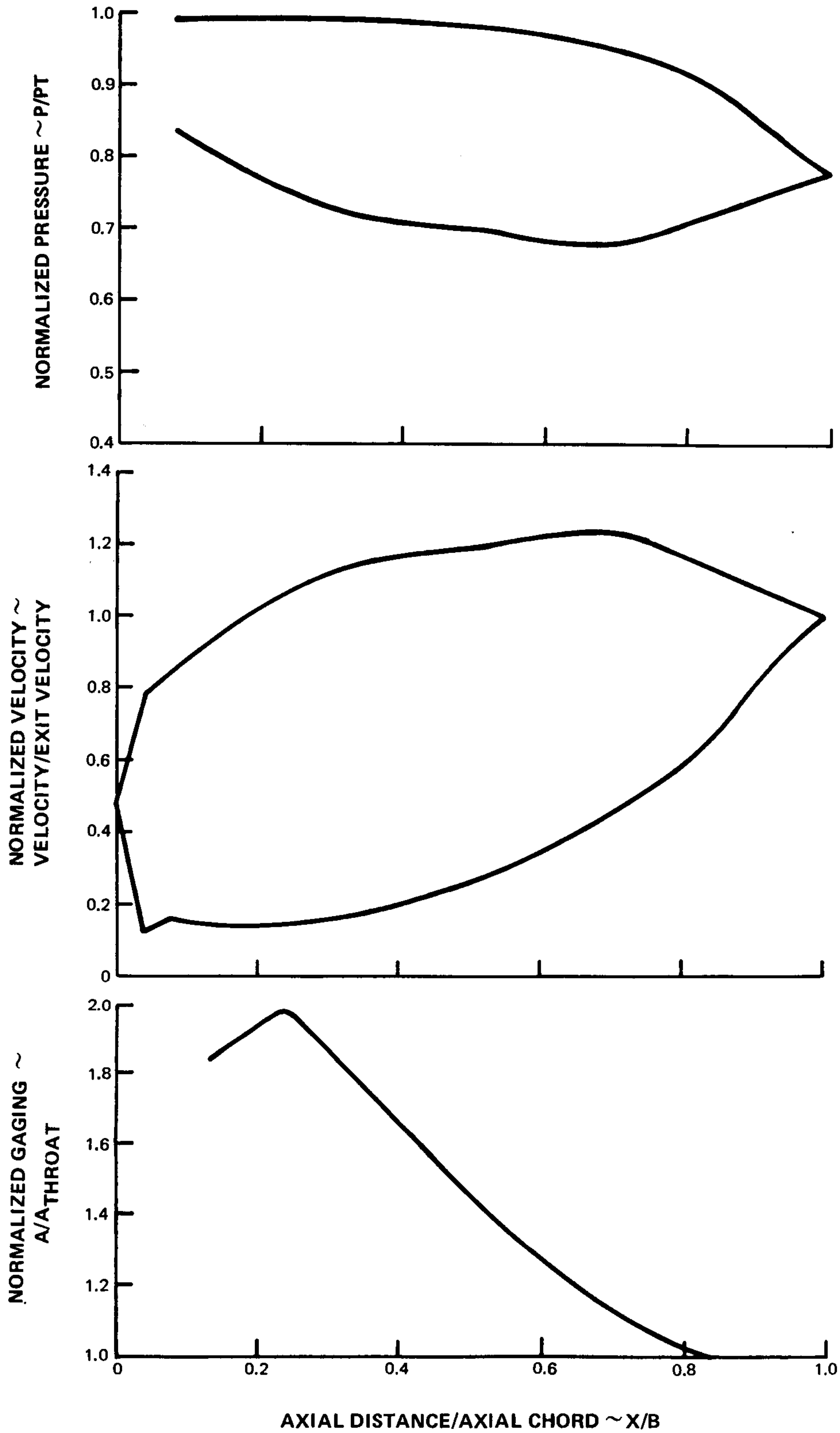

FIG. 76 FOURTH STAGE VANE TIP NORMALIZED PRESSURE VELOCITY AND GAGING DIAGRAMS

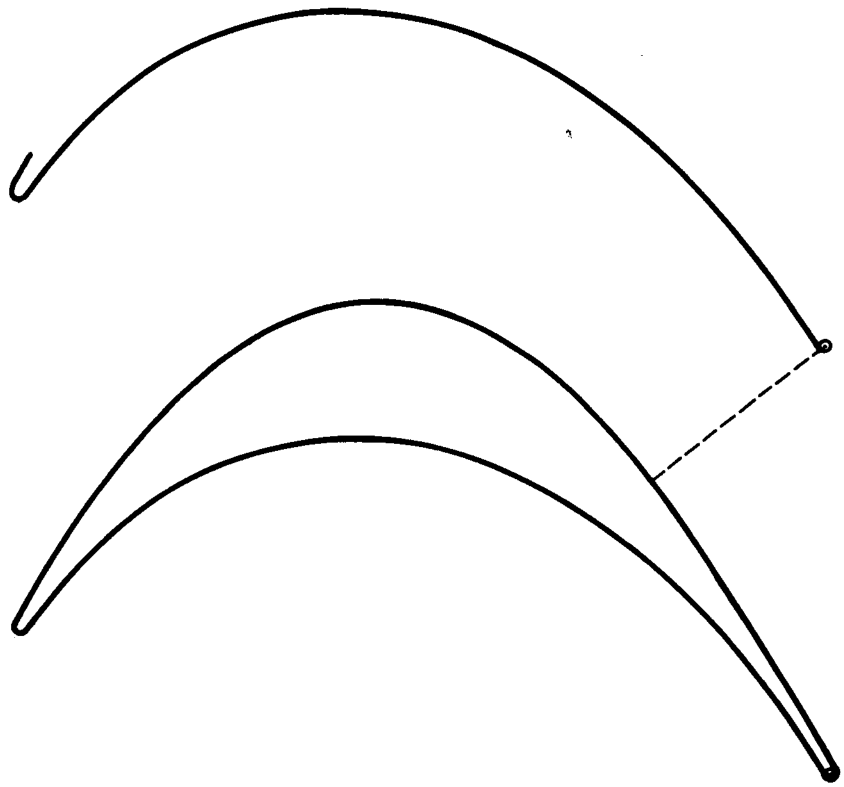

FIG. 77 FOURTH STAGE BLADE ROOT 2.5 SCALE

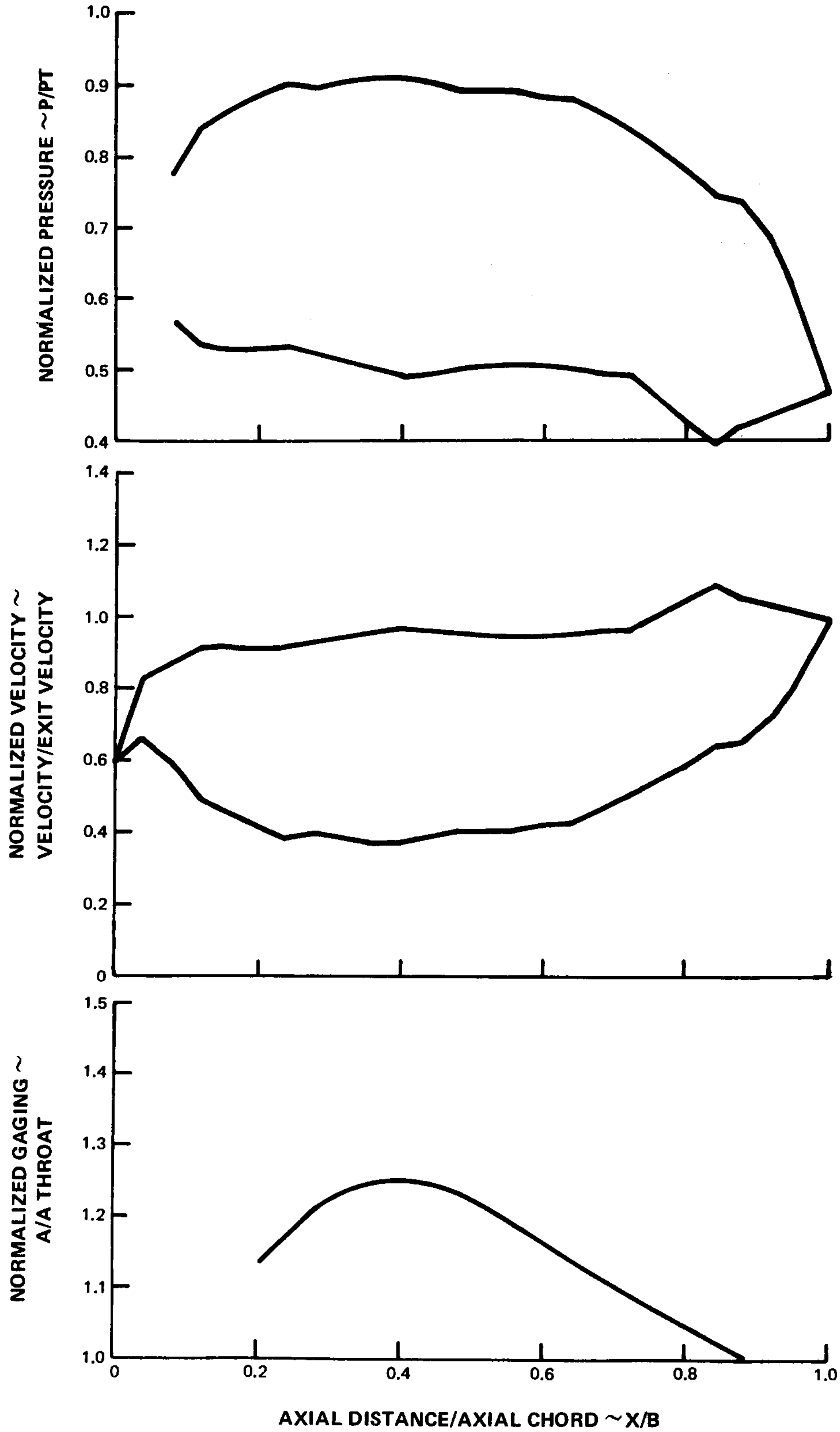

FIG. 78 FOURTH STAGE BLADE ROOT NORMALIZED PRESSURE VELOCITY AND GAGING DIAGRAMS

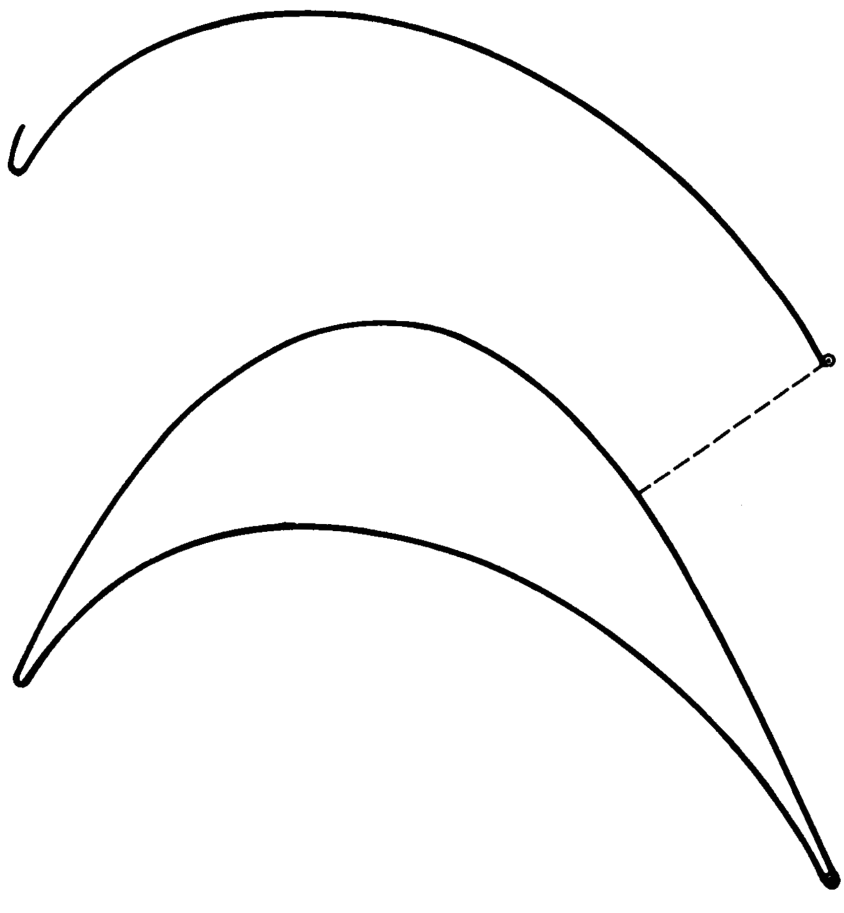

FIG. 79 FOURTH STAGE BLADE QUARTER ROOT

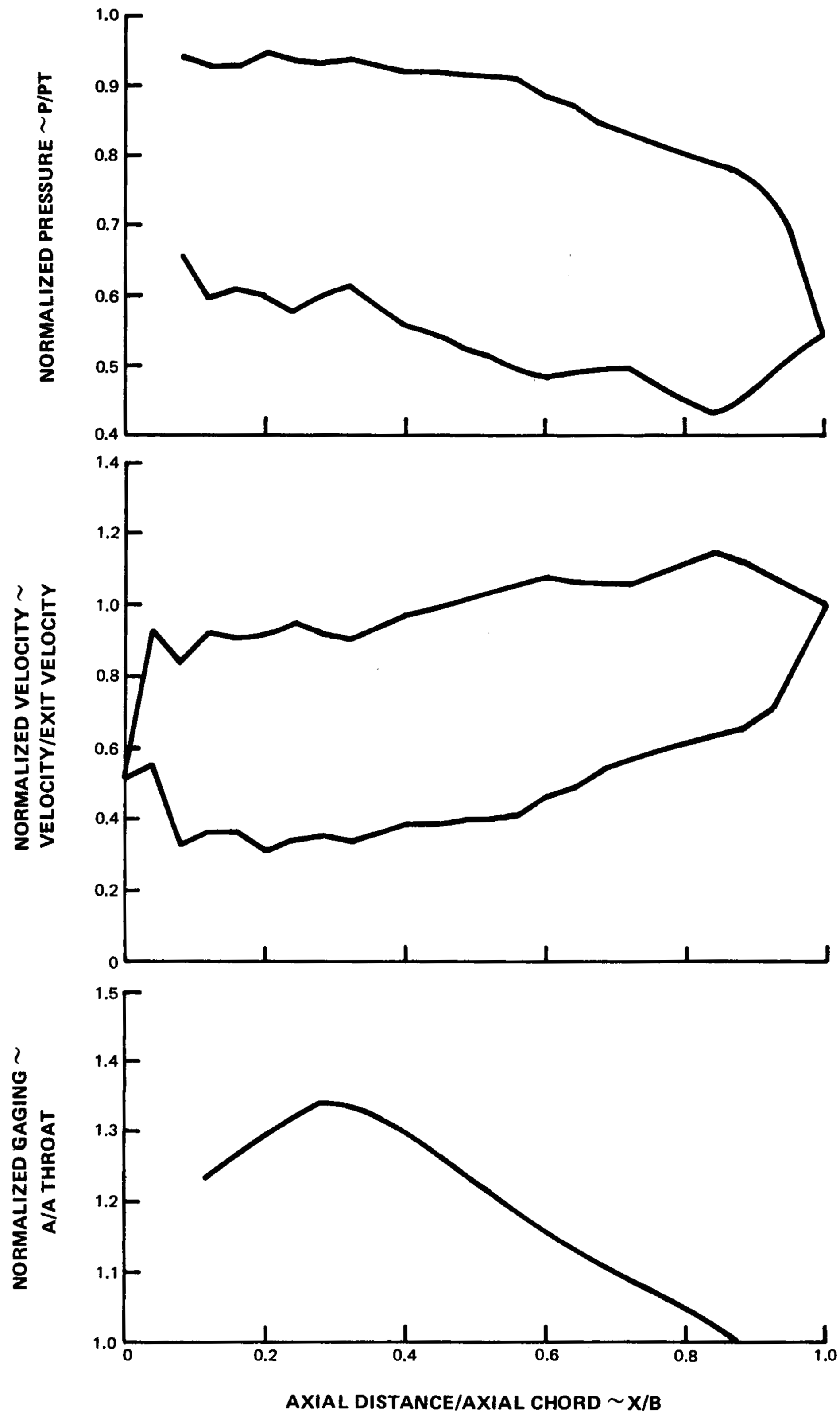

FIG. 80 FOURTH STAGE BLADE QUARTER ROOT NORMALIZED PRESSURE VELOCITY AND GAGING DIAGRAMS

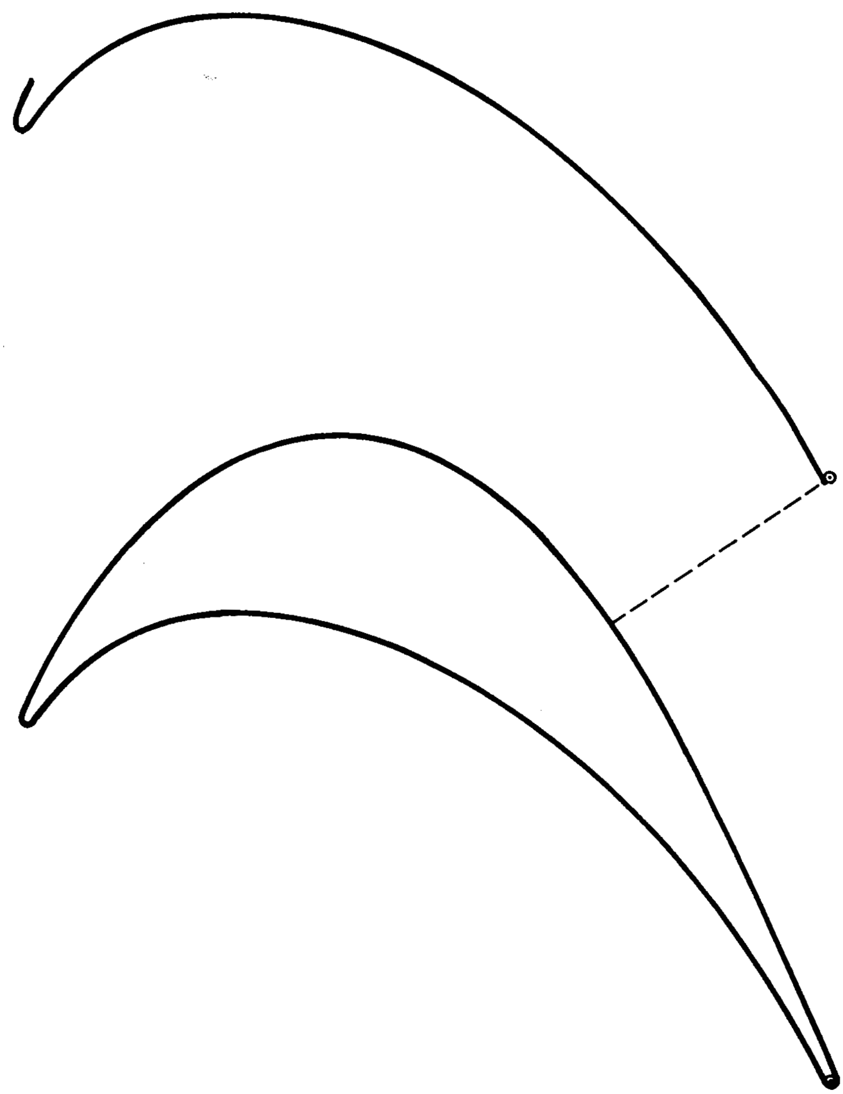

FIG. 81 FOURTH STAGE BLADE MEAN 2.5 SCALE

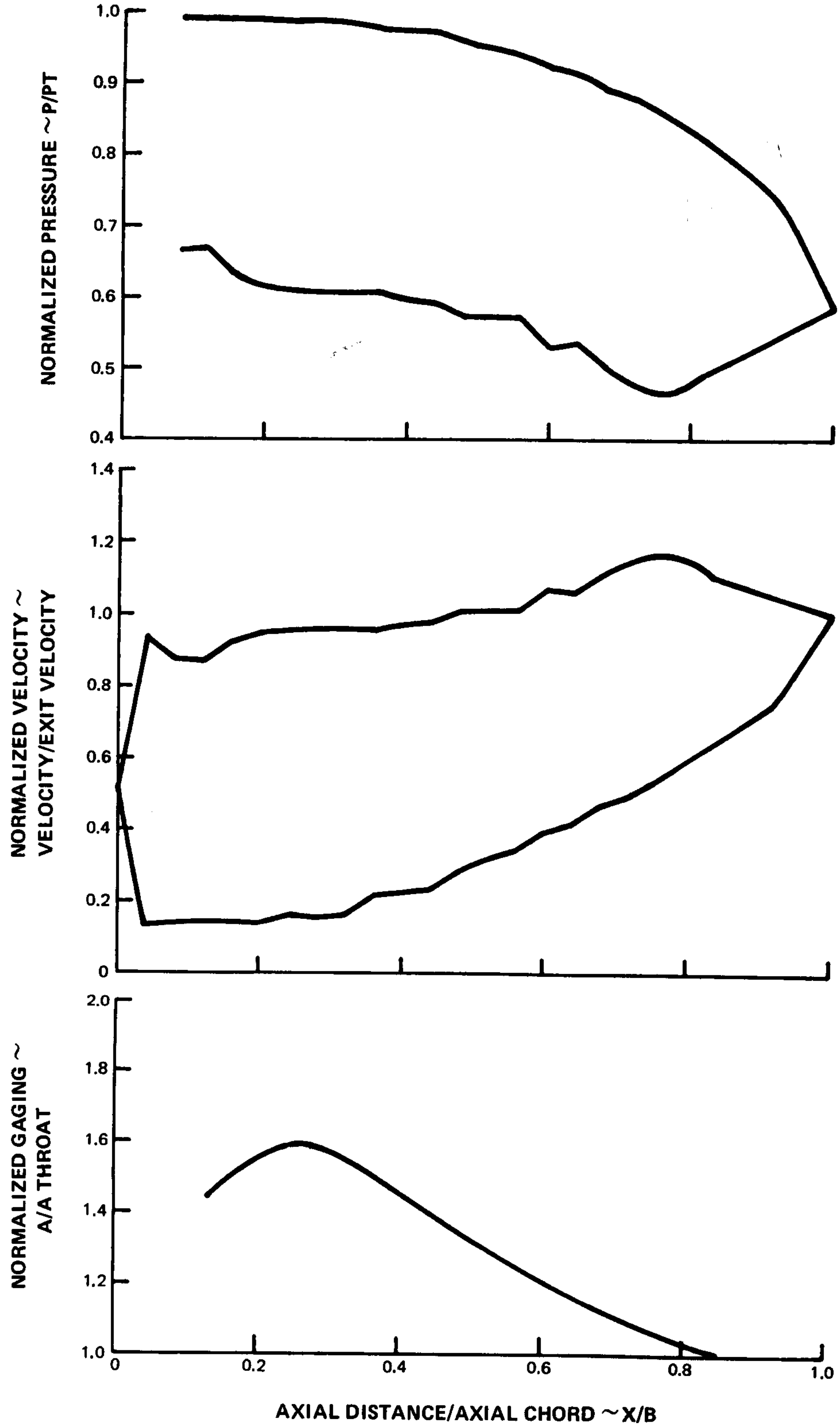

FIG. 82 FOURTH STAGE BLADE MEAN NORMALIZED PRESSURE VELOCITY AND GAGING DIAGRAMS

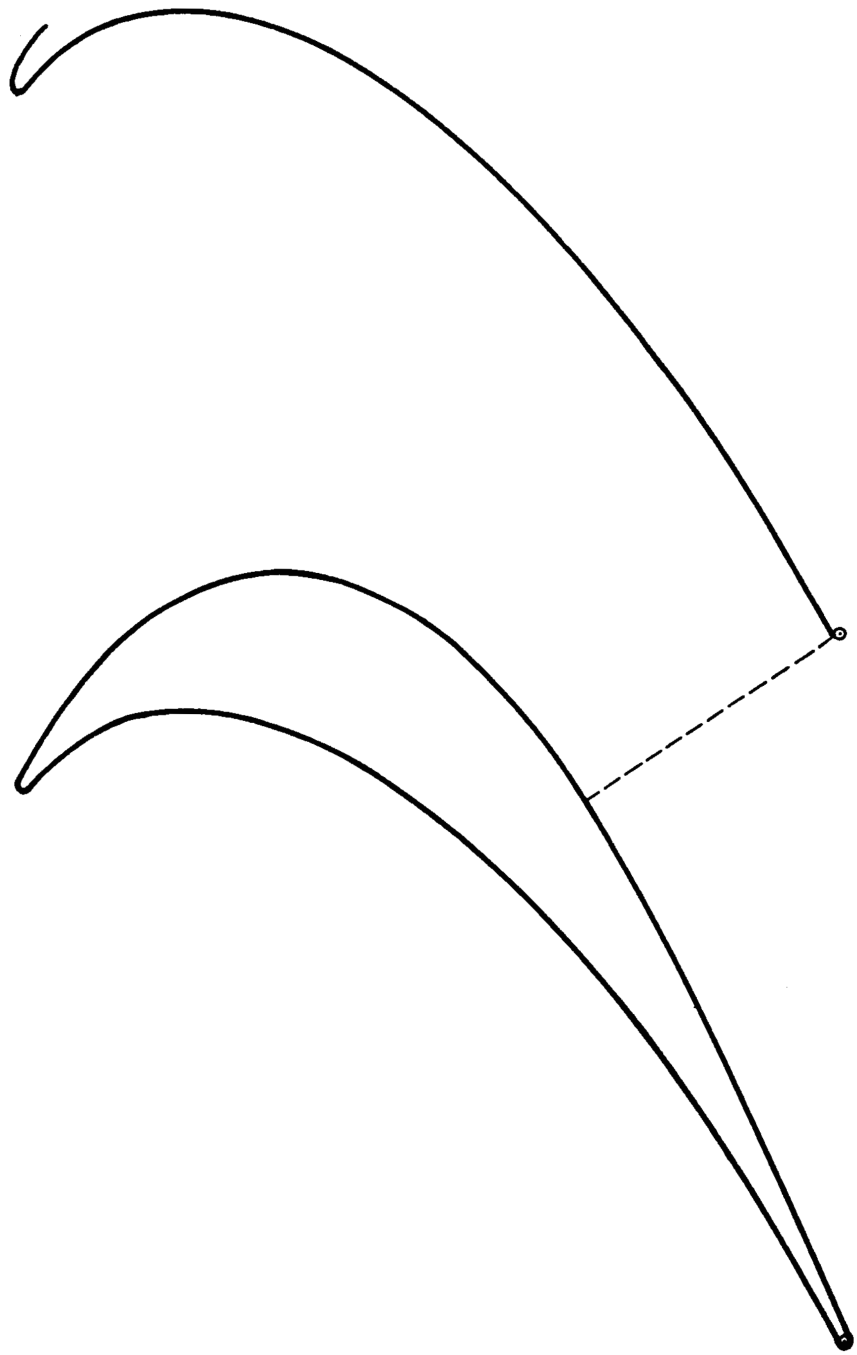

FIGURE 83 FOURTH STAGE BLADE QUARTER TIP 2.5 SCALE

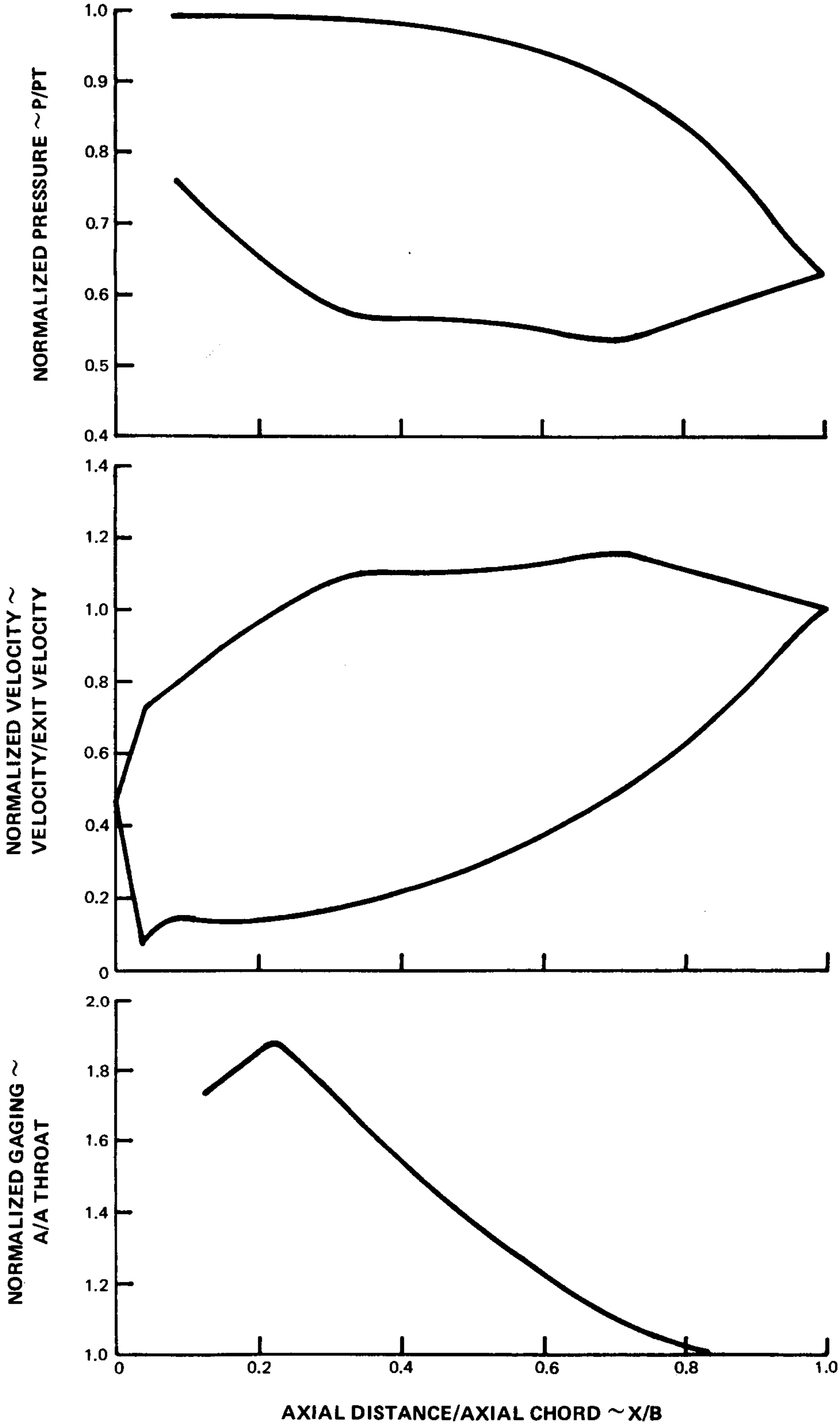

FIG. 84 FOURTH STAGE BLADE QUARTER TIP NORMALIZED PRESSURE VELOCITY AND GAGING DIAGRAMS

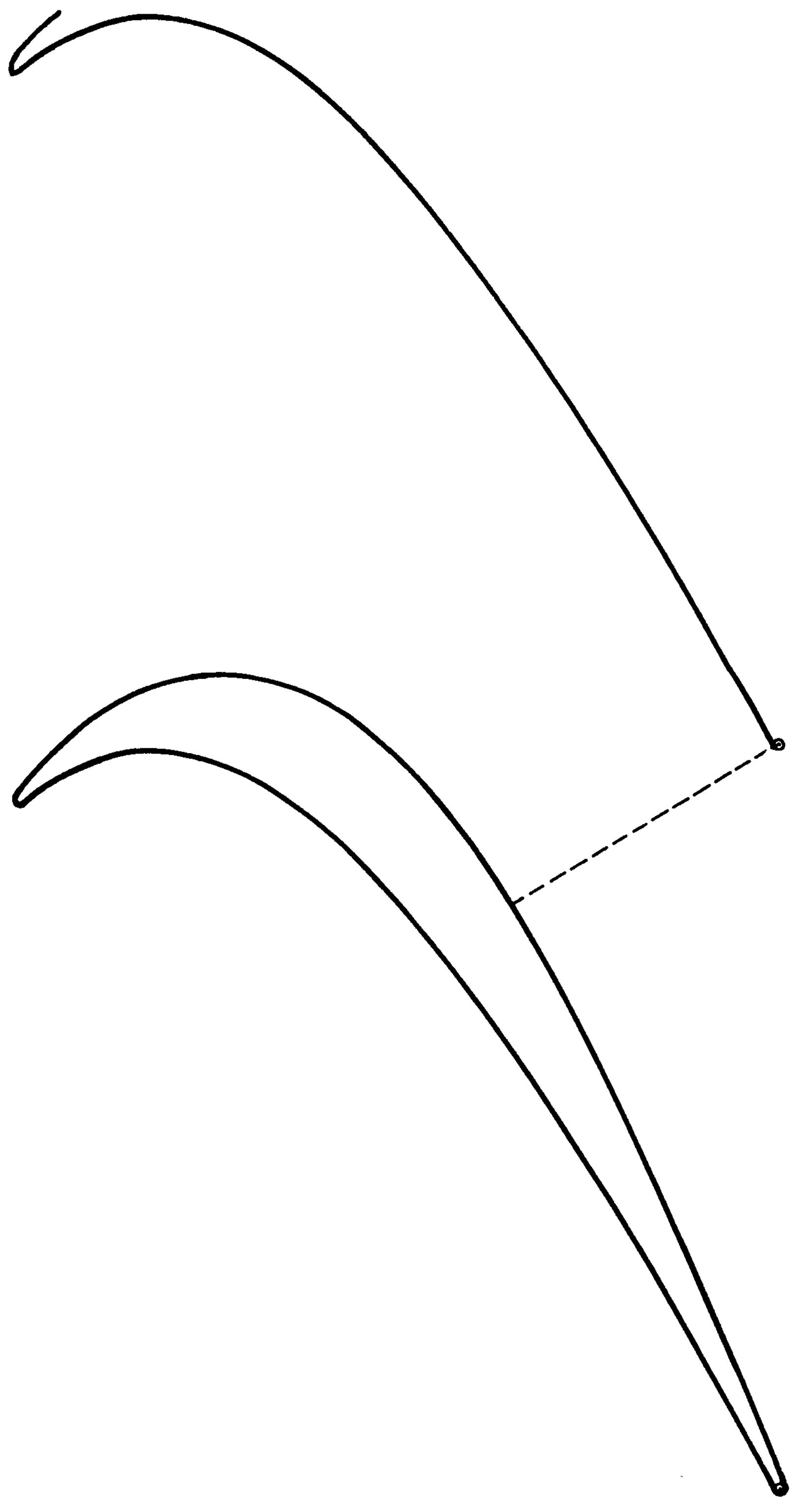

FIGURE 85 FOURTH STAGE BLADE TIP 2.5 SCALE

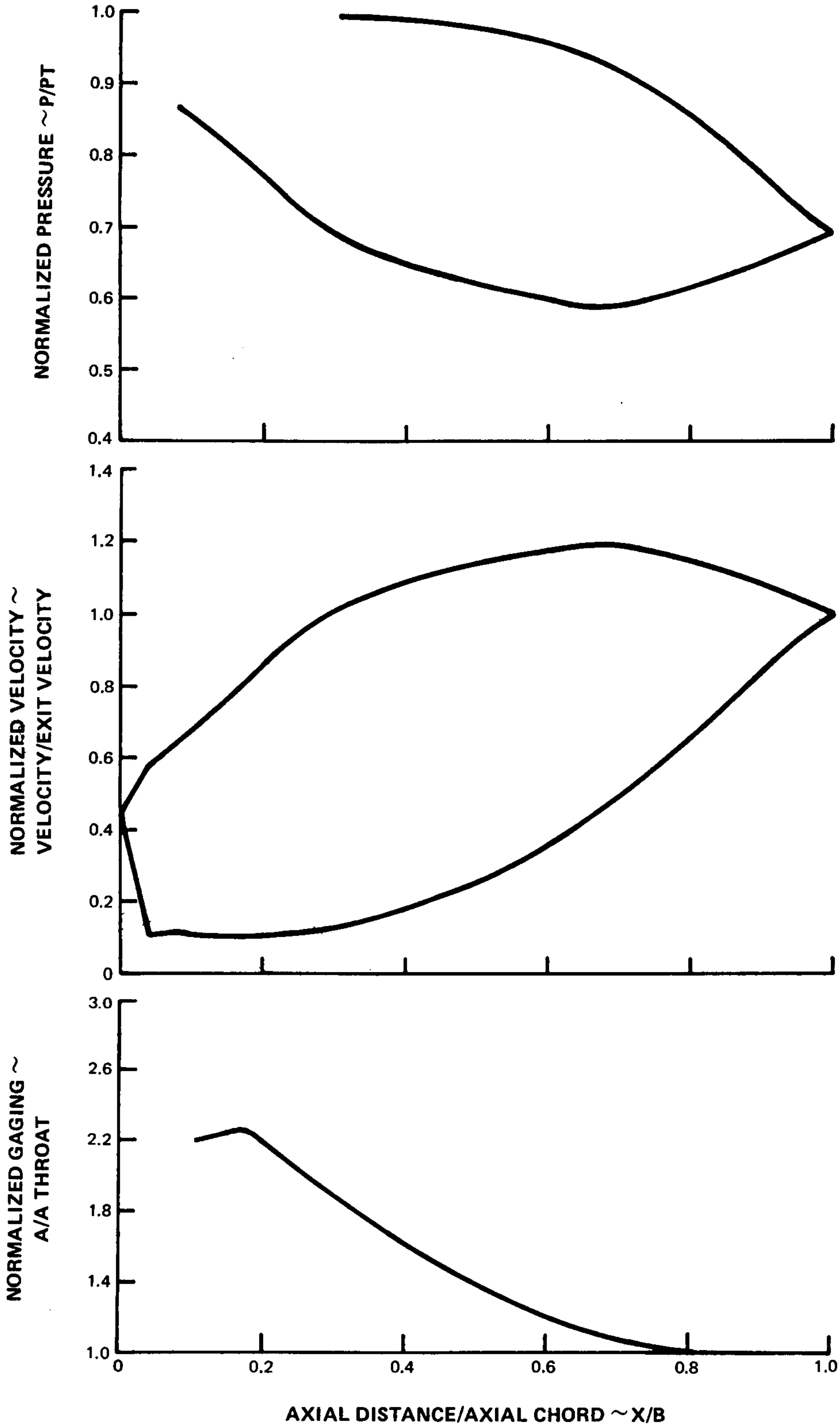

FIG. 86 FOURTH STAGE BLADE TIP NORMALIZED PRESSURE VELOCITY AND GAGING DIAGRAMS

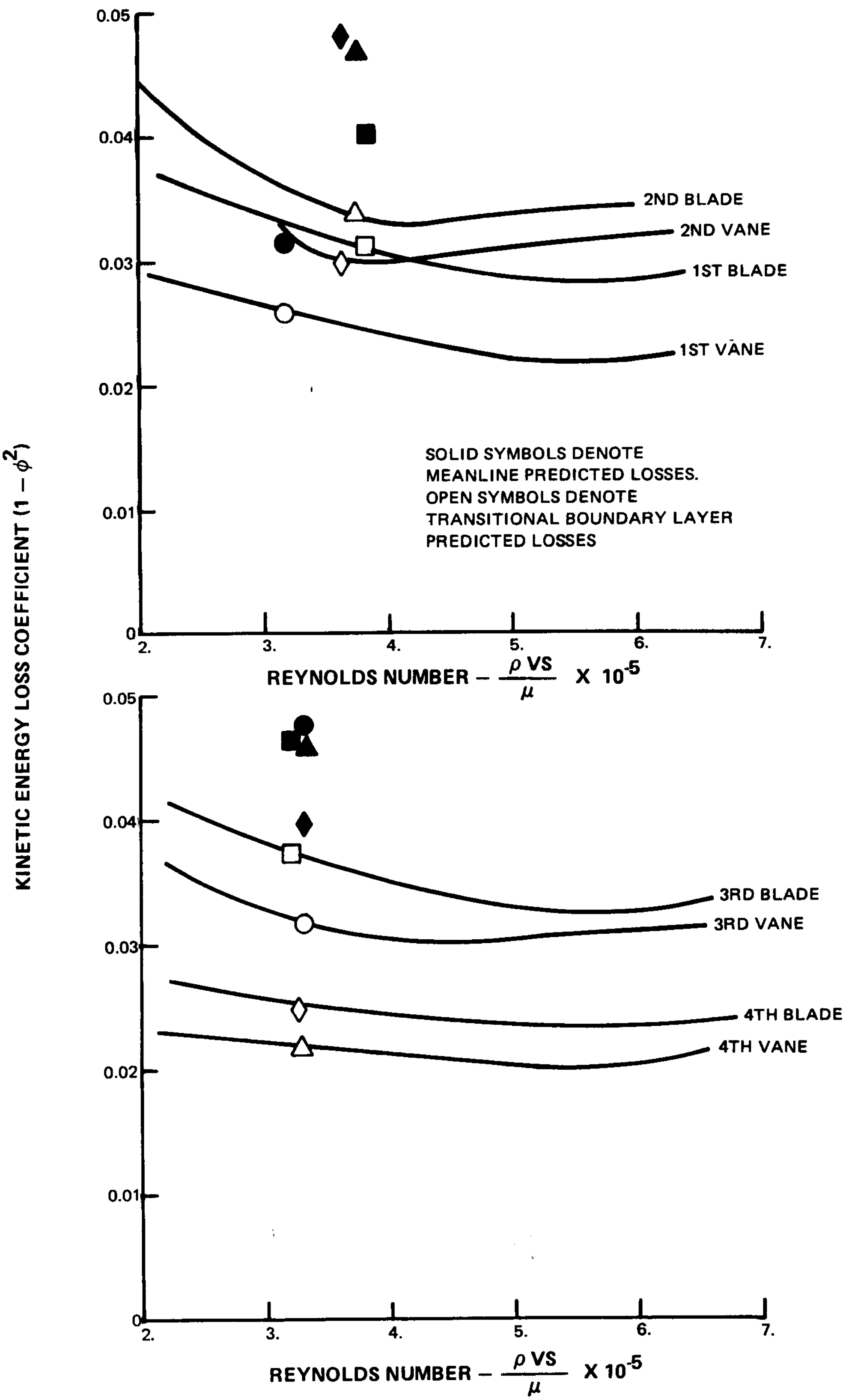

FIG. 87 AIRFOIL PROFILE LOSS VERSUS AIRFOIL REYNOLDS NUMBER

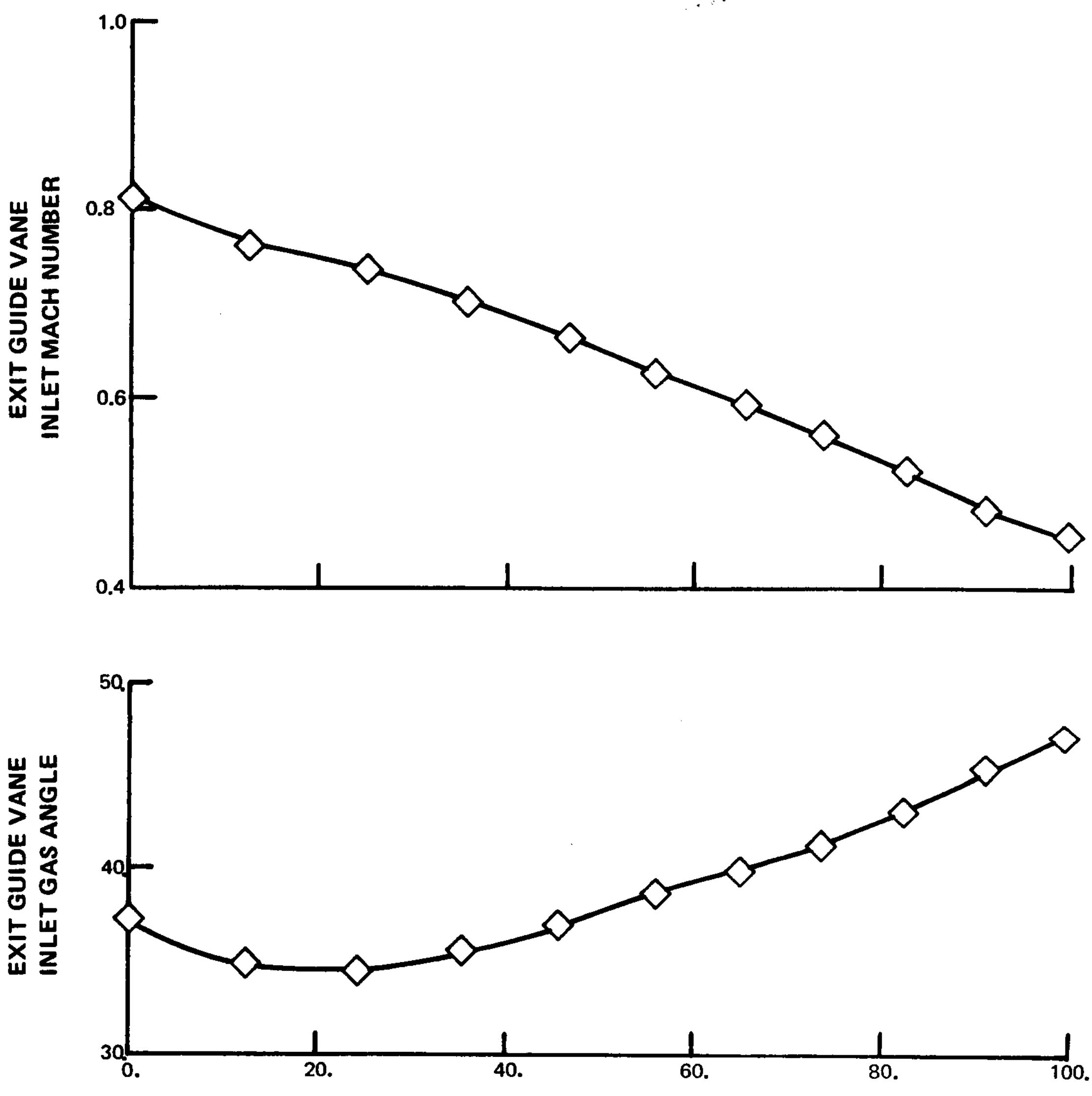

FIGURE 88 EXIT GUIDE VANE INLET CONDITIONS

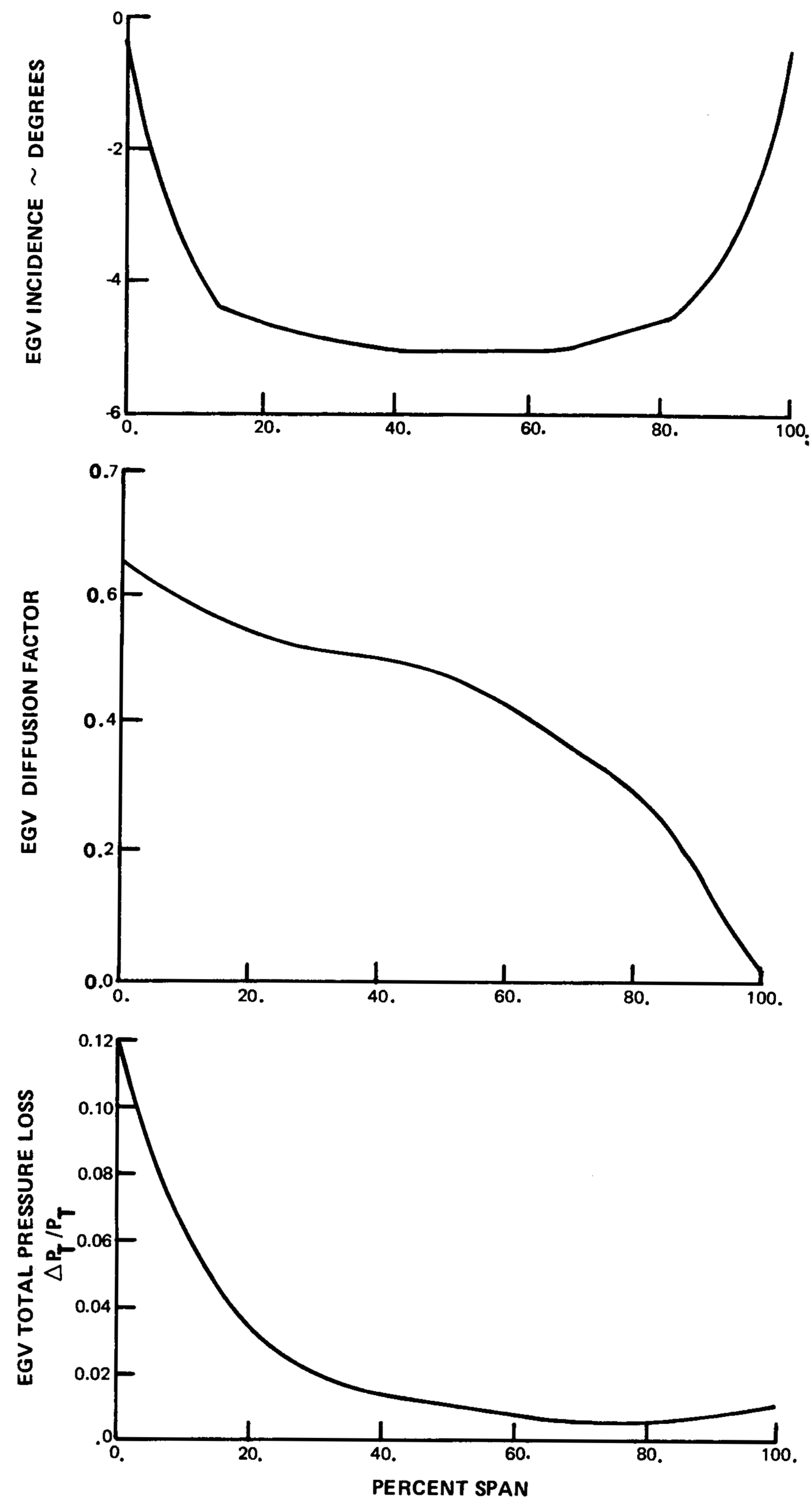

FIG. 89 EGV INCIDENCE, DIFFUSION FACTOR AND LOSS VERSUS PERCENT SPAN

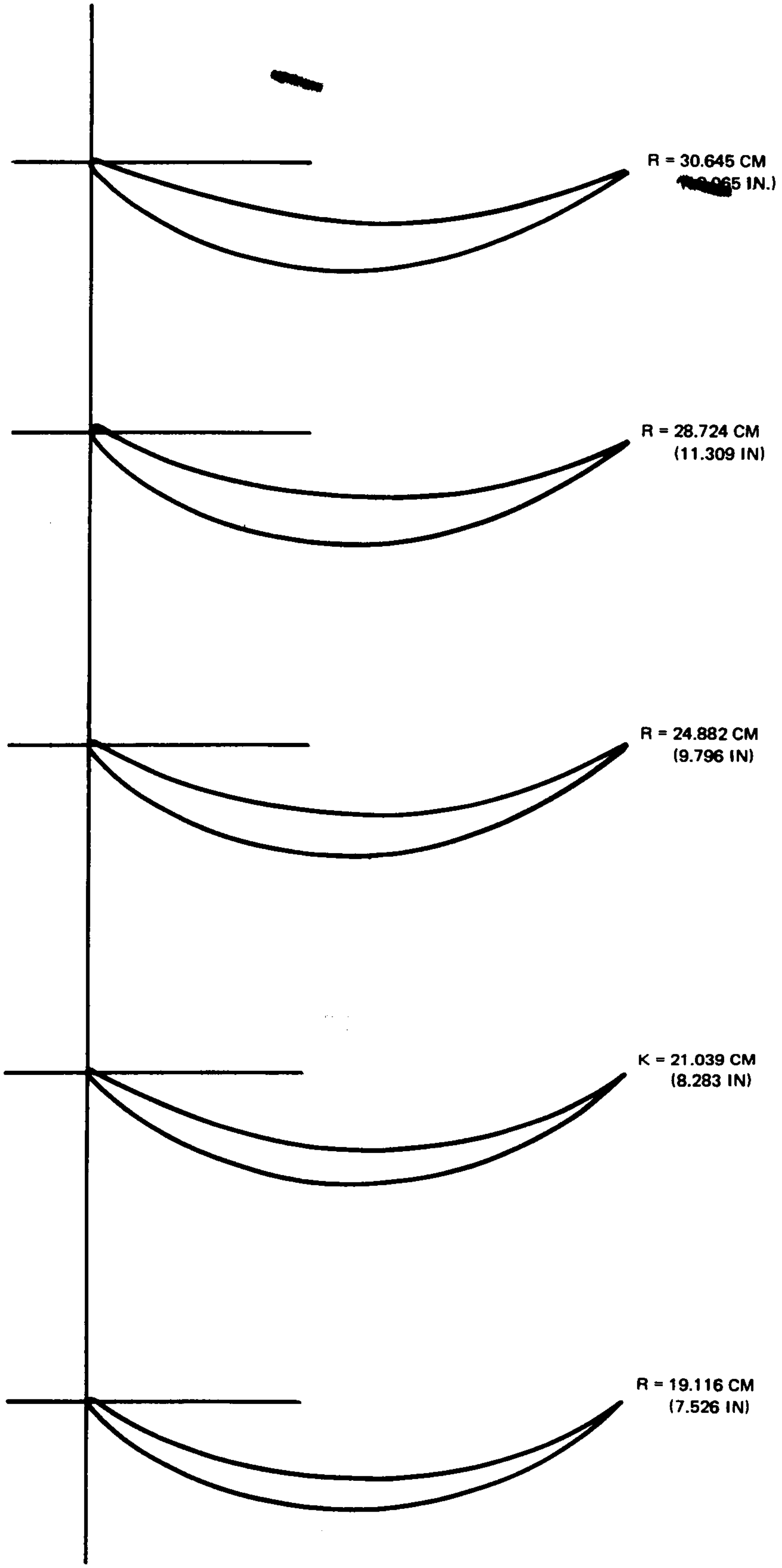

FIG. 90 TURBINE EXIT GUIDE VANE – 1.0 SCALE

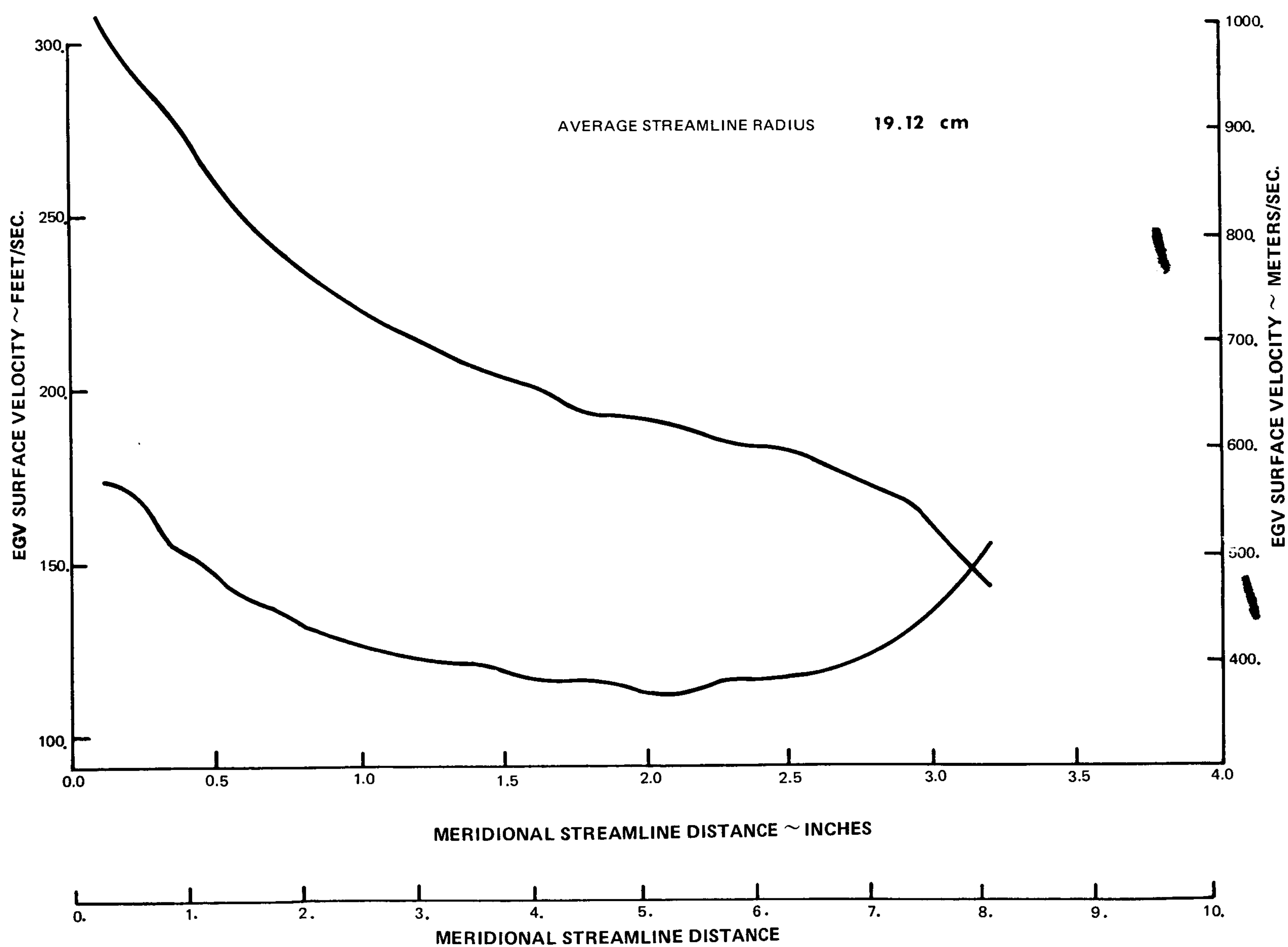

FIG. 91 EGV SURFACE VELOCITY VERSUS MERIDIONAL STREAMLINE DISTANCE

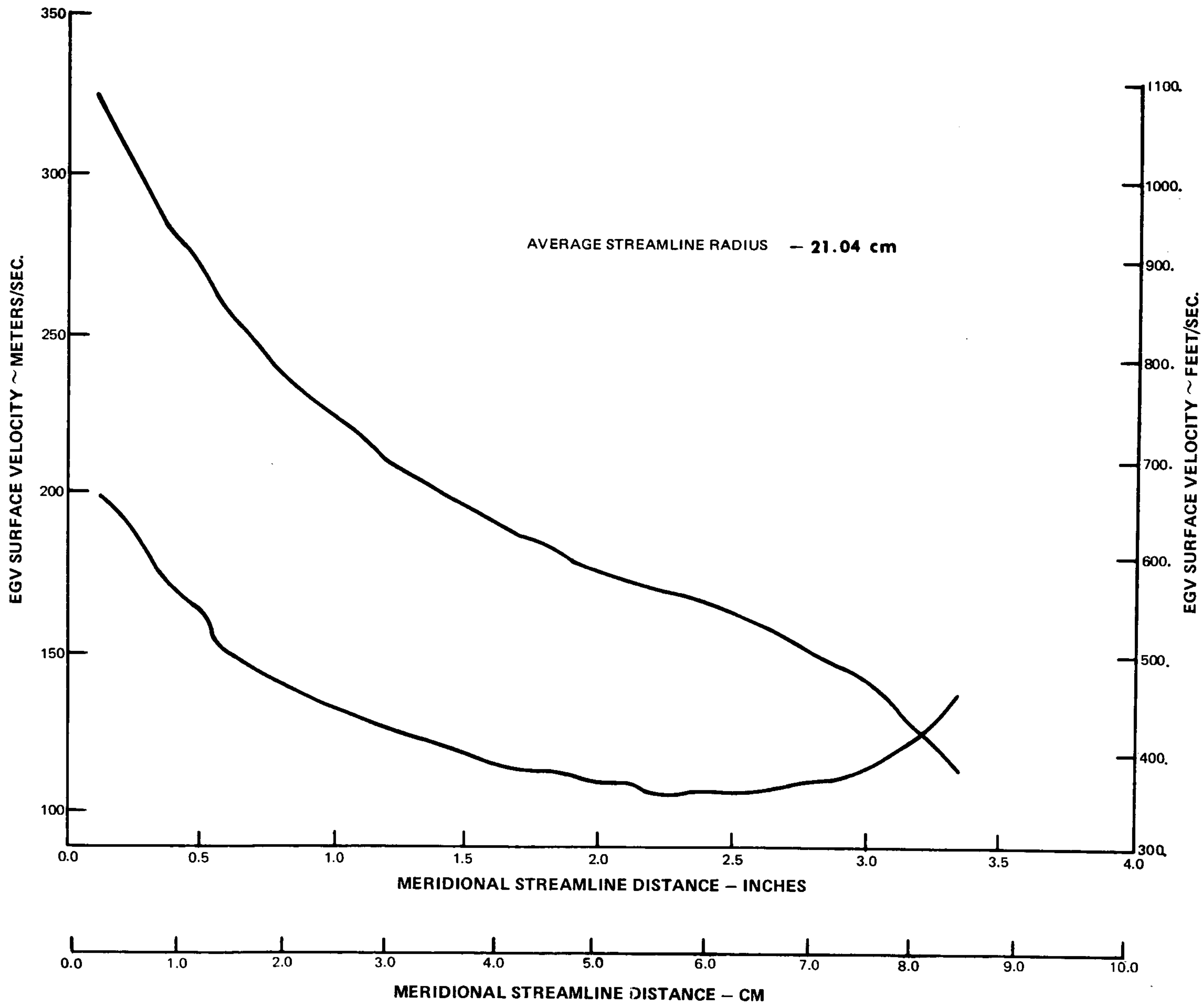

FIG. 92 EGV SURFACE VELOCITY VERSUS MERIDIONAL STREAMLINE DISTANCE

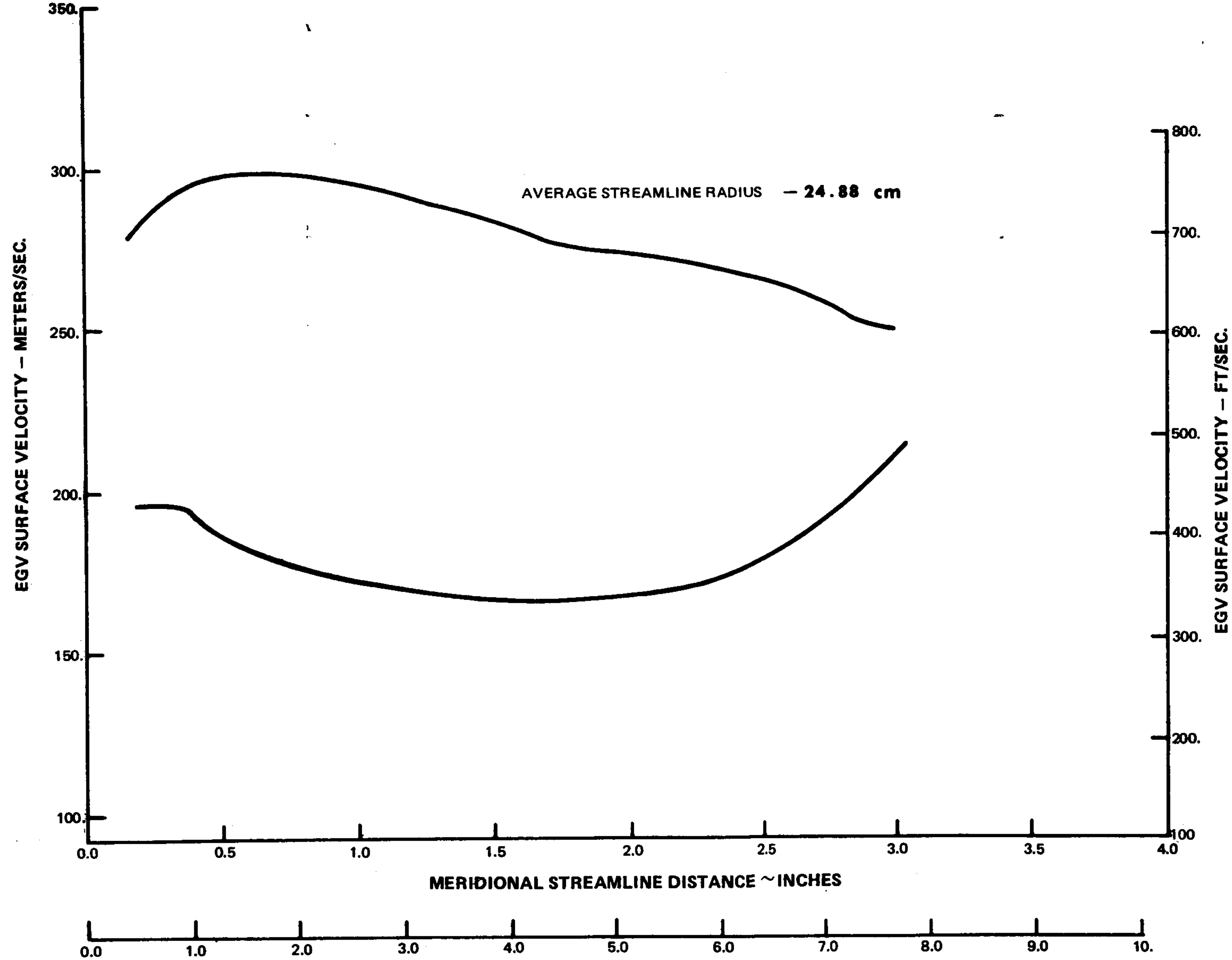

FIG. 93 EGV SURFACE VELOCITY VERSUS MERIDIONAL STREAMLINE DISTANCE

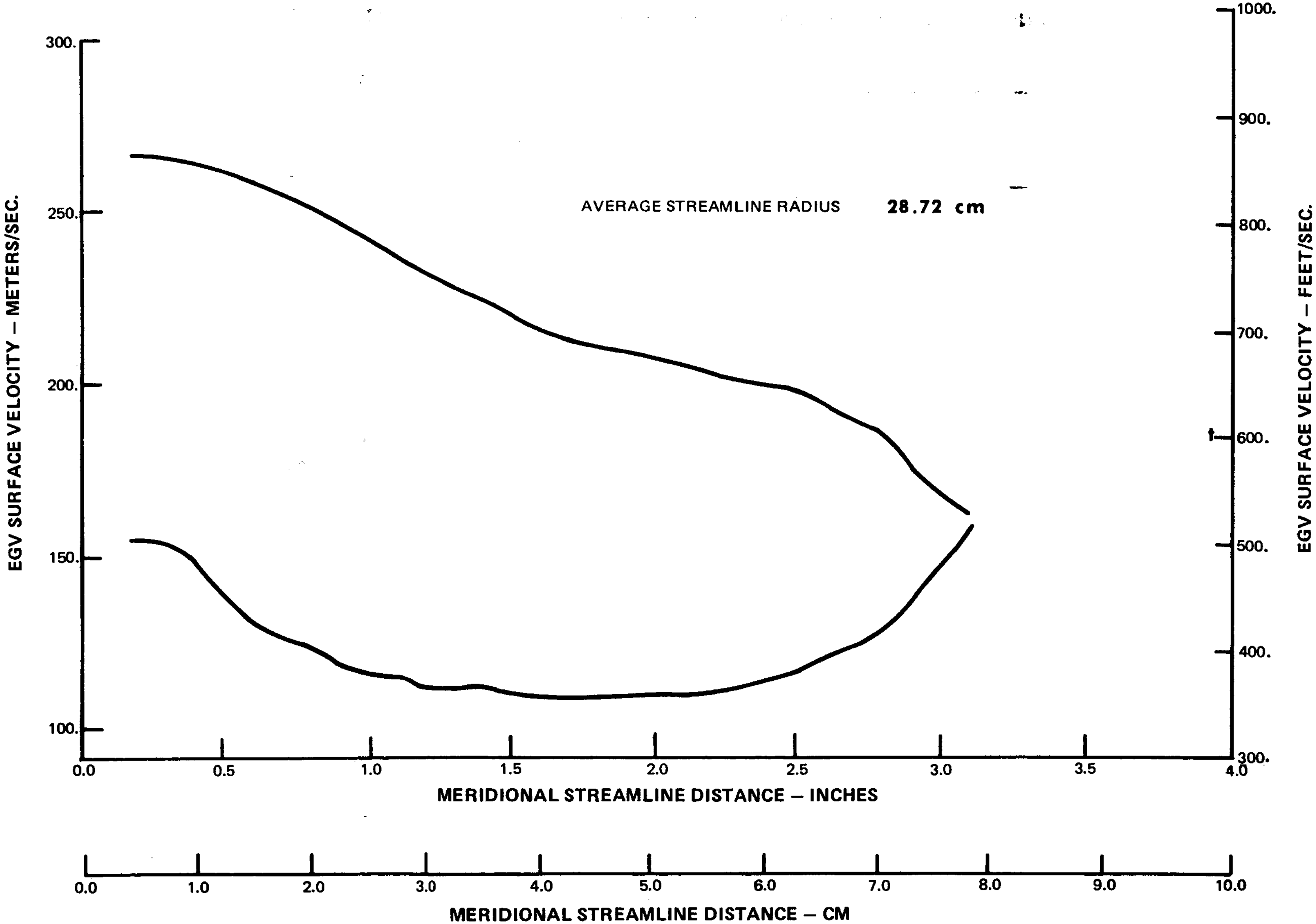

FIG. 94 EGV SURFACE VELOCITY VERSUS MERIDIONAL STREAMLINE DISTANCE

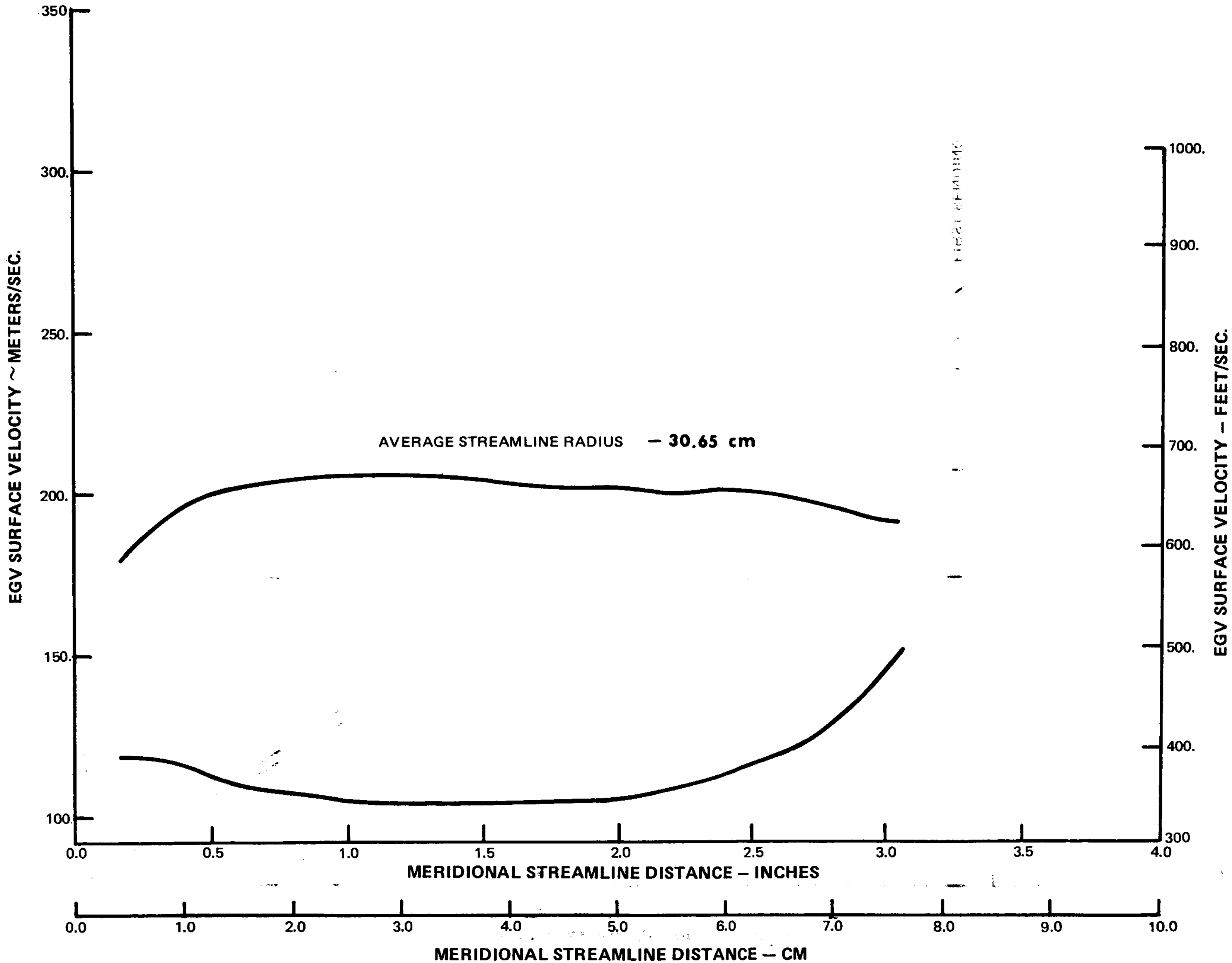

FIG. 95 EGV SURFACE VELOCITY VERSUS MERIDIONAL STREAMLINE DISTANCE

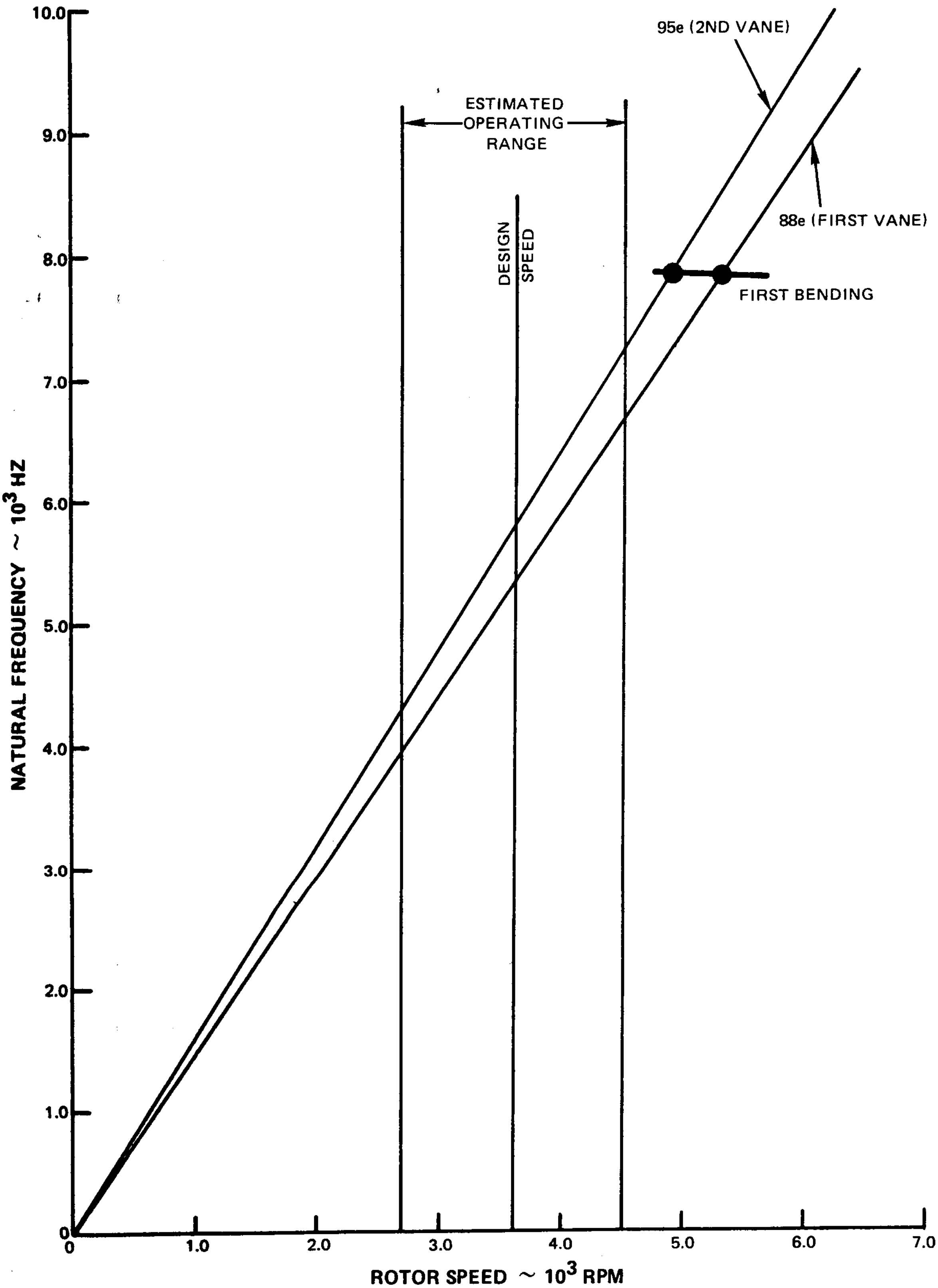

FIG 96 FIRST BLADE RESONANCE DIAGRAM

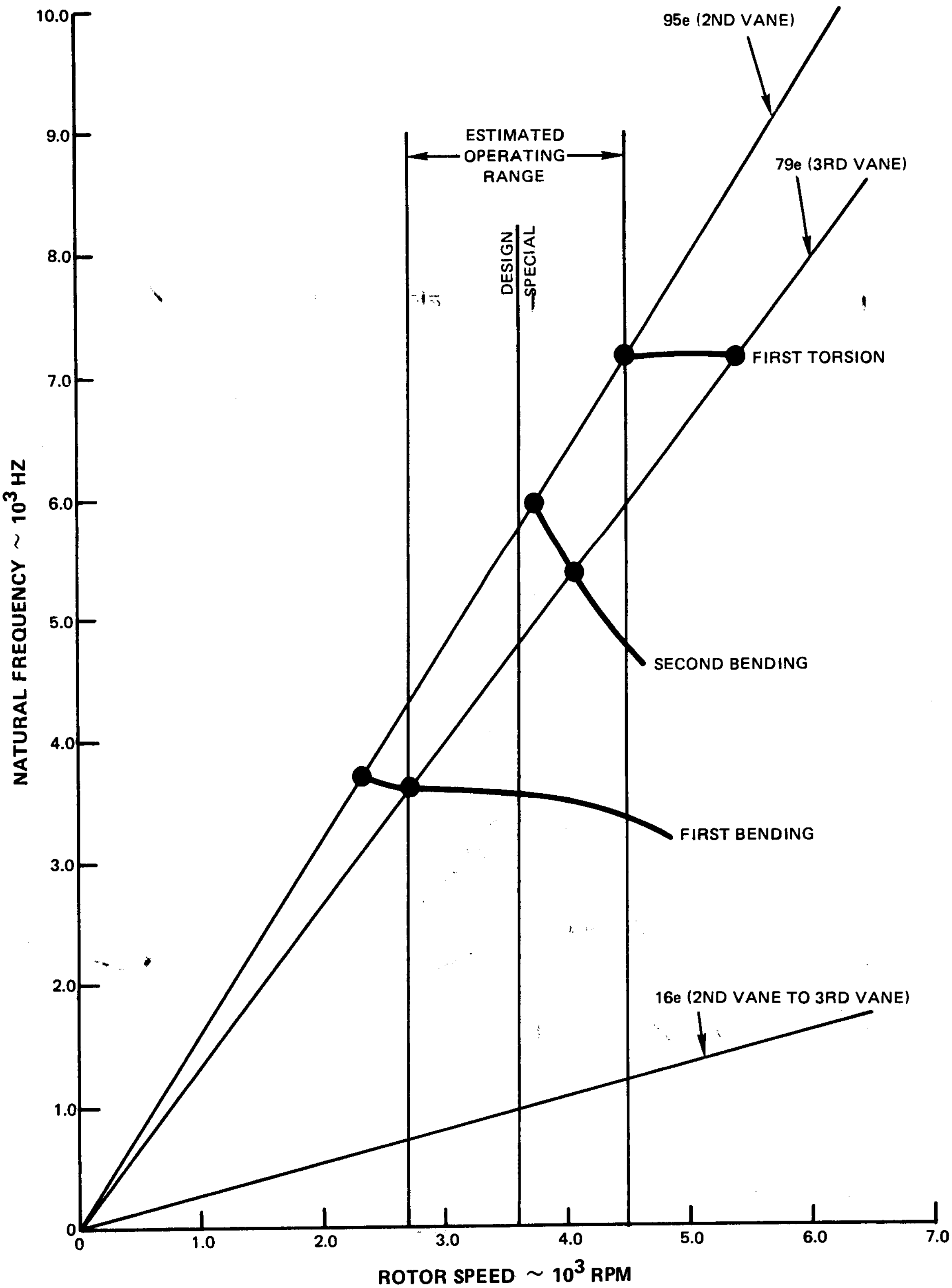

FIG. 97 SECOND BLADE RESONANCE DIAGRAM

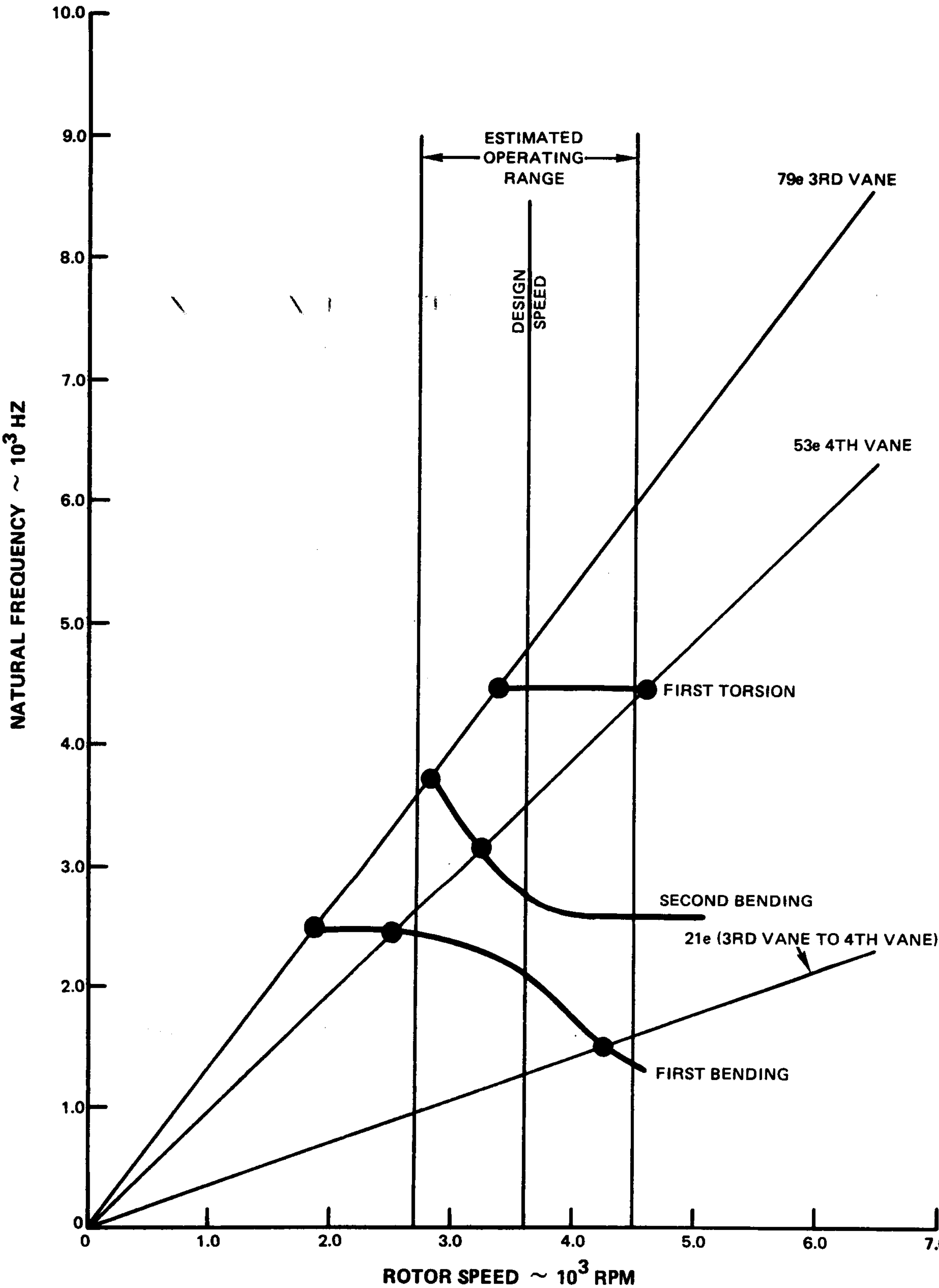

FIG. 98 THIRD BLADE RESONANCE DIAGRAM

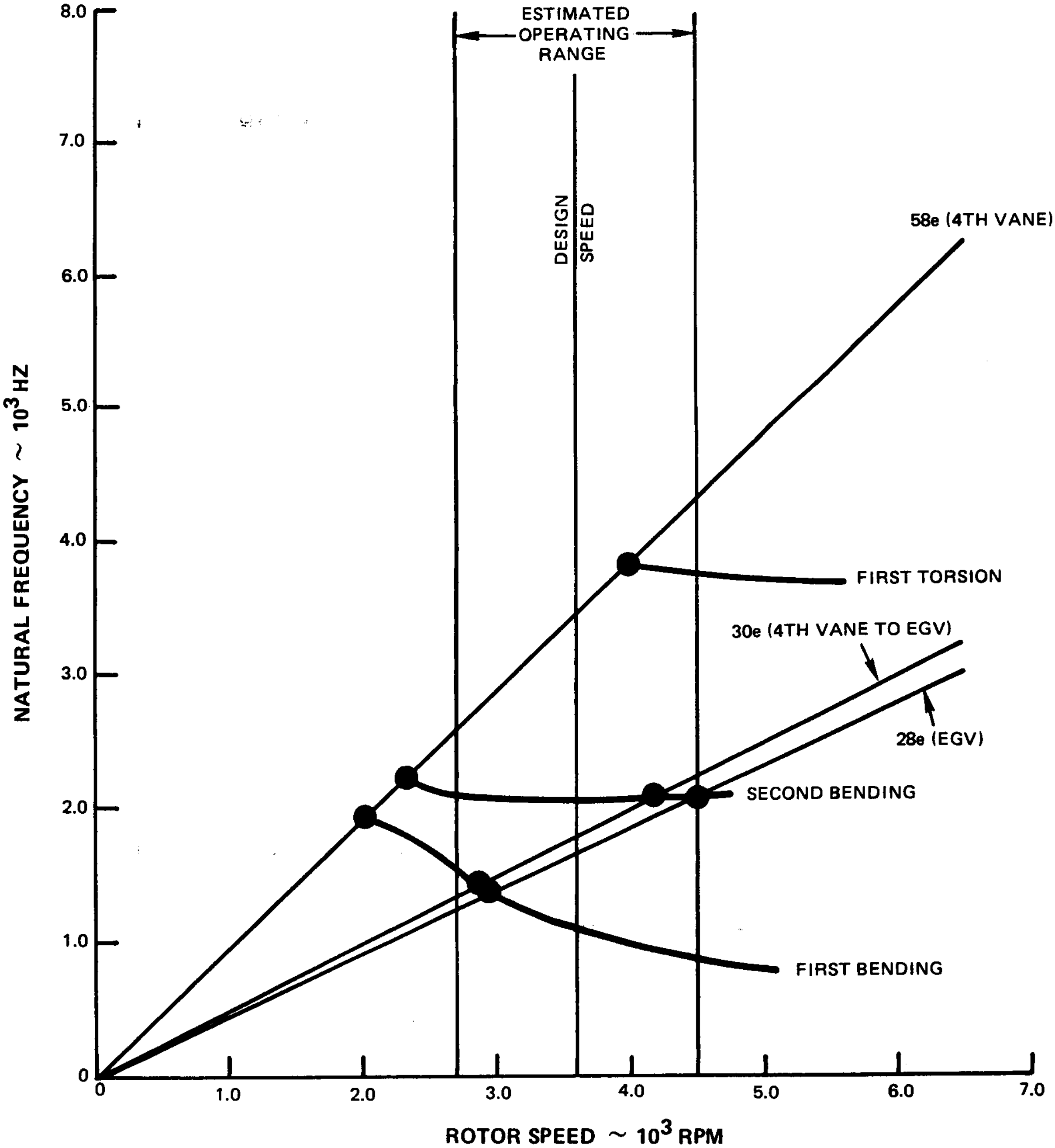

FIG. 99 FOURTH BLADE RESONANCE DIAGRAM

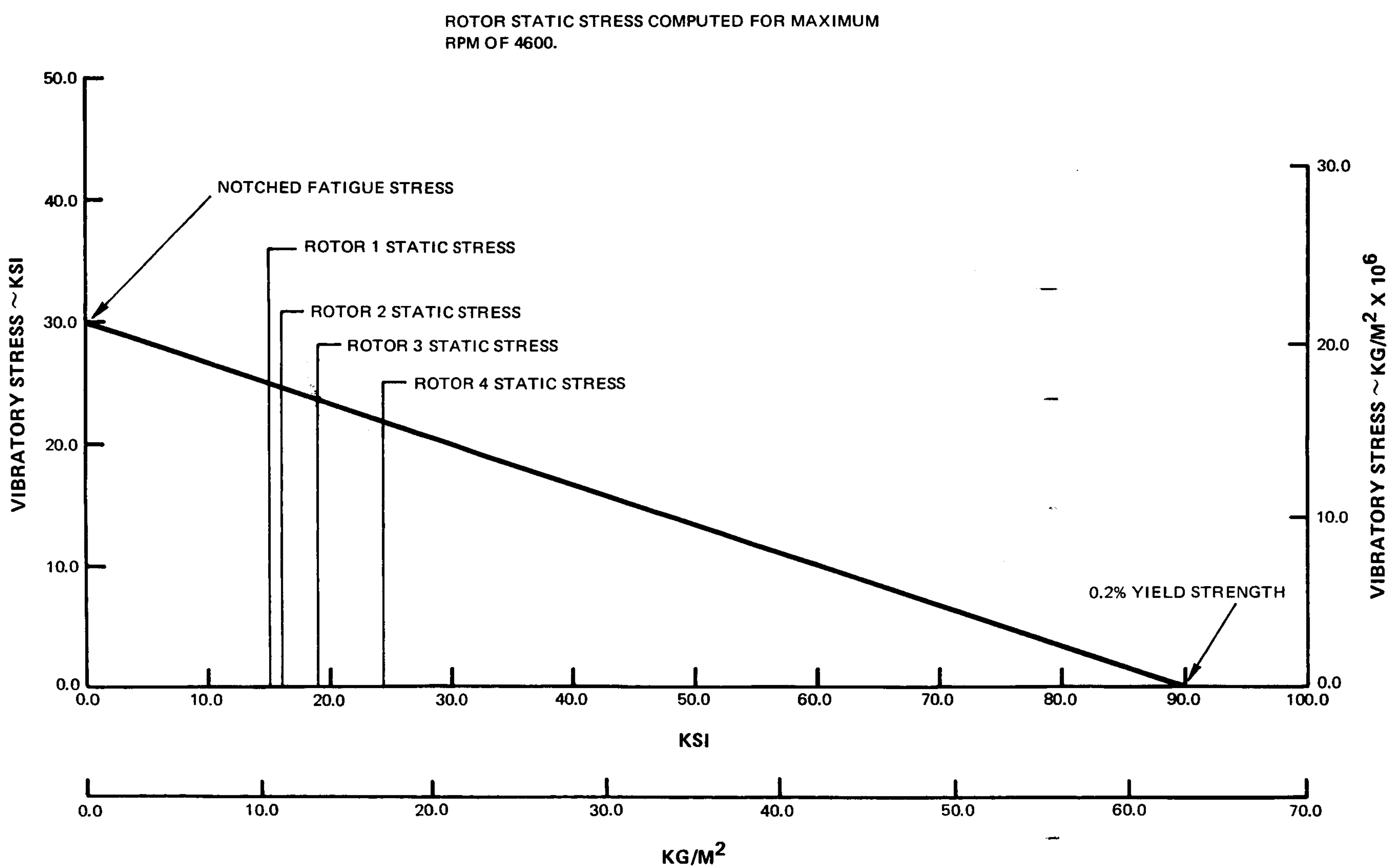

FIG. 100 ROTOR GOODMAN DIAGRAM

TABLE I

TURBINE AERODYNAMICS

RADIAL STATION	FIRST STAGE			SECOND STAGE		
	ROOT	MEAN	TIP	ROOT	MEAN	TIP
R_0 (VANE INLET) CM	20.264	22.240	24.13	19.632	20.898	26.025
(IN.)	(7.978)	(8.756)	(9.500)	(7.729)	(9.015)	(10.246)
R_1 (VANE EXIT) CM	19.939	22.209	24.486	19.454	23.126	26.208
(IN.)	(7.850)	(8.744)	(9.640)	(7.659)	(9.105)	(10.515)
$R_{1.5}$ (BLADE INLET) CM	19.733	22.253	24.887	19.279	23.236	27.087
(IN.)	(7.769)	(8.761)	(9.798)	(7.590)	(9.148)	(10.664)
R_2 (BLADE EXIT) CM	19.733	22.738	25.596	19.279	23.810	27.894
(IN.)	(7.769)	(8.952)	(10.077)	(7.590)	(9.374)	(10.982)
U_2 WHEEL SPEED MPS	74.37	85.95	96.62	72.85	89.92	105.16
(FPS)	(244.)	(282)	(317.)	(239.)	(295.)	(345.)
Δh Joules/kg	35306.	39864.	36980.	36678.	40725.	35515.
(BTU/lb)	(15.18)	(17.14)	(15.90)	15.97).	(17.51)	(15.27)
VEL. RATIO	0.280	0.304	0.355	0.269	0.315	0.395
$\alpha 0$ Deg.	90.00	90.00	90.00	32.12	28.66	31.21
α_1 Deg.	31.53	25.73	23.93	26.64	21.63	20.64
θ_v Deg.	58.47	64.27	66.07	121.24	129.71	128.15
$\beta_{1.5}$ Deg.	37.46	31.82	29.47	31.48	28.22	32.75
β_2 Deg.	26.66	22.66	22.66	25.37	21.37	21.37
θ_B Deg.	115.88	125.52	127.87	123.15	130.41	125.88
α_2 Deg.	34.09	30.94	35.05	32.48	30.29	35.93
REACTION (PRESS.)	0.375	0.335	0.377	0.430	0.468	0.534
$(P_S/P_S)_V$	1.457	1.434	1.375	1.285	1.249	1.213
$(P_S/P_S)_B$	1.343	1.261	1.250	1.260	1.259	1.291
$(C_L)_V$	0.757	0.740	0.773	0.910	0.901	0.957
$(C_L)_B$	0.851	0.884	0.980	0.823	0.857	0.896
$(M_R)_B$ INLET	0.600	0.573	0.456	0.698	0.584	0.375
$(M_R)_B$ EXIT	0.857	0.814	0.678	0.882	0.817	0.671
$(M_A)_V$ INLET	.317	.283	.300	0.674	0.589	0.431
$(M_A)_V$ EXIT	.782	.782	.708	0.881	0.813	0.684
C_{X1}/C_{X2} FPS (MPS)	517.(476)	433.(388)	366.(327)	475.(444)	362.(350)	276.(294)
STAGE WORK Joules/Kg		38934.			39494.	
(BTU/lb)		(16.74)			(16.98)	

TABLE I (Cont'd)

TURBINE AERODYNAMICS

	THIRD STAGE STREAMLINE			FOURTH STAGE STREAMLINE		
RADIAL STATION	ROOT	MEAN	TIP	ROOT	MEAN	TIP
R_0 (VANE INLET) CM	19.202	23.944	28.298	18.519	25.042	30.698
(IN.)	(7.560)	(9.427)	(11.141)	(7.291)	(9.859)	(12.086)
R_1 (VANE EXIT) CM	18.849	24.158	29.108	18.064	25.194	31.458
(IN.)	(7.421)	(9.511)	(11.460)	(7.112)	(9.919)	(12.385)
$R_{1.5}$ (BLADE INLET) CM	18.621	24.257	29.487	17.787	25.237	31.836
(IN.)	(7.331)	(9.550)	(11.609)	(7.003)	(9.936)	(12.534)
R_2 (BLADE EXIT) CM	18.621	24.928	30.320	17.788	26.070	32.593
(IN.)	(7.331)	(9.814)	(11.937)	(7.003)	(10.264)	(12.832)
U_2 WHEEL SPEED MPS	70.41	94.18	114.60	67.06	98.45	123.14
(FPS)	(231.)	(309.)	(376.)	(220.)	(323.)	(404.)
Δh joules/kg	34724.	38771.	33608.	33.189	38212.	34922.
(BTU/lb)	14.93	16.67	14.45	14.27	16.43	14.8
VEL. RATIO	0.267	0.338	0.441	0.261	0.356	0.469
α_0 Deg.	32.52	28.73	33.10	34.17	32.54	39.95
α_1 Deg.	26.82	21.78	20.82	29.54	24.47	23.54
θ_v Deg.	120.67	129.49	126.09	116.29	122.99	116.51
$\beta_{1.5}$ Deg.	31.86	30.05	38.80	35.55	35.60	48.74
β_2 Deg.	26.75	22.75	22.75	29.99	25.99	25.99
θ_B Deg.	121.40	127.20	118.45	114.46	118.40	105.27
α_2 Deg.	34.07	33.81	42.19	37.25	38.57	47.94
REACTION	0.406	0.462	0.553	0.401	0.522	0.585
$(P_S/P_S)_V$	1.303	1.257	1.205	1.355	1.278	1.224
$(P_S/P_S)_B$	1.253	1.266	1.312	1.319	1.410	1.423
$(C_L)_V$	0.857	0.909	0.999	0.824	0.956	1.062
$(C_L)_B$	0.815	0.904	0.933	0.803	0.953	0.986
$(M_R)_B$ INLET	0.739	0.563	0.321	0.811	0.544	0.297
$(M_R)_B$ EXIT	0.912	0.807	0.660	1.018	0.897	0.740
$(M_A)_V$ INLET	0.708	0.577	0.400	0.739	0.548	0.364
$(M_A)_V$ EXIT	0.921	0.810	0.604	0.981	0.806	0.601
C_{X1}/C_{X2} MPS (FPS)	472.(456)	344.(356)	254.(293)	517.(528)	360.(405)	271.(351)
STAGE WORK						
Joules/Kg		37445.			36887.	
(BTU/lb)		(16.10)			(15.86)	

TABLE I (Cont'd)
EXIT GUIDE VANE AERODYNAMICS

RADIAL STATION	ROOT	MEAN	TIP
R_o (VANE INLET) CM.	17.787	26.167	32.822
IN.	7.003	10.302	12.922
R_1 (VANE EXIT) CM.	20.447	26.570	31.031
IN.	8.050	10.461	12.217
α_0	36.16	38.41	46.18
α_1	90.0	90.0	90.0
θ_v	53.84	51.59	43.82
P_S/P_S	0.7923	0.9418	1.0877
(M_A) V INLET	0.8295	0.6268	0.4190
(M_A) V EXIT	0.4385	0.5292	0.5440

TABLE II
FIRST STAGE AIRFOILS

VANE GEOMETRY

AVERAGE LENGTH (L) = 4.206 CM   HUB/TIP RATIO = 0.827
ASPECT RATIO (L/B) = 1.705   NO. OF VANES = 88

RADIAL STATION	ROOT	QUARTER ROOT	MEAN	QUARTER TIP	TIP
DEFINING RADIUS CM (IN.)	19.939 (7.850)	21.014 (8.297)	22.212 (8.745)	23.348 (9.192)	24.486 (9.640)
AXIAL CHORD CM (IN.)	1.676 (0.660)	1.676 (0.660)	1.676 (0.660)	1.676 (0.660)	1.676 (0.660)
ACTUAL CHORD CM (IN.)	2.261 (0.890)	2.393 (0.942)	2.466 (0.971)	2.543 (1.001)	2.639 (1.039)
GAP/AXIAL CHORD	0.849	0.898	0.946	0.994	1.043
α_0^*/α_0 - DEGREES	90.00/90.00	90.00/90.00	90.00/90.00	90.00/90.00	90.00/90.00
α_1^*/α_1 - DEGREES	31.53/31.53	26.68/26.68	25.73/25.73	24.76/24.80	23.93/23.93
$\theta^* = (180 - \alpha_0^* - \alpha_1^*)$ - DEGREES	58.47	68.62	64.27	65.24	66.07
α_1 GAGING	31.16	26.73	25.68	24.93	24.30
LED CM (IN.)	0.076 (0.030)	0.076 (0.030)	0.076 (0.030)	0.076 (0.030)	0.076 (0.030)
TED CM (IN.)	0.038 (0.015)	0.038 (0.015)	0.038 (0.015)	0.038 (0.015)	0.038 (0.015)
UNCOVERED TURN -DEGREES	8.068	8.097	8.449	8.826	9.232

BLADE GEOMETRY

AVERAGE LENGTH (L) = 5.509 CM   HUB/TIP RATIO = 0.782
ASPECT RATIO (L/B) = 2.763   NO. OF BLADES = 102

RADIAL STATION	ROOT	QUARTER ROOT	MEAN	QUARTER TIP	TIP
DEFINING RADIUS CM (IN.)	19.733 (7.769)	21.199 (8.346)	22.664 (8.923)	24.130 (9.500)	25.596 (10.077)
AXIAL CHORD CM (IN.)	1.880 (0.740)	1.880 (0.740)	1.880 (0.740)	1.880 (0.740)	1.88 (0.740)
ACTUAL CHORD CM (IN.)	1.887 (0.743)	1.991 (0.764)	1.994 (0.785)	2.068 (0.814)	2.139 (0.842)
GAP/AXIAL CHORD	0.647	0.695	0.743	0.791	0.839
β_1^*/β_1 DEGREES	34.44/37.44	26.8/31.8	25.60/31.60	24.0/30.0	23.47/29.47
β_2^*/β_2 DEGREES	26.66/26.66	22.66/22.66	22.66/22.66	22.66/22.66	22.66/22.66
$\theta^* = (180 - B_1^* - B_2^*)$ DEGREES	118.90	130.5	131.74	133.34	133.87
β_2 GAGING - DEGREES	26.90	23.00	22.73	22.40	22.05
LED CM (IN.)	0.076 (0.130)	0.076 (0.030)	0.076 (0.030)	0.076 (0.030)	0.076 (0.030)
TED CM (IN.)	0.038 (0.015)	0.038 (0.015)	0.038 (0.015)	0.038 (0.015)	0.038 (0.015)
UNCOVERED TURN - DEGREES	14.735	13.07	12.516	12.20	12.852

TABLE II (Cont'd)
SECOND STAGE AIRFOILS

VANE GEOMETRY

AVERAGE LENGTH = 6.825 CM. HUB/TIP RATIO = .741
ASPECT RATIO (L/B) = 3.176 NO. OF VANES = 95

RADIAL STATION	ROOT	QUARTER ROOT	MEAN	QUARTER TIP	TIP
DEFINING RADIUS CM (IN.)	19.454 (7.659)	21.267 (8.373)	23.081 (0.087)	24.895 (9.801)	26.708 (10.515)
AXIAL CHORD CM (IN.)	1.981 (0.780)	1.981 (0.780)	1.981 (0.780)	1.981 (0.780)	1.981 (0.780)
ACTUAL CHORD CM (IN.)	2.002 (0.788)	2.019 (0.795)	2.149 (0.846)	2.273 (0.895)	2.383 (0.938)
GAP/AXIAL CHORD	0.649	0.710	0.771	0.831	0.892
α_0^*/α_0 – DEGREES	30.30/33.30	22.5/27.5	22.80/28.80	24.4/30.4	25.60/31.60
α_1^*/α_1 - DEGREES	26.64/26.64	22.2/22.2	21.63/21.63	21.1/21.1	20.64/20.64
$\theta^* = (180 - \alpha_0^* - \alpha_1^*)$ - DEGREES	123.06	135.3	135.57	134.5	133.76
α_1 GAGING - DEGREES	26.64	22.2	21.64	21.1	20.48
LED CM (IN.)	0.076 (0.030)	0.076 (0.030)	0.076 (0.030)	0.076 (0.030)	0.076 (0.030)
TED CM (IN.)	0.038 (0.015)	0.038 (0.015	0.038 (0.015)	0.038 (0.015)	0.038 (0.015)
UNCOVERED TURN ~ DEGREES	13.326	11.77	10.998	11.56	11.674

BLADE GEOMETRY

AVERAGE LENGTH (L) = 82/2 CM HUB/TIP RATIO = .701
ASPECT RATIO (L/B) = 3.382 NO. OF BLADES = 86

RADIAL STATION	ROOT	QUARTER ROOT	MEAN	QUARTER TIP	TIP
DEFINING RADIUS CM (IN.)	19.279 (7.590)	21.933 (8.438)	23.586 (9.286)	25.740 (10.134)	27.894 (10.982)
AXIAL CHORD CM (IN.)	2.337 (0.920)	2.337 (0.920)	2.337 (0.920)	2.337 (0.920)	2.337 (0.920)
ACTUAL CHORD CM (IN.)	2.350 (0.925)	2.362 (0.930)	2.428 (0.956)	2.550 (1.004)	2.708 (1.066)
GAP/AXIAL CHORD	0.603	0.670	0.737	0.805	0.872
β_1^*/β_1^* DEGREES	26.48/31.48	22.47/27.47	22.40/28.40	24.0/30.0	26.73/32.73
β_2^*/β_2 DEGREES	25.37/25.37	21.45/21.45	21.37/21.37	21.37/21.37	21.37/21.37
$\theta^* = (180 - \beta_1^* - \beta_2^*)$ DEGREES	128.15	136.08	136.23	134.63	131.90
β_2 GAGING	25.57	21.60	21.40	21.15	20.85
LED CM (IN.)	0.076 (0.030)	0.076 (0.030)	0.076 (0.030)	0.076 (0.030)	0.076 (0.030)
TED CM (IN.)	0.038 (0.015)	0.038 (0.015)	0.038 (0.015)	0.038 (0.030)	0.038 (0.015)
UNCOVERED TURN DEGREES	12.441	11.98	11.597	11.14	10.771

TABLE II (Cont'd)
THIRD STAGE AIRFOILS

VANE GEOMETRY

AVERAGE LENGTH (L) = 9.678 CM HUB/TIP RATIO = 0.663
ASPECT RATIO (L/B) = 3.605 NO. OF VANES = 79

RADIAL STATION	ROOT	QUARTER ROOT	MEAN	QUARTER TIP	TIP
DEFINING RADIUS CM(IN.)	18.847 (7.420)	21.412 (8.430)	23.978 (9.440)	26.543 (10.450)	29.108 (11.460)
AXIAL CHORD CM (IN.)	2.464 (0.970)	2.464 (0.970)	2.464 (0.970)	2.464 (0.970)	2.464 (0.970)
ACTUAL CHORD CM (IN.)	2.499 (0.984)	2.543 (1.001)	2.685 (1.057)	2.893 (1.139)	3.170 (1.248)
GAP/AXIAL CHORD	0.608	0.691	0.774	0.857	0.940
α_0^*/α_0 – DEGREES	28.90/33.90	22.70/27.22	22.80/28.80	25.13/31.13	27.80/33.80
α_1^*/α_1 – DEGREES	26.82/26.82	22.38/22.38	21.81/21.81	21.24/21.34	20.82/20.82
$\theta^* = (180 - \alpha_0^* - \alpha_1^*)$ DEGREES	124.28	134.92	135.39	133.53	131.38
α_1 GAGING – DEGREES	27.02	22.46	21.78	21.24	20.60
LED CM (IN.)	0.076 (0.030)	0.076 (0.030)	0.076 (0.030)	0.076 (0.030)	0.076 (0.030)
TED CM (IN.)	0.038 (0.015)	0.038 (0.015)	0.038 (0.015)	0.038 (0.015)	0.038 (0.015)
UNCOVERED TURN – DEGREES	12.271	11.73	10.129	10.72	11.165

BLADE GEOMETRY

AVERAGE LENGTH (L) = 11.282 CM HUB/TIP RATIO = 0.623
ASPECT RATIO (L/B) = 3.702 NO. OF BLADES = 72

RADIAL STATION	ROOT	QUARTER ROOT	MEAN	QUARTER TIP	TIP
DEFINING RADIUS CM(IN.)	18.621 (7.331)	21.547 (8.483)	24.600 (9.685)	27.394 (10.785)	30.320 (11.937)
AXIAL CHORD CM (IN.)	2.870 (1.130)	2.870 (1.130)	2.870 (1.130)	2.870 (1.130)	2.870 1.130)
ACTUAL CHORD CM (IN.)	2.865 (1.128)	2.916 (1.148)	3.048 (1.200)	3.279 (1.291)	3.617 (1.424)
GAP/AXIAL CHORD	0.566	0.655	0.748	0.833	0.922
β_1^*/β_1 – DEGREES	28.84/31.84	23.5/28.50	24.05/30.05	27.35/33.35	32.78/38.78
β_2^*/β_2 – DEGREES	26.75/26.75	22.9/22.9	22.75/22.75	22.75/22.75	22.75/22.75
$\theta^* = (180 - B_1^* - B_2^*)$ DEGREES	124.41	133.6	133.20	129.9	124.47
B_2 GAGING – DEGREES	26.99	23.0	22.60	22.40	21.93
LED CM(IN.)	0.076 (0.030)	0.076 (0.030)	0.076 (0.030)	0.076 (0.030)	0.076 (0.030)
TED CM (IN.)	0.038 (0.015)	0.038 (0.015)	0.038 (0.015)	0.038 (0.015)	0.038 (0.015)
UNCOVERED TURN – DEGREES	10.951	11.13	10.593	11.18	10.437

TABLE II (Cont'd)
FOURTH STAGE AIRFOILS

VANE GEOMETRY

AVERAGE LENGTH (L) = 12.786 CM HUB/TIP RATIO = .589
ASPECT RATIO (L/B) = 3.431 NO. OF VANES = 58

RADIAL STATION	ROOT	QUARTER ROOT	MEAN	QUARTER TIP	TIP
DEFINING RADIUS CM (IN.)	18.064 (7.112)	21.412 (8.430)	24.762 (9.749)	28.110 (11.067)	31.458 (12.385)
AXIAL CHORD CM (IN.)	3.556 (1.400)	3.556 (1.400)	3.556 (1.400)	3.556 (1.400)	3.556 (1.400)
ACTUAL CHORD CM (IN.)	3.534 (1.407)	3.589 (1.413)	3.726 (1.467)	3.975 (1.565)	4.392 (1.729)
GAP/AXIAL CHORD CM (IN.)	0.550	0.652	0.754	0.856	0.958
α_0^*/α_0 – DEGREES	34.30/37.30	24.43/29.92	26.30/32.30	30.1/36.0	35.30/41.30
α_1^*/α_1 – DEGREES	29.54/29.54	25.1/25.1	24.52/24.52	24.0/24.02	22.97/22.97
$\theta^* = (180 - \alpha_0^* - \alpha_1^*)$ DEGREES	116.16	130.47	129.18	125.88	121.73
α_1 GAGING DEGREES	29.87	25.12	24.30	23.66	22.97
LED CM(IN.)	0.076 (0.030)	0.076 (0.030)	0.076 (0.030)	0.076 (0.030)	0.076 (0.030)
TED CM(IN.)	0.038 (0.015)	0.038 (0.015)	0.038 (0.015)	0.038 (0.015)	0.038 (0.015)
UNCOVERED TURN DEGREES	12.010	10.58	10.027	11.23	12.277

BLADE GEOMETRY

AVERAGE LENGTH (L) = 14.427 CM HUB/TIP RATIO = .552
ASPECT RATIO (L/B) = 3.111 NO. OF BLADES = 50

RADIAL STATION	ROOT	QUARTER ROOT	MEAN	QUARTER TIP	TIP
DEFINING RADIUS CM(IN.)	17.788 (7.003)	21.488 (8.460)	25.190 (9.9175)	28.890 (11.374)	32.593 (12.832)
AXIAL CHORD CM(IN.)	4.2672 (1.680)	4.267 (1.680)	4.267 (1.680)	4.267 (1.680)	4.267 (1.680)
ACTUAL CHORD CM (IN.)	4.313 (1.698)	4.361 (1.717)	4.638 (1.826)	5.108 (2.011)	5.687 (2.239)
GAP/AXIAL CHORD	0.524	0.633	0.742	0.851	0.960
β_1^*/β_1 – DEGREE Sq	32.50/35.50	27.6/32.6	29.51/34.80	34.38/40.4	46.00/52.00
β_2^*/β_2 – DEGREES	29.99/29.99	26.1/26.1	25.9/25.95	25.99/25.99	25.99/25.99
$\theta^* = (180 - B_1^* - B_2^*)$ DEGREES	117.51	126.3	124.54	119.63	108.01
B_2 GAGING – DEGREES	30.69	26.58	26.00	25.70	24.84
LED CM (IN.)	0.076 (0.030)	0.076 (0.030)	0.076 (0.030)	0.076 (0.030)	0.036 (0.030)
TED CM (IN.)	0.038 (0.015)	0.038 (0.015)	0.038 (0.015)	0.038 (0.015)	0.038 (0.015)
UNCOVERED TURN – DEGREES	8.935	10.58	9.872	8.7	8.786

TABLE III
FIRST STAGE VANE
NON-DIMENSIONAL AIRFOIL COORDINATES

X/B*	ROOT		QUARTER ROOT		MEAN		QUARTER TIP		TIP	
	YS/B*	YP/B*	YS/B	YP/B	YS/B	YP/B	YS/B	YP/B	YS/B	YP/B
0.0	.8983	.8983	1.0142	1.0142	1.0722	1.0722	1.1349	1.1349	1.2074	1.2074
.05	0.9227	.8714	1.0394	0.9877	1.0980	1.0449	1.1607	1.1076	1.2330	1.1798
.10	0.9223	.8579	1.0415	0.9780	1.1008	1.0339	1.1626	1.0959	1.2341	1.1668
.15	0.9172	.8383	1.0399	0.9638	1.0993	1.0188	1.1597	1.0795	1.2295	1.1477
.20	0.9069	.8136	1.0341	0.9448	1.0929	.9991	1.1511	1.0577	1.2183	1.1217
.25	0.8911	.7848	1.0230	0.9209	1.0806	.9744	1.1361	1.0302	1.2000	1.0885
.30	0.8695	.7521	1.0056	0.8917	1.0615	.9443	1.1139	.9963	1.1737	1.0479
.35	0.8419	.7158	0.9810	0.8571	1.0348	.9082	1.0838	.9555	1.1388	1.0002
.40	0.8082	.6762	0.9484	0.8171	0.9996	.8655	1.0452	.9077	1.0952	0.9460
.45	0.7684	.6335	0.9070	0.7714	0.9556	.8159	0.9977	.8534	1.0425	0.8862
.50	0.7224	.5876	0.8567	0.7203	0.9025	.7600	0.9414	.7930	0.9812	0.8211
.55	0.6706	.5385	0.7978	0.6639	0.8406	.6980	0.8764	.7272	0.9114	0.7513
.60	0.6131	.4865	0.7309	0.6022	0.7705	.6309	0.8033	.6565	0.8340	0.6771
.65	.5502	.4316	0.6569	0.5355	0.6929	.5589	0.7226	.5814	0.7495	0.5988
.70	.4824	.3736	0.5768	0.4641	0.6088	.4829	0.6352	.5020	0.6588	0.5167
.75	.4101	.3126	0.4914	0.3884	0.5190	.4029	0.5417	.4189	0.5622	0.4308
.80	.3341	.2486	0.4013	0.3085	0.4240	.3192	0.4427	.3320	0.4602	0.3414
.85	.2548	.1816	0.3070	0.2449	0.3244	.2324	0.3388	.2418	0.3531	0.2486
.90	.1728	.1114	0.2089	0.1378	0.2207	.1423	0.2305	.1482	0.2410	0.1524
.95	.0888	.0380	0.1073	0.0476	0.1132	.0492	0.1182	.0514	0.1240	0.0530
1.0	0.0000	0.0000	0.0000	0.0000	0.0000	0.0000	0.0000	0.0000	0.0000	0.0000

* X/B = NON DIMENSIONAL AXIAL COORDINATE USING THE AXIAL CHORD
YS/B = NON DIMENSIONAL TANGENTIAL COORDINATE FOR THE SUCTION SURFACE USING THE AXIAL CHORD
YP/B = NON DIMENSIONAL TANGENTIAL COORDINATE FOR THE PRESSURE SURFACE USING THE AXIAL CHORD

TABLE III (CONTINUED)
FIRST STAGE BLADE
NON-DIMENSIONAL AIRFOIL COORDINATES

X/B*	ROOT		QUARTER ROOT		MEAN		QUARTER TIP		TIP	
	YS/B*	YP/B*	YS/B	YP/B	YS/B	YP/B	YS/B	YP/B	YS/B	YP/B
0.0	0.1939	0.1939	0.3248	0.3248	0.4072	0.4072	0.5042	0.5042	0.5818	0.5818
.05	0.2808	0.1975	0.4374	0.3329	0.5234	0.4166	0.6261	0.5151	0.7053	0.5935
.10	0.3513	0.2439	0.5239	0.3847	0.6099	0.4738	0.7132	0.5765	0.7919	0.6585
.15	0.4119	0.2773	0.5933	0.4161	0.6773	0.5087	0.7782	0.6129	0.8551	0.6970
.20	0.4634	0.3018	0.6484	0.4356	0.7291	0.5300	0.8260	0.6336	0.9001	0.7179
.25	0.5064	0.3194	0.6912	0.4468	0.7677	0.5414	0.8594	0.6429	0.9299	0.7258
.30	0.5411	0.3311	0.7227	0.4515	0.7946	0.5450	0.8802	0.6431	0.9466	0.7232
.35	0.5678	0.3378	0.7438	0.4507	0.8107	0.5419	0.8897	0.6355	0.9515	0.7116
.40	0.5864	0.3400	0.7550	0.4450	0.8166	0.5330	0.8885	0.6212	0.9453	0.6923
.45	0.5970	0.3378	0.7565	0.4348	0.8126	0.5186	0.8771	0.6006	0.9287	0.6658
.50	0.5993	0.3315	0.7483	0.4203	0.7988	0.4991	0.8557	0.5742	0.9018	0.6328
.55	0.5927	0.3212	0.7303	0.4017	0.7750	0.4746	0.8242	0.5422	0.8647	0.5936
.60	0.5768	0.3067	0.7021	0.3789	0.7408	0.4451	0.7822	0.5046	0.8171	0.5484
.65	0.5507	0.2879	0.6629	0.3517	0.6955	0.4105	0.7292	0.4614	0.7587	0.4972
.70	0.5129	0.2645	0.6116	0.3199	0.6379	0.3705	0.6642	0.4124	0.6886	0.4400
.75	0.4617	0.2360	0.5467	0.2830	0.5664	0.3246	0.5857	0.3572	0.6057	0.3768
.80	0.3941	0.2017	0.4656	0.2400	0.4786	0.2720	0.4922	0.2953	0.5088	0.3073
.85	0.3098	0.1602	0.3672	0.1898	0.3745	0.2116	0.3840	0.2257	0.3982	0.2311
.90	0.2134	0.1096	0.2543	0.1298	0.2578	0.1413	0.2641	0.1473	0.2753	0.1477
.95	0.1098	0.0456	0.1313	0.0548	0.1325	0.0573	0.1358	0.0577	0.1424	0.0563
1.0	0.0000	0.0000	0.0000	0.0000	0.0000	0.0000	0.0000	0.0000	0.0000	0.0000

* X/B = NON DIMENSIONAL AXIAL COORDINATE USING THE AXIAL CHORD
YS/B = NON DIMENSIONAL TANGENTIAL COORDINATE FOR THE SUCTION SURFACE USING THE AXIAL CHORD
YP/B = NON DIMENSIONAL TANGENTIAL COORDINATE FOR THE PRESSURE SURFACE USING THE AXIAL CHORD

TABLE III (CONTINUED)
SECOND STAGE VANE
NON-DIMENSIONAL AIRFOIL COORDINATES

X/B*	ROOT		QUARTER ROOT		MEAN		QUARTER TIP		TIP	
	YS/B*	YP/B*	YS/B	YP/B	YS/B	YP/B	YS/B	YP/B	YS/B	YP/B
0.0	0.2234	0.2234	0.2816	0.2816	0.2816	0.2816	0.4662	0.4662	0.6021	0.6021
.05	0.3219	0.2330	0.4224	0.2980	0.6012	0.4807	0.7244	0.6148	0.8147	0.7111
.10	0.4020	0.2868	0.5294	0.3669	0.6977	0.5386	0.8090	0.6659	0.8944	0.7617
.15	0.4694	0.3250	0.6136	0.4131	0.7697	0.5722	0.8705	0.6923	0.9518	0.7877
.20	0.5253	0.3524	0.6796	0.4450	0.8230	0.5914	0.9145	0.7042	0.9921	0.7983
.25	0.5703	0.3715	0.7300	0.4664	0.8609	0.6003	0.9440	0.7056	1.0185	0.7975
.30	0.6050	0.3837	0.7668	0.4793	0.8854	0.6011	0.9610	0.6987	1.0316	0.7876
.35	0.6298	0.3900	0.7911	0.4850	0.8979	0.5950	0.9666	0.6850	1.0338	0.7700
.40	0.6448	0.3908	0.8036	0.4842	0.8991	0.5829	0.9618	0.6651	1.0253	0.7455
.45	0.6503	0.3867	0.8049	0.4775	0.8897	0.5651	0.9467	0.6396	1.0066	0.7148
.50	0.6460	0.3777	0.7951	0.4652	0.8697	0.5421	0.9217	0.6089	0.9777	0.6783
.55	0.6320	0.3641	0.7743	0.4473	0.8392	0.5141	0.8864	0.5730	0.9384	0.6361
.60	0.6077	0.3457	0.7421	0.4240	0.7977	0.4809	0.8406	0.5321	0.8882	0.5883
.65	0.5729	0.3225	0.6980	0.3950	0.7447	0.4425	0.7833	0.4860	0.8261	0.5348
.70	0.5268	0.2942	0.6412	0.3600	0.6792	0.3986	0.7134	0.4344	0.7509	0.4754
.75	0.4685	0.2603	0.5702	0.3185	0.5996	0.3487	0.6289	0.3769	0.6601	0.4098
.80	0.3969	0.2202	0.4833	0.2697	0.5040	0.2920	0.5276	0.3128	0.5522	0.3374
.85	0.3118	0.1728	0.3797	0.2121	0.3927	0.2272	0.4105	0.2409	0.4286	0.2573
.90	0.2157	0.1165	0.2624	0.1437	0.2694	0.1523	0.2814	0.1595	0.2933	0.1680
.95	0.1116	0.0480	0.1352	0.0603	0.1381	0.0633	0.1441	0.0652	0.1500	0.0673
1.0	0.0000	0.0000	0.0000	0.0000	0.0000	0.0000	0.0000	0.0000	0.0000	0.0000

* X/B = NON DIMENSIONAL AXIAL COORDINATE USING THE AXIAL CHORD
YS/B = NON DIMENSIONAL TANGENTIAL COORDINATE FOR THE SUCTION SURFACE USING THE AXIAL CHORD
YP/B = NON DIMENSIONAL TANGENTIAL COORDINATE FOR THE PRESSURE SURFACE USING THE AXIAL CHORD

TABLE III (CONTINUED)
SECOND STAGE BLADE
NON-DIMENSIONAL AIRFOIL COORDINATES

X/B*	ROOT		QUARTER ROOT		MEAN		QUARTER TIP		TIP	
	YS/B*	YP/B*	YS/B	YP/B	YS/B	YP/B	YS/B	YP/B	YS/B	YP/B
0.0	0.1951	0.1951	0.2341	0.2341	0.3366	0.3366	0.4780	0.4780	0.6146	0.6146
.05	0.3058	0.2165	0.3664	0.2605	0.4753	0.3620	0.6076	0.5001	0.7303	0.6342
.10	0.3912	0.2707	0.4660	0.3217	0.5772	0.4225	0.7011	0.5519	0.8130	0.6870
.15	0.4599	0.3073	0.5448	0.3620	0.6559	0.4617	0.7719	0.5825	0.8749	0.7206
.20	0.5152	0.3330	0.6077	0.3897	0.7169	0.4876	0.8252	0.5998	0.9204	0.7401
.25	0.5589	0.3508	0.6573	0.4084	0.7633	0.5037	0.8642	0.6074	0.9523	0.7483
.30	0.5922	0.3621	0.6954	0.4200	0.7970	0.5120	0.8906	0.6073	0.9722	0.7469
.35	0.6161	0.3680	0.7229	0.4255	0.8192	0.5136	0.9056	0.6006	0.9810	0.7372
.40	0.6310	0.3690	0.7405	0.4258	0.8306	0.5093	0.9099	0.5880	0.9793	0.7200
.45	0.6372	0.3655	0.7484	0.4210	0.8317	0.4994	0.9038	0.5699	0.9674	0.6956
.50	0.6347	0.3577	0.7468	0.4116	0.8224	0.4843	0.8874	0.5468	0.9452	0.6646
.55	0.6233	0.3458	0.7353	0.3976	0.8027	0.4641	0.8603	0.5186	0.9123	0.6272
.60	0.6027	0.3297	0.7135	0.3789	0.7719	0.4387	0.8221	0.4854	0.8679	0.5833
.65	0.5723	0.3091	0.6804	0.3554	0.7292	0.4080	0.7716	0.4470	0.8109	0.5329
.70	0.5309	0.2840	0.6346	0.3267	0.6732	0.3717	0.7072	0.4032	0.7392	0.4759
.75	0.4770	0.2536	0.5736	0.2924	0.6015	0.3292	0.6264	0.3535	0.6495	0.4120
.80	0.4082	0.2175	0.4933	0.2514	0.5106	0.2797	0.5258	0.2970	0.5399	0.3406
.85	0.3224	0.1741	0.3901	0.2023	0.3996	0.2217	0.4076	0.2326	0.4150	0.2611
.90	0.2227	0.1216	0.2688	0.1425	0.2741	0.1529	0.2777	0.1581	0.2812	0.1723
.95	0.1145	0.0554	0.1376	0.0663	0.1401	0.0687	0.1414	0.0697	0.1426	0.0727
1.0	0.0000	0.0000	0.0000	0.0000	0.0000	0.0000	0.0000	0.0000	0.0000	0.0000

* X/B = NON DIMENSIONAL AXIAL COORDINATE USING THE AXIAL CHORD
YS/B = NON DIMENSIONAL TANGENTIAL COORDINATE FOR THE SUCTION SURFACE USING THE AXIAL CHORD
YP/B = NON DIMENSIONAL TANGENTIAL COORDINATE FOR THE PRESSURE SURFACE USING THE AXIAL CHORD

TABLE III (CONTINUED)
THIRD STAGE VANE
NON-DIMENSIONAL AIRFOIL COORDINATES

X/B*	ROOT		QUARTER ROOT		MEAN		QUARTER TIP		TIP	
	YS/B*	YP/B*	YS/B	YP/B	YS/B	YP/B	YS/B	YP/B	YS/B	YP/B
0.0	0.2344	0.2344	0.3126	0.3126	0.4689	0.4689	0.6447	0.6447	0.8303	0.8303
.05	0.3315	0.2590	0.4471	0.3426	0.5992	0.4978	0.7603	0.6688	0.9314	0.8495
.10	0.4108	0.3212	0.5504	0.4070	0.6961	0.5568	0.8436	0.7155	1.0005	0.8833
.15	0.4772	0.3678	0.6317	0.4498	0.7703	0.5928	0.9052	0.7393	1.0488	0.8940
.20	0.5318	0.4024	0.6951	0.4787	0.8262	0.6143	0.9496	0.7488	1.0807	0.8908
.25	0.5753	0.4272	0.7431	0.4974	0.8666	0.6250	0.9793	0.7478	1.0989	0.8776
.30	0.6082	0.4437	0.7775	0.5076	0.8933	0.6271	0.9961	0.7386	1.1050	0.8565
.35	0.6310	0.4526	0.7995	0.5107	0.9076	0.6218	1.0011	0.7224	1.1000	0.8286
.40	0.6440	0.4547	0.8097	0.5075	0.9101	0.6100	0.9949	0.7000	1.0844	0.7950
.45	0.6472	0.4504	0.8088	0.4983	0.9013	0.5921	0.9780	0.6718	1.0587	0.7559
.50	0.6408	0.4399	0.7969	0.4836	0.8814	0.5686	0.9504	0.6383	1.0229	0.7119
.55	0.6247	0.4235	0.7740	0.4634	0.8503	0.5396	0.9119	0.5997	0.9768	0.6630
.60	0.5987	0.4011	0.7400	0.4378	0.8078	0.5051	0.8623	0.5558	0.9197	0.6094
.65	0.5624	0.3727	0.6945	0.4067	0.7532	0.4650	0.8007	0.5068	0.8510	0.5509
.70	0.5156	0.3382	0.6368	0.3697	0.6855	0.4190	0.7260	0.4523	0.7691	0.4874
.75	0.4575	0.2973	0.5659	0.3264	0.6034	0.3666	0.6364	0.3919	0.6720	0.4186
.80	0.3875	0.2494	0.4802	0.2760	0.5051	0.3072	0.5307	0.3251	0.5591	0.3439
.85	0.3051	0.1939	0.3789	0.2173	0.3919	0.2397	0.4108	0.2508	0.4322	0.2626
.90	0.2118	0.1300	0.2633	0.1486	0.2678	0.1622	0.2804	0.1676	0.2949	0.1735
.95	0.1098	0.0560	0.1364	0.0663	0.1367	0.0716	0.1431	0.0729	0.1504	0.0744
1.0	0.0000	0.0000	0.0000	0.0000	0.0000	0.0000	0.0000	0.0000	0.0000	0.0000

* X/B = NON DIMENSIONAL AXIAL COORDINATE USING THE AXIAL CHORD
YS/B = NON DIMENSIONAL TANGENTIAL COORDINATE FOR THE SUCTION SURFACE USING THE AXIAL CHORD
YP/B = NON DIMENSIONAL TANGENTIAL COORDINATE FOR THE PRESSURE SURFACE USING THE AXIAL CHORD

TABLE III (CONTINUED)
THIRD STAGE BLADE
NON-DIMENSIONAL AIRFOIL COORDINATES

X/B*	ROOT		QUARTER ROOT		MEAN		QUARTER TIP		TIP	
	YS/B*	YP/B*	YS/B	YP/B	YS/B	YP/B	YS/B	YP/B	YS/B	YP/B
0.0	0.1294	0.1294	0.2450	0.2450	0.3920	0.3920	0.5783	0.5783	0.7841	0.7841
.05	0.2270	0.1601	0.3662	0.2813	0.5116	0.4265	0.6859	0.6052	0.8723	0.8039
.10	0.3089	0.2173	0.4606	0.3391	0.6027	0.4810	0.7658	0.6472	0.9341	0.8376
.15	0.3794	0.2597	0.5366	0.3772	0.6743	0.5150	0.8265	0.6697	0.9786	0.8535
.20	0.4391	0.2917	0.5977	0.4033	0.7301	0.5361	0.8717	0.6795	1.0091	0.8564
.25	0.4887	0.3156	0.6461	0.4205	0.7725	0.5475	0.9033	0.6800	1.0274	0.8490
.30	0.5287	0.3327	0.6830	0.4307	0.8028	0.5513	0.9229	0.6729	1.0349	0.8332
.35	0.5591	0.3440	0.7093	0.4349	0.8221	0.5485	0.9314	0.6593	1.0323	0.8099
.40	0.5803	0.3500	0.7256	0.4338	0.8309	0.5400	0.9293	0.6400	1.0200	0.7800
.45	0.5921	0.3509	0.7321	0.4277	0.8293	0.5260	0.9168	0.6153	0.9981	0.7439
.50	0.5945	0.3472	0.7289	0.4170	0.8175	0.5069	0.8940	0.5856	0.9665	0.7021
.55	0.5872	0.3387	0.7156	0.4018	0.7952	0.4829	0.8606	0.5510	0.9247	0.6548
.60	0.5697	0.3254	0.6919	0.3819	0.7617	0.4359	0.8163	0.5116	0.8721	0.6021
.65	0.5410	0.3073	0.6568	0.3573	0.7161	0.4197	0.7600	0.4673	0.8073	0.5441
.70	0.5019	0.2840	0.6090	0.3276	0.6570	0.3802	0.6906	0.4197	0.7282	0.4807
.75	0.4495	0.2551	0.5466	0.2924	0.5821	0.3348	0.6061	0.3630	0.6323	0.4118
.80	0.3829	0.2197	0.4664	0.2508	0.4883	0.2829	0.5052	0.3020	0.5204	0.3371
.85	0.3010	0.1768	0.3662	0.2015	0.3777	0.2232	0.3903	0.2341	0.3977	0.2563
.90	0.2071	0.1243	0.2513	0.1422	0.2568	0.1539	0.2658	0.1580	0.2686	0.1688
.95	0.1062	0.0589	0.1263	0.0683	0.1305	0.0715	0.1353	0.0713	0.1359	0.0737
1.0	0.0000	0.0000	0.0000	0.0000	0.0000	0.0000	0.0000	0.0000	0.0000	0.0000

* X/B = NON DIMENSIONAL AXIAL COORDINATE USING THE AXIAL CHORD
YS/B = NON DIMENSIONAL TANGENTIAL COORDINATE FOR THE SUCTION SURFACE USING THE AXIAL CHORD
YP/B = NON DIMENSIONAL TANGENTIAL COORDINATE FOR THE PRESSURE SURFACE USING THE AXIAL CHORD

TABLE III (CONTINUED)
FOURTH STAGE VANE
NON-DIMENSIONAL AIRFOIL COORDINATES

X/B*	ROOT		QUARTER ROOT		MEAN		QUARTER TIP		TIP	
	YS/B*	YP/B*	YS/B	YP/B	YS/B	YP/B	YS/B	YP/B	YS/B	YP/B
0.0	0.1574	0.1574	0.1968	0.1968	0.3444	0.3444	0.5215	0.5215	0.5215	0.5215
.05	0.2370	0.1885	0.3121	0.2427	0.4613	0.3829	0.6250	0.5529	0.8238	0.7609
.10	0.3052	0.2375	0.4059	0.3048	0.5535	0.4381	0.7049	0.6002	0.8868	0.7956
.15	0.3649	0.2752	0.4835	0.3487	0.6276	0.4772	0.7678	0.6331	0.9338	0.8167
.20	0.4163	0.3042	0.5473	0.3805	0.6864	0.5044	0.8162	0.6543	0.9675	0.8263
.25	0.4594	0.3258	0.5986	0.4029	0.7318	0.5220	0.8518	0.6656	0.9892	0.8260
.30	0.4942	0.3410	0.6384	0.4176	0.7651	0.5316	0.8757	0.6681	1.0002	0.8169
.35	0.5207	0.3506	0.6674	0.4258	0.7869	0.5340	0.8887	0.6627	1.0010	0.7996
.40	0.5387	0.3550	0.6860	0.4280	0.7978	0.5300	0.8909	0.6500	0.9919	0.7750
.45	0.5480	0.3543	0.6942	0.4246	0.7979	0.5198	0.8827	0.6304	0.9730	0.7433
.50	0.5485	0.3489	0.6922	0.4160	0.7871	0.5038	0.8639	0.6042	0.9440	0.7050
.55	0.5399	0.3387	0.6797	0.4022	0.7653	0.4821	0.8340	0.5717	0.9047	0.6603
.60	0.5219	0.3237	0.6561	0.3833	0.7318	0.4547	0.7924	0.5330	0.8540	0.6094
.65	0.4940	0.3039	0.6208	0.3591	0.6857	0.4215	0.7380	0.4879	0.7909	0.5523
.70	0.4557	0.2790	0.5726	0.3294	0.6256	0.3822	0.6692	0.4366	0.7132	0.4892
.75	0.4065	0.2485	0.5098	0.2936	0.5494	0.3366	0.5836	0.3787	0.6191	0.4199
.80	0.3454	0.2121	0.4303	0.2511	0.4558	0.2840	0.4818	0.3140	0.5102	0.3444
.85	0.2722	0.1688	0.3344	0.2009	0.3494	0.2235	0.3688	0.2422	0.3906	0.2626
.90	0.1886	0.1174	0.2279	0.1410	0.2362	0.1537	0.2493	0.1626	0.2643	0.1742
.95	0.0974	0.0559	0.1160	0.0685	0.1195	0.0726	0.1262	0.0746	0.1339	0.0788
1.0	0.0000	0.0000	0.0000	0.0000	0.0000	0.0000	0.0000	0.0000	0.0000	0.0000

* X/B = NON DIMENSIONAL AXIAL COORDINATE USING THE AXIAL CHORD
YS/B = NON DIMENSIONAL TANGENTIAL COORDINATE FOR THE SUCTION SURFACE USING THE AXIAL CHORD
YP/B = NON DIMENSIONAL TANGENTIAL COORDINATE FOR THE PRESSURE SURFACE USING THE AXIAL CHORD

TABLE III (CONTINUED)
FOURTH STAGE BLADE
NON-DIMENSIONAL AIRFOIL COORDINATES

X/B*	ROOT		QUARTER ROOT		MEAN		QUARTER TIP		TIP	
	YS/B*	YP/B*	YS/B	YP/B	YS/B	YP/B	YS/B	YP/B	YS/B	YP/B
0.0	.1845	.1845	0.2467	0.2467	0.4440	0.4440	0.6709	0.6709	0.8880	0.8880
.05	0.2692	0.2238	0.3470	0.2908	0.5388	0.4817	0.7525	0.7003	0.9453	0.9057
.10	0.3426	0.2780	0.4299	0.3418	0.6127	0.5236	0.8143	0.7337	0.9878	0.9307
.15	0.4066	0.3208	0.4990	0.3770	0.6710	0.5494	0.8609	0.7516	1.0191	0.9440
.20	0.4611	0.3540	0.5558	0.4014	0.7161	0.5641	0.8942	0.7578	1.0393	0.9458
.25	0.5057	0.3790	0.6011	0.4176	0.7493	0.5703	0.9152	0.7545	1.0487	0.9366
.30	0.5403	0.3966	0.6356	0.4270	0.7717	0.5694	0.9248	0.7431	1.0474	0.9170
.35	0.5647	0.4074	0.6598	0.4306	0.7839	0.5624	0.9237	0.7247	1.0356	0.8879
.40	0.5789	0.4120	0.6739	0.4290	0.7863	0.5500	0.9120	0.7000	1.0133	0.8499
.45	0.5829	0.4105	0.6781	0.4224	0.7790	0.5324	0.8902	0.6693	0.9806	0.8042
.50	0.5766	0.4032	0.6724	0.4112	0.7621	0.5100	0.8581	0.6332	0.9373	0.7514
.55	0.5601	0.3902	0.6565	0.3954	0.7352	0.4829	0.8157	0.5919	0.8834	0.6925
.60	0.5336	0.3715	0.6301	0.3750	0.6979	0.4511	0.7626	0.5454	0.8189	0.6282
.65	0.4972	0.3471	0.5927	0.3499	0.6495	0.4146	0.6984	0.4939	0.7434	0.5590
.70	0.4512	0.3167	0.5436	0.3199	0.5888	0.3731	0.6224	0.4373	0.6570	0.4857
.75	0.3958	0.2802	0.4817	0.2844	0.5142	0.3263	0.5341	0.3757	0.5606	0.4087
.80	0.3313	0.2371	0.4657	0.2430	0.4252	0.2738	0.4360	0.3087	0.4564	0.3285
.85	0.2582	0.1868	0.3158	0.1944	0.3256	0.2147	0.3315	0.2363	0.3468	0.2455
.90	0.1778	0.1287	0.2160	0.1372	0.2200	0.1479	0.2232	0.1581	0.2336	0.1600
.95	0.0916	0.0616	0.1102	0.0683	0.1114	0.0713	0.1128	0.0735	0.1181	0.0723
1.0	0.0000	0.0000	0.0000	0.0000	0.0000	0.0000	0.0000	0.0000	0.0000	0.0000

* X/B = NON DIMENSIONAL AXIAL COORDINATE USING THE AXIAL CHORD
YS/B = NON DIMENSIONAL TANGENTIAL COORDINATE FOR THE SUCTION SURFACE USING THE AXIAL CHORD
YP/B = NON DIMENSIONAL TANGENTIAL COORDINATE FOR THE PRESSURE SURFACE USING THE AXIAL CHORD

TABLE IV
EGV AIRFOIL DATA

AVG. PCT. SPAN	0	15%	45%	75%	90%
DEFINING RADIUS ~ CM.	19.116	21.039	24.882	28.722	30.645
DEFINING RADIUS ~ IN.	7.526	8.283	9.796	11.308	12.065
α_1°	30.52	30.27	32.99	36.53	38.96
α_2°	105.87	106.95	107.18	106.16	104.42
θ°	75.35	76.68	74.19	69.62	65.45
B CM	8.636	8.636	8.636	8.636	8.636
IN.	3.400	3.400	3.400	3.400	3.400
τ/B	0.4967	0.5467	0.6465	0.7464	0.7963
LER CM.	0.0208	0.0251	0.0358	0.0480	0.0549
IN.	0.0082	0.0099	0.0141	0.0189	0.0216
TER CM.	0.0239	0.0264	0.0312	0.0361	0.0383
IN.	0.0094	0.0104	0.0123	0.0142	0.0151

TABLE V

EXIT GUIDE VANE
NONDIMENSIONAL COORDINATES

T/B_T*	0%		15%		45%		75%		100%	
	S/B_T*	P/B_T*	S/B_T	P/B_T	S/B_T	P/B_T	S/B_T	P/B_T	S/B_T	P/B_T
0.0	0.0	0.0	0.0	0.0	0.0	0.0	0.0	0.0	0.0	0.0
0.052	0.0221	0.0542	0.0214	0.0569	0.0172	0.0586	0.0121	0.0588	0.0087	0.0576
0.110	0.0506	0.0941	0.0500	0.0981	0.0432	0.0995	0.0345	0.0984	0.0284	0.0957
0.160	0.0724	0.1221	0.0719	0.1267	0.0635	0.1260	0.0524	0.1260	0.0443	0.1222
0.211	0.0911	0.1451	0.0907	0.1503	0.0810	0.1513	0.0680	0.1485	0.0584	0.1439
0.261	0.1064	0.1638	0.1062	0.1694	0.0956	0.1702	0.0811	0.1667	0.0704	0.1613
0.311	0.1190	0.1783	0.1189	0.1842	0.1076	0.1847	0.0920	0.1807	0.0804	0.1748
0.362	0.1237	0.1890	0.1287	0.1950	0.1170	0.1954	0.1006	0.1910	0.0883	0.1847
0.419	0.1357	0.1960	0.1368	0.2022	0.1238	0.2023	0.1070	0.1975	0.0943	0.1908
0.462	0.1400	0.1994	0.1402	0.2056	0.1283	0.2055	0.114	0.2004	0.0985	0.1935
0.513	0.1417	0.1993	0.1421	0.2054	0.1304	0.2050	0.1137	0.1997	0.1009	0.1926
0.563	0.1409	0.1956	0.1414	0.2015	0.1301	0.2009	0.1139	0.1954	0.1014	0.1883
0.613	0.1375	0.1883	0.1331	0.1939	0.1274	0.1931	0.1120	0.1874	0.1001	0.1804
0.664	0.1313	0.1773	0.1320	0.1826	0.1221	0.1816	0.1078	0.1759	0.0966	0.1690
0.714	0.1220	0.1628	0.1228	0.1676	0.1139	0.1665	0.1007	0.1609	0.0905	0.1543
0.764	0.1093	0.1447	0.1103	0.1497	0.1023	0.1498	0.0906	0.1425	0.0815	0.1364
0.815	0.0932	0.1228	0.0940	0.1266	0.0872	0.1253	0.0773	0.1206	0.0695	0.1152
0.865	0.0732	0.0968	0.0739	0.0998	0.0634	0.0938	0.0605	0.0949	0.0543	0.0905
0.915	0.0483	0.0661	0.0492	0.0683	0.0453	0.0676	0.0398	0.0650	0.0355	0.0620
0.951	0.0283	0.0411	0.0234	0.0425	0.0258	0.0423	0.0223	0.0403	0.0197	0.0390
1.00	0.0	0.0	0.0	0.0	0.0	0.0	0.0	0.0	0.0	0.0

T/B_T = COORDINATE ALONG THE TRUE CHORD, NONDIMENSIONALIZED BY THE TRUE CHORD

NS/B_T = SUCTION SURFACE COORDINATE NORMAL TO THE TRUE CHORD, NONDIMENSIONALIZED BY THE TRUE CHORD

NP/B_T = PRESSURE SURFACE COORDINATE NORMAL TO THE TRUE CHORD, NONDIMENSIONALIZED BY THE TRUE CHORD

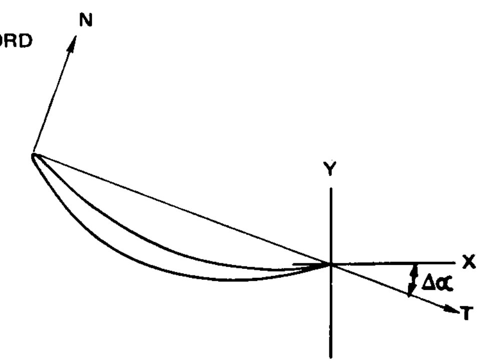

NOTE: NONDIMENSIONAL CORRDINATES ARE GIVEN RELATIVE TO THE AIRFOIL TRUE CHORD WHICH IS STAGGERED FROM THE AXIAL DIRECTION BY A $\Delta\alpha$ OF -21.8°, -21.4°, -29.9°, -18.7° AND -18.3° FOR THE 0%, 15%, 45%, 75% AND 100% SECTIONS RESPECTIVELY.

*U.S. GOVERNMENT PRINTING OFFICE: 1976 - 635-275/86

NATIONAL AERONAUTICS AND SPACE ADMINISTRATION
WASHINGTON, D.C. 20546

OFFICIAL BUSINESS
PENALTY FOR PRIVATE USE $300

SPECIAL FOURTH-CLASS RATE
BOOK

POSTAGE AND FEES PAID
NATIONAL AERONAUTICS AND
SPACE ADMINISTRATION
451

U.S.MAIL

POSTMASTER: If Undeliverable (Section 158 Postal Manual) Do Not Return

"The aeronautical and space activities of the United States shall be conducted so as to contribute . . . to the expansion of human knowledge of phenomena in the atmosphere and space. The Administration shall provide for the widest practicable and appropriate dissemination of information concerning its activities and the results thereof."

—NATIONAL AERONAUTICS AND SPACE ACT OF 1958

NASA SCIENTIFIC AND TECHNICAL PUBLICATIONS

TECHNICAL REPORTS: Scientific and technical information considered important, complete, and a lasting contribution to existing knowledge.

TECHNICAL NOTES: Information less broad in scope but nevertheless of importance as a contribution to existing knowledge.

TECHNICAL MEMORANDUMS: Information receiving limited distribution because of preliminary data, security classification, or other reasons. Also includes conference proceedings with either limited or unlimited distribution.

CONTRACTOR REPORTS: Scientific and technical information generated under a NASA contract or grant and considered an important contribution to existing knowledge.

TECHNICAL TRANSLATIONS: Information published in a foreign language considered to merit NASA distribution in English.

SPECIAL PUBLICATIONS: Information derived from or of value to NASA activities. Publications include final reports of major projects, monographs, data compilations, handbooks, sourcebooks, and special bibliographies.

TECHNOLOGY UTILIZATION PUBLICATIONS: Information on technology used by NASA that may be of particular interest in commercial and other non-aerospace applications. Publications include Tech Briefs, Technology Utilization Reports and Technology Surveys.

Details on the availability of these publications may be obtained from:

SCIENTIFIC AND TECHNICAL INFORMATION OFFICE

NATIONAL AERONAUTICS AND SPACE ADMINISTRATION

Washington, D.C. 20546